Boundedly Rational User Equilibrium: Models and Applications

A THESIS
SUBMITTED TO THE FACULTY OF THE GRADUATE SCHOOL
OF THE UNIVERSITY OF MINNESOTA
BY

Xuan Di

IN PARTIAL FULFILLMENT OF THE REQUIREMENTS
FOR THE DEGREE OF
DOCTOR OF PHILOSOPHY

Henry X. Liu

August, 2014

Acknowledgements

There are many people that have earned my gratitude for their contribution to my time in graduate school.

I would like to first give my gratitude to my beloved parents for their unconditional support. They never complain even when I only visited them once in the past six years.

In addition, I am so grateful to my advisor, Professor Henry Liu, for his precious advice for my graduate research and career development.

Also, I would like to thank my seniors, Dr. Sean (Xiaozheng) He for initiating valuable discussions and offering insights into my graduate study, Dr. Xiaolei Guo and Dr. Shanjiang Zhu for their helpful comments and suggestions for my research, Dr. Saif Jabari for his life suggestions, Dr. Xinkai Wu for his assistance when I was suffering from transition, Adam Danczyk for bringing liveliness and passion to the lab. I also want to extend my gratitude to my lab mates, Heng Hu, Jie Sun, Jiangfeng Zheng, and my colleagues, Indrajit Chatterjee, Huina Yuan, Andrew Owen, David Giacomin, Carlos Carrion and Abhisek Mudgal. Their accompany makes my graduate life smooth, exciting and fruitful.

Last but not least, thank my committee members, Prof. Davis, Prof. Levinson and Prof. Zhang for their inspiration in the process of preparing this thesis.

Dedication

To my dear parents, my love and those who held me up over the years

Abstract

Efficient transportation management requires good understanding of people's travel behavior. Most transportation planning models assume travelers are perfectly rational in decision-making. However, much of the empirical evidence from psychology, economics, and transportation has shown that perfect rationality is not realistic in modeling travelers' decision-making process. Thus existing transportation planning models may provide inaccurate predictions to transportation planners.

Motivated by travelers' route choice changes in response to the reopening of the I-35W Bridge in Minneapolis, this dissertation shows that travelers are boundedly rational (BR) in making route choices. Though the BR travel behavioral model was proposed in the 1980's, empirical validation of such behavioral principle using real-world data along with a theoretical framework was non-existent. This study is dedicated to bridging these gaps from both empirical and theoretical perspectives.

The first contribution of this dissertation is the empirical verification and estimation of boundedly rational route choice behavior. By analyzing recorded GPS trajectories from 143 commuters before and after the reopening of the I-35W Bridge in Minneapolis, we employ a probit model to estimate the bounded rationality parameters in Twin Cities.

Despite the behavioral appeal of bounded rationality, a rigorous study of boundedly rational user equilibria (BRUE) solution has been lacking, partly due to its mathematical complexity. This research offers a systematic approach of deriving the BRUE solutions analytically on networks with fixed travel demands. Based on the definition of ε-BRUE, where ε is the indifference band for perceived travel times, we formulate the ε-BRUE problem as a nonlinear complementarity problem (NCP). With the increase of the indifference band, the path set that contains equilibrium flows will be augmented and the critical values of the indifference band to augment the path set can be identified by solving a sequence of mathematical programs with equilibrium constraints (MPEC). A novel solution method is provided to obtain the BRUE solution set and numerical examples are given to illustrate this finding.

To provide guidelines to policy-makers for congestion mitigation, this research also explores an important phenomenon which should be avoided in transportation network

design, i.e., Braess paradox. The classical Braess paradox was built upon the perfectly rational behavioral assumption. Under the framework of bounded rationality, each equilibrium flow pattern leads to a different total system travel time, resulting in non-unique network performance measures. Because of the non-uniqueness of BRUE solutions, which particular equilibrium pattern should be used to compare network performances before and after new roads are built remains a question. This dissertation aims to study the analytical properties of Braess paradox under bounded rationality by exploring the relationships between the occurrence of Braess paradox and the indifference band as well as the demand level. The unveiled relationships offer a guideline for transportation planners to prevent the occurrence of Braess paradox and pave the way for strategic transportation management under the bounded rationality assumption.

Contents

Acknowledgements i

Dedication ii

Abstract iii

List of Tables ix

List of Figures x

1 Introduction 1

1.1 Problem statement 1

1.2 Research objectives and scope 2

1.3 Research contributions 3

1.4 Dissertation organization 5

2 Literature review 6

2.1 Introduction 6

2.2 Behavioural evidence on bounded rationality 7

2.2.1 Why not perfect rationality 7

2.2.2 Why bounded rationality 10

2.2.3 Boundedly rational travel choice models 12

2.3 Boundedly rational static traffic assignment 19

2.3.1 A unifying framework for game-theoretical approach 19

2.3.2 Static user equilibria 20

2.3.3 Boundedly rational Nash equilibria with finite players 22
2.3.4 Threshold discrete choice model 24
2.4 Boundedly rational dynamic traffic assignment 27
2.4.1 A unifying framework for dynamic travel choice process 27
2.4.2 Day-to-day traffic dynamic 28
2.4.3 Within-day traffic dynamic 33
2.4.4 Boundedly rational dynamical game with finite players 34
2.4.5 Boundedly rational learning behavior estimation 35
2.5 Boundedly rational cognitive process 39
2.5.1 A unifying framework for boundedly rational cognitive processes 39
2.5.2 Boundedly rational network recognition and route generation . . 40
2.5.3 Path information search 41
2.5.4 Minimum perceivable difference model 43

3 Empirical analysis of boundedly rational route choice behavior 45
3.1 Introduction 45
3.2 Theoretical Background 47
3.2.1 Boundedly rational route choice behavior 47
3.2.2 Threshold stimulus-response models 49
3.3 Route choice observations 51
3.3.1 Subject classification 51
3.3.2 Bridge usage analysis for switchers and stayers 55
3.4 Travel time saving calculation 58
3.5 Route switching analysis 59
3.5.1 Old-users and non-users 59
3.5.2 Factors contributing to route switching 61
3.6 Indifference band estimation 63
3.6.1 Unsupervised learning 65
3.6.2 Logit regression model formulation 65

4 Boundedly rational user equilibrium (BRUE) 71
4.1 Introduction 71
4.2 Definition of ε-BRUE and nonlinear complementarity formulation . . . 73

4.2.1 Definition . . . 73
4.2.2 BRUE-NCP formulation . . . 75
4.3 Monotonically non-decreasing acceptable path set . . . 78
4.3.1 Monotonically non-decreasing property . . . 78
4.3.2 Definition of ε-acceptable path set . . . 81
4.4 Generation of the ε-acceptable path set . . . 82
4.4.1 Solving critical points sequentially . . . 84
4.4.2 ε-acceptable path set for multiple OD pairs . . . 85
4.5 Construction of $\boldsymbol{\varepsilon}$-BRUE path flow set . . . 89
4.5.1 $\boldsymbol{\varepsilon}$-BRUE path flow set for one OD pair . . . 90
4.5.2 $\boldsymbol{\varepsilon}$-BRUE path flow set for multiple OD pairs . . . 93
4.6 Topological properties of the BRUE set . . . 94
4.6.1 Closedness and compactness . . . 94
4.6.2 Connectedness . . . 94
4.6.3 Non-convexity . . . 95

5 Boundedly rational Braess paradox 96
5.1 Introduction and motivation . . . 96
5.1.1 Literature review on the Braess paradox . . . 96
5.1.2 Contribution . . . 97
5.2 Braess paradox under boundedly rational user equilibrium . . . 98
5.3 Braess paradox analysis on the Braess network . . . 102
5.3.1 UE and BRUE . . . 103
5.3.2 Graphical solutions of the best and the worst cases . . . 106
5.3.3 Paradox synthesis over (d, ε) region . . . 112
5.3.4 Braess paradox regions under three different attitudes . . . 114
5.4 Braess paradox analysis in grid networks . . . 117
5.4.1 A grid network with one OD pair . . . 117
5.4.2 A grid network with four OD pairs . . . 121

6 Conclusions and Future Research Directions 125
6.1 Conclusions . . . 125
6.2 Research gaps of this dissertation . . . 126

6.2.1 Empirical verification and estimation 126
6.2.2 Mathematical properties of BRUE 127
6.2.3 Transportation network design under bounded rationality 127
6.3 Future Research Directions 128
6.3.1 Cognitive process 128
6.3.2 Game-theoretical BRUE model 128
6.3.3 Boundedly rational multi-modal and route choice 129

References **130**

Appendix A. Acronyms and Appendix **142**

List of Tables

2.1 Summary of boundedly rational travel behavior models 14
3.1 Statistics of crossers and non-crossers 52
3.2 Descriptive statistics of duration of bridge stabilization 58
3.3 Estimated time saving statistics 59
3.4 Contingency table of subjects' categories 60
3.5 Probit regression coefficients 66
A.1 Notation 142
A.2 Acronyms 143
A.3 Bridge usage distribution for each subject 145

List of Figures

1.1 Dissertation components 3
2.1 Boundedly rational game-theoretical framework in route choice 20
2.2 Boundedly rational travel learning process 28
2.3 Boundedly rational cognitive processes with random utility 40
3.1 Examples of subjects 54
3.2 Bridges over the Mississippi River 56
3.3 Cross-river trip distribution among bridges for study subjects 57
3.4 Boxplot of travel time saving proportions 61
3.5 Travel time saving distribution 64
3.6 Frequency and cumulative distribution for old-users 68
3.7 Frequency and cumulative distribution for non-users 69
4.1 Monotonically non-decreasing property illustration 82
4.2 Single-OD pair network illustration 85
4.3 Two-OD pair network and paths illustration 87
4.4 Acceptable paths for critical point pairs $(\varepsilon^1,\varepsilon^2)$ 89
4.5 Single OD pair network illustration 92
4.6 BRUE solution set illustration composed of two pieces 93
5.1 Braess network illustration 103
5.2 Relative positions of UE_3 and SO_3 109
5.3 Case 1: $0 \leqslant d < \frac{a_1-a_2}{2(b_1+b_2)}$ 110
5.4 STT intervals over (d, ε) region 113
5.5 Risk-averse paradox 114
5.6 Risk-averse, risk-neutral and risk-prone Braess paradox 116
5.7 A grid network with BPR link cost functions 117

5.8 UE travel time comparison without and with the new link 118
5.9 Risk-averse Braess paradox frontier over (p, ε) region 121
5.10 A grid network connecting four OD pairs with BPR link cost functions . 122
5.11 Paradox analysis in the grid network connecting four OD pairs 123
5.12 Paradox analysis in the grid network connecting four OD pairs 124
A.1 Case 2: $\frac{a_1-a_2}{2(b_1+b_2)} \leqslant d < \frac{2(a_1-a_2)}{3b_1+b_2}$ 152
A.2 Case 3: $\frac{2(a_1-a_2)}{3b_1+b_2} \leqslant d < \frac{a_1-a_2}{b_1+b_2}$ 153
A.3 Case 4: $\frac{a_1-a_2}{b_1+b_2} \leqslant d < \frac{a_1-a_2}{b_1}$ 154
A.4 Case 5: $\frac{a_1-a_2}{b_1} \leqslant d < \frac{a_1-a_2}{b_1-b_2}$ 155
A.5 Case 6: $\frac{a_1-a_2}{b_1-b_2} \leqslant d < \frac{4(a_1-a_2)}{3b_1+b_2}$ 156
A.6 Case 7: $\frac{4(a_1-a_2)}{3b_1+b_2} \leqslant d < \frac{2(a_1-a_2)}{b_1-b_2}$ 157
A.7 Case 8: $d \geqslant \frac{2(a_1-a_2)}{b_1-b_2}$ 158

Chapter 1

Introduction

1.1 Problem statement

The I-35W Bridge has been playing a critical role in transporting commuters to downtown Minneapolis and East Bank Campus of the University of Minnesota, Twin Cities. Its collapse in 2007 forced 140,000 daily users (Danczyk et al. 2010) to switch to other parallel bridges or to cancel trips. At the same time, an extra lane was added to the parallel I-94 Bridge in each direction to reduce cross river traffic burdens. A year later, the new I-35W Bridge was rebuilt and the addition of the bridge offered commuters a new option to cross the river. Surprisingly, only 100,000 daily trips on average were observed on the new bridge (Danczyk et al. 2010), which was more than 25% daily trip decrease. This phenomenon was referred to as 'irreversible network disruption' (Guo and Liu 2011). According to Zhu (2011), the total travel demand in the Twin Cities area only dropped slightly in 2008 due to economic crisis and the average daily trip on the I-94 Bridge returned to the original level after the temporarily added lanes were closed.

In reality, there may exist many possible reasons for irreversible network disruption. This dissertation aims to explain the observed phenomenon from route choice behavior perspective by employing the theory of bounded rationality.

As opposed to 'rationality as optimization', Herbert Simon, in 1957, proposed that people are boundedly rational in their decision-making processes. This is either because people are lack of accurate information, or they are incapable of obtaining the optimized

decision due to the complexity of the situations. They tend to seek a satisfactory choice solution instead. Since then, 'bounded rationality' has been studied extensively in economic and psychology literature (See Conlisk 1996 for a detailed review). Bounded rationality (BR) was introduced into transportation science by Mahmassani and Chang (1987).

Although the concept of boundedly rational route choice behavior is not new, empirical validation of such behavioral principle using real-world data and a BR theoretical framework are non-existent. This study is dedicated to bridging these gaps from both empirical and theoretical perspectives.

1.2 Research objectives and scope

This research aims to first understand boundedly rational route choice behavior from empirical analysis and then build a theoretical framework of boundedly rational user equilibria. The goal of this study is to offer thorough insights into implication of bounded rationality for transportation planning. In summary, the objectives of this study are primarily focused on:

1. providing a comprehensive survey on boundedly rational travel behavior models and methodologies;

2. analyzing empirical travel survey data from the Twin Cities and estimating bounded rationality parameters;

3. developing a mathematical framework of solving boundedly rational user equilibria;

4. exploring Braess paradox under bounded rationality and offering guidelines for transportation network design.

In light of these objectives, this research is restricted to route choice behavior in transportation networks with fixed travel demands and a single user class for each origin-destination (OD) pair. Travel time is the only determinant in route choice. In other words, travel factors, such as travel time reliability and behavioral heterogeneity within the same OD pair, are not considered.

Accordingly, the scope of this research includes four components (illustrated in Figure (1.1)):

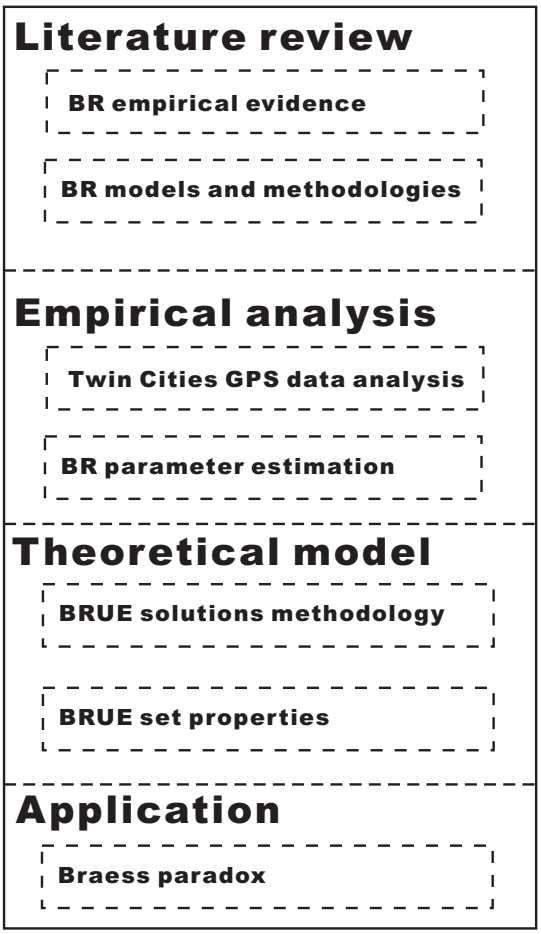

Figure 1.1: Dissertation components

1.3 Research contributions

Perfect rationality (PR) has been widely used in modeling travel behavior. As opposed to PR, bounded rationality (BR) has regained researchers' attention since its first introduction into transportation in the 1980s, due to its power in better modeling and predicting travel behavior. Despite a small but growing body of studies on employing bounded rationality principle, BR travel behavior remains understudied due to the

following reasons:

1. BR parameters are usually latent and difficult to identify and estimate;
2. The existence of BR thresholds leads to mathematically intractable properties of equilibria;
3. The non-uniqueness of boundedly rational user equilibria complicates transportation planning under the BR principle.

This dissertation aims to address the above three challenges and contributes significantly to the state-of-the-art of boundedly rational travel behavior from both empirical and theoretical aspects.

Firs of all, the disruption and the rebuilding of the I-35W Bridge in Minneapolis provides us a rare opportunity to empirically study people's route choices in response to the change in road network's topology. Accordingly, we propose an alternative route choice theory, bounded rationality, to explain observed irreversible network disruption. Though the concept of boundedly rational route choice is not new, its empirical verification has been lacking. To verify this behavioral assumption, a hypothesis is developed that travelers will not switch to the new I-35W Bridge unless the saved travel time exceeds an indifference band. Then GPS travel data are analyzed from 143 commuters tracked before and after the bridge's reopening to test the hypothesis and the indifference band is estimated by employing the probit model. Unlike a large body of existing literature employing experimental laboratory data to discover route choice behavior, this dissertation makes the first effort of utilizing empirical field data to uncover bounded rationality and estimate associated behavioral parameters.

Theoretically, due to the existence of indifference bands, the boundedly rational user equilibria (BRUE) is generally non-unique and the BRUE set is usually non-convex. As a result, there exists little literature on developing equilibrium solution algorithms and exploring its mathematical properties. To the best of our knowledge, this dissertation is the first study that provides a systematic approach of constructing the BRUE set based on the finding that the BRUE set can be decomposed into finite subsets. Accordingly, the topological properties of the BRUE set are studied based on each subset's property. These two theoretical contributions offer a tool of predicting traffic flow patterns and lay the foundations of BR related applications, such as network design problem.

With the methodology of solving BRUE sets in place, our third contribution is to explore relationships between the occurrence of the Braess paradox and the indifference band in the setting of BRUE. The ultimate goal of studying boundedly rational route choice behavior is to provide insights into transportation network design so that Braess paradox can be avoided in the first place. The Braess paradox and its variants have been extensively studied under the perfectly rational behavior assumption. However, when the perfect rationality assumption is relaxed to bounded rationality, it remains unclear under what conditions the Braess paradox occurs. This dissertation studies the occurrence conditions in the classical Braess network as well as in grid networks with Bureau of Public Roads (BPR) link performance functions. We reveal that Braess paradox can happen in general networks if certain conditions are fulfilled and bounded rationality may worsen the Braess paradox.

1.4 Dissertation organization

- Chapter 2 presents a comprehensive survey on existing boundedly rational travel behavior models.
- Chapter 3 conducts an empirical analysis of irreversible network disruption of the I-35W Bridge in Minneapolis by using boundedly rational route choice behavioral assumption.
- In Chapter 4, the theoretical aspects of boundedly rational user equilibria are discussed.
- Chapter 5 discusses the occurrence of Braess paradox under bounded rationality.
- Chapter 6 summarizes the research findings and the research gaps of this dissertation. Future research directions are also presented.

Chapter 2

Literature review

2.1 Introduction

Perfect rationality is widely used in modeling travelers' decision-making behavior. As opposed to 'rationality as optimization', Herbert Simon, in 1957, proposed that people are boundedly rational in their decision-making processes (Simon 1957). This is either because people lack accurate information, or they are incapable of obtaining an optimized decision due to complexity of the situations. They tend to seek a satisfactory choice solution instead. Since then, 'bounded rationality' has been studied extensively in economics and psychology.

Mahmassani and Chang (1987) first employed bounded rationality (BR) in modeling pre-trip departure time selection for a single bottleneck. Since then, there is small but growing literature on incorporating bounded rationality into various transportation models, such as hyperpath assignment (Fonzone and Bell 2010), transportation planning (Gifford and Checherita 2007; Khisty and Arslan 2005), traffic policy making (Marsden et al. 2012) and traffic safety (Sivak 2002). All these studies indicated that the BR assumption plays a very important role in transportation modeling. However, "there is not yet much convergence among them" (Ridwan 2004). In other words, there does not exist a standard BR framework for travel behavior study.

In this chapter, we aim to conduct a comprehensive survey on boundedly rational travel behavior and propose a unifying framework. There are two types of behavioral research (Simon 1982): "studies that are aimed at discovering and testing invariant

laws of human individual or social behavior" and "studies that estimate parameters we need for fitting theoretical models incorporating known/believed laws to particular situations where we wish to make predictions". The former is to reveal behavior while the latter is to model behavior. Accordingly, we will first review behavioral studies on discovering and verifying bounded rationality. Then we will summarize research on modeling boundedly rational travel behavior.

The rest of the chapter is organized as follows: in Section 2.2, empirical and experimental evidence is listed to support bounded rationality in modeling people's travel behavior. In Section 2.3, 2.4 and 2.5, BR formulations are introduced in static traffic assignment, dynamic traffic assignment and cognitive process models. Methodologies of estimating boundedly rational learning parameters by utilizing static and panel data from laboratory experiments are also introduced for each category.

2.2 Behavioural evidence on bounded rationality

2.2.1 Why not perfect rationality

In the following, we will present empirical evidence and anomalies to show that perfect rationality is too ideal and a new behavioral framework is needed. Three cognitive reasons are listed and are then followed by their manifestation.

Heuristic and bias

Psychologists and experimental economists verified that people use heuristic rules when making decisions, leading to biases or systematic errors (Conlisk 1996). For example, people react differently under the same situations when the problem is presented in different ways, called "framing effect" (Tversky et al. 1981).

'Debiasing' experiments were conducted to test whether biases caused by heuristic processes can be eliminated through repeated practice and adequate incentives or punishments. However, many research indicated that biases are "substantial and importation behavioral regularities" (Conlisk 1996) and will not disappear due to deliberation costs.

On the other hand, heuristics are also critical tools people employ when making decisions. People try to tradeoff "between cognitive effort and judgemental accuracy".

Due to high costs of deliberation and information search, people tend to use heuristics to find the first alternative which they are satisfied with instead of calculating an optimal one.

Cognitive limit and deliberation cost

Hiraoka et al. (2002) showed that cognitive limits and deliberation costs play important roles in route choices. They designed an experiment where subjects spoke aloud while choosing routes. A protocol analysis was conducted to analyze subjects' cognitive processes from verbal data. Results indicated that drivers had the desire to choose routes with less travel time, involving less cognitive resources and making them feel comfortable while driving along. Among the above three route choice criteria, a choice consuming less cognitive process dominated the other two criteria and drivers chose routes dynamically when one route satisfying their criteria was found.

Behavioral heterogeneity

Drivers are heterogeneous in terms of their ages, genders, familiarity within a road network and so on. There are two aspects regarding the impact of familiarity on route choices. Lotan (1997) showed that more familiar drivers took longer habitual routes than unfamiliar drivers. Hiraoka et al. (2002) showed that familiar drivers were more responsive to current traffic conditions and had flexibility to switch more frequently en route for shorter paths, while new drivers preferred staying in their predetermined routes no matter how traffic conditions changed.

Contini and Morini (2007) investigated job changing behavior from Worker Histories Italian Panel (WHIP) data in Italy. Two variables, future wages and risk-on-the-job, were identified as two driving forces of the job change. A full rationality model should imply "a positive relationship between future wages and risk-on-the-job". In other words, the higher future wages are, the higher the risk-on-the-job is. However, Contini and Morini (2007) revealed from WHIP data that when individual effects from wage growth were included, the future wage was negatively proportional to risk-on-the-job, which was inconsistent with the full rationality model. On the other hand, when individual effects were removed, future wage was positively proportional to risk-on-the-job. In conclusion, while market forces drove towards a rational outcome, individual

characteristics led towards an opposite direction. Though it is not related to travel behavior, this study revealed behavioral heterogeneity across the population in response to a system change.

Violation of taking shortest paths

Transportation researchers from across the world found evidence that people do not usually take the shortest paths and the utilized paths generally have higher costs than shortest ones.

After evaluating habitual routes, only 59% respondents from Cambridge, Massachusetts (Bekhor et al. 2006), 30% from Boston (Ramming 2001), 86.8% from Turin, Italy (Prato and Bekhor 2006) chose paths with the shortest distance or the shortest travel time. According to GPS studies, 60% of subject commuters in the Twin Cities, Minnesota took paths longer than the shortest travel time paths (Zhu 2011) and high percentage of commuting routes in Nagoya, Japan (Morikawa et al. 2005) and Lexington, Kentucky (Jan et al. 2000) were found to differ considerably from the shortest paths.

Nonexistence of perfect rationality via learning processes

Some opponents in economics claimed that people can improve their rationality via repeated learning process. In other words, people can approach to unbounded rationality while making decisions everyday based on previous experiences. Conlisk (1996) argued that learning mechanism does improve people's decision-making towards the optimal in some situations, but it can also hinder learning and adaptation due to habit. This has been validated by a sequence of route choice experiments. Compared to unfamiliar drivers, familiar drivers stick mostly to their usual driving routes which may be longer than the shortest path (Lotan 1997). Under four different route choice rules, simulated drivers' route choice behavior did not become rational through learning (Nakayama et al. 2001). Instead, there were fewer rational drivers even after a long process of route choices and they did not necessarily perceive system status accurately even after a sufficient period of time.

Infeasibility of dynamic traffic assignment

From modeling's perspective, Szeto and Lo (2006) indicated that a dynamic traffic assignment model with a physical queue paradigm might not even converge. To solve this anomaly, a tolerance-based principle was proposed that a route carrying flow at a time interval has a travel cost which is less than an acceptable tolerance from the shortest travel cost.

In summary, all above statements show that perfect rationality cannot capture people's cognitive processes in decision-making and more realistic assumption is needed in travel behavior modeling.

2.2.2 Why bounded rationality

Many researchers showed that perfectly rational models cause estimation and prediction errors without considering people's cognitive limits and deliberation costs, habits and myopia. On the contrary, models considering these factors give better prediction.

Habit and inertia

People "place higher value on an opportunity if it is associated with the status quo" (Samuelson and Zeckhauser 1988), because it can provide significant energy saving to cognitive thinking. Much empirical evidence suggested that habit plays a significant role in people's behavior in stable situations (Bamberg and Schmidt 2003).

Habit may result from searching for an optimal solution in prevailing circumstances, but it also prevents people from pursuing better alternatives when situation changes and can collapse to "bad habit" (Jager 2003). Lotan (1997) compared the impact of information on familiar and unfamiliar drivers. Ten familiar drivers and fifteen unfamiliar drivers were selected to drive in the Newton network in Massachusetts coded in traffic simulators. Results indicated that familiar drivers were reluctant to receive new information and only considered salient information. Therefore most of them stuck to their usual driving routes and did not necessarily minimize travel time.

Habit can be represented by a threshold in modeling travel choices. Cantillo et al. (2006, 2007) applied a discrete choice model with thresholds to simulated SP/RP

datasets to estimate and predict people's mode choices, showing that a model not considering inertia overestimated the benefits of transport investments substantially. Lotan (1997) fit an approximate-reasoning based model and a random utility model respectively to driving simulation data in order to estimate and predict route choices. Results showed that the approximate-reasoning based model outperformed the random utility model. Carrion and Levinson (2012) studied commuters' day-to-day route choices from GPS data collected from 65 subjects for about 30 days, concluding that commuters chose routes based on a specific threshold and might abandon a route if its travel time exceeded the margin.

Mahmassani and his colleagues conducted a series of route choice experiments in the 1990s showing that even when all path cost information was available to travelers, commuters would not switch to shorter paths due to existence of inertia, which was quantified by the 'indifference band' (Hu and Mahmassani 1997; Jayakrishnan et al. 1994a; Mahmassani and Chang 1987; Mahmassani and Jayakrishnan 1991; Mahmassani and Liu 1999; Srinivasan and Mahmassani 1999). Accordingly a boundedly rational route choice framework was proposed to capture people's travel behavior with information provision. By comparing commuter departure time and route choice switch behavior in laboratory experiments with field surveys in Dallas and Austin, Texas, Mahmassani and Jou (2000) showed that boundedly rational route choice modeling observed from experiments provided a valid description of actual commuter daily behavior.

Myopia

Myopia refers to the fact that people do not usually concern for wider interests or longer-term consequences while making decisions. Consumers manifest myopia when purchasing large appliances and tend to buy models with lower price but higher energy consumption (Conlisk 1996). Gabaix et al. (2006) conducted an experiment involving a class of complex decision problems. Two behavioral models were proposed to predict choices: one with partial myopia and one with full rationality. The model with partial myopia fit laboratory experiments better.

Similarly when making travel choices, travelers tend to switch to a link at an intersection which seems shorter for the time being but may lead to a longer route. Recent

travel experiences also impact people's travel choice more profoundly. Bogers et al. (2005) used an interactive travel simulator "TSL" developed by Delft University of Technology to investigate travel behavior. Subjects were asked to make route choices among two alternative paths for 25 simulation days. En route information was provided by a built-in dynamic traffic model and ex post information of realized travel times were given in three different scenarios: travel time on the chosen route for the latest period, travel times on both routes for the latest period and travel times on both routes for all past periods. Experiential results showed that people were myopic because their previous day's travel experiences, such as lateness and experience travel time, greatly impacted their choices in the next day.

Less computational burden and solution existence

From modeling's perspective, bounded rationality requires less computational burdens and ensures existence of a satisficing solution.

In large scale problems, it is difficult to attain optimal solutions analytically. The perfectly rational search model proposed by Gabaix et al. (2006) is not solvable and suffers from curse of dimensionality and no convergence. A heuristic algorithm usually admits a computationally tractable solution without losing too much accuracy.

According to Simon (1957), decisions are sought dynamically and will not terminate till an alternative meeting a certain threshold level is found. This level will be adjusted if a satisficing alternative is difficult to find. "Such changes in aspiration level...tend to guarantee the existence of satisfactory solutions" (Simon 1957). Similar results are found in transportation literature. The traditional dynamic traffic assignment model with perfect rationality may be infeasible, while a tolerance-based traffic dynamic ensures existence of an equilibrium (Szeto and Lo 2006).

2.2.3 Boundedly rational travel choice models

Simon (1986) classified two types of rationality: substantive rationality ('rationality is viewed in terms of the choices it produces') and procedural rationality (rationality is viewed 'in terms of the processes it employs'). Substantive rationality focuses on the choice results subjective to certain goals, while procedural rationality describes the cognitive process of a decision-maker. According to Simon (1982), bounded rationality

is a more "ambitious" rationality concept, trying to capture both the substance of the final decision and the dynamical process of decision-making, based on empirical studies and psychological research.

In terms of travel decision choices, there also exist two categories of travel behavioral models: static traffic assignment (i.e., stable and time-invariant route choices) and dynamic traffic assignment (i.e., temporal travel behavioral changes). Static traffic assignment can be embedded with substantive bounded rationality. However, dynamic traffic assignment does not correspond to procedural bounded rationality. Accordingly, we add another category of "dynamic bounded rationality" to represent rationality when decisions have to be made repeatedly as time progresses. In addition, there is another school of literature on modeling human beings' cognitive processes in route choices, which is associated with procedural bounded rationality.

Bounded rationality (BR) is rather a more realistic behavioral foundation than a new theory. Thus it permeates every part of travel behavioral modeling. To review BR related models and methodologies, a thorough survey on static and dynamic traffic assignment models should come along. Therefore, we will introduce various travel behavior models and show how substantive, dynamic and procedural bounded rationality are represented.

All relevant models are summarized in Table (2.1). Column "Category" represents three major types of bounded rationality. Column "Model" summarizes all the route choice models we will discuss in this chapter. Column "Aspect" illustrates the decision which is incorporated with bounded rationality, column "Representation" further explains how it is incorporated while column "Specification" lists the specific form of the associated bounded rationality parameter. Column "Estimated" indicates whether the bounded rationality parameter is estimated or given in the corresponding model.

Table 2.1: Summary of boundedly rational travel behavior models

Category	Model	Aspect	Representation	Specification	Estimated or not	References
Substantive BR	BRUE	route choice	not take the shortest paths	indifference band	N	Lou et al. (2010); Di et al. (2013)
	BR Nash game	static decision	not choose the alternative with least disutility	rationality parameter	N	Chen et al. (1997); McKelvey and Palfrey (1995); Seim (2006); Zhao (1994)
	Stimulus-response threshold model	behavioral response	not respond till stimulus exceeds a threshold	random variable	Y	Krishnan (1977)
	Threshold choice model	mode choice	no mode switch unless travel cost exceeds a threshold	random utility with state dependence and serial correlation	Y	Cantillo et al. (2006, 2007)
Dynamic BR	Day-to-day BR dynamic	deterministic route choice	take an acceptable path every day	indifference band	N	Guo and Liu (2011)

	stochastic route choice	not always update perceived path costs	indifference band	N	Wu et al. (2013)
BR-DUE	simultaneous departure-time and route choices	not take the shortest paths at each time interval	tolerance	N	Szeto and Lo (2006)
Dynamic Nash game	dynamic decision	not choose the alternative with least disutility	rationality parameter	N	Chen et al. (1997)
Learning process model	travel time update	only learn salient travel information	random utility	Y	Chen and Mahmassani (2004); Nakayama et al. (2001)

	departure-time choice	no switch unless schedule delay exceeds a threshold	random utility	Y	Chen and Mahmassani (2004); Hu and Mahmassani (1997); Jayakrishnan et al. (1994a); Mahmassani and Chang (1987); Mahmassani and Jayakrishnan (1991); Mahmassani and Liu (1999); Srinivasan and Mahmassani (1999)
			stochastic automation	N	Yanmaz-Tuzel and Ozbay (2009)

		route choice	no switch unless difference between experienced and best travel time exceeds a threshold	random utility	Y	Chen and Mahmassani (2004); Hu and Mahmassani (1997); Jayakrishnan et al. (1994a); Mahmassani and Chang (1987); Mahmassani and Jayakrishnan (1991); Mahmassani and Liu (1999); Srinivasan and Mahmassani (1999)
Procedural BR	Network recognition	choice set generation	generate a mental map with partial alternative paths	a fixed parameter	N	Hato and Asakura (2000)
	Route generation model	path selection	evaluate partial attributes	a fixed parameter	N	Hato and Asakura (2000)
	Cognitive cost model	path information search	not search all path information	random utility	Y	Gao et al. (2011)

	Indifference model	alternative preference	indifference to alternatives with small utility difference	a constant parameter	Y	Guilford (1954)

The survey of each category of models is arranged as follows: at the beginning of each section, a unifying framework diagram serves as a navigation map, providing a general picture of each category (including elements and their relations) and how the BR piece fits the whole picture. Then we will introduce analytical models and estimation methodologies under the unifying framework.

2.3 Boundedly rational static traffic assignment

2.3.1 A unifying framework for game-theoretical approach

Figure (2.1) illustrates a framework of equilibrium models. A large population of travelers make route choices in a road network and suffer from congestion effects leading to travel costs or disutilities. The travel cost or the disutility is indicated in ovals which represent latent variables (Walker 2001) and is also enclosed in a big box with dotted borders because they are unobservable. Every traveler aims to minimize his own travel cost or disutility. Bounded rationality thresholds can be embedded into either cost or disutility functions in the form of "random error" or "rationality parameter" or represented by the route choice principle, indicated in dotted hexagons. Individual's route choices and various types of equilibria, such as boundedly rational user equilibria (BRUE), quantal response equilibrium (QRE) and boundedly rational Nash equilibria (BRNE), are indicated in solid parallelograms, representing observable outputs. In this section, we will introduce how different specifications of travel costs or disutilities and route choice behavior lead to different types of equilibria.

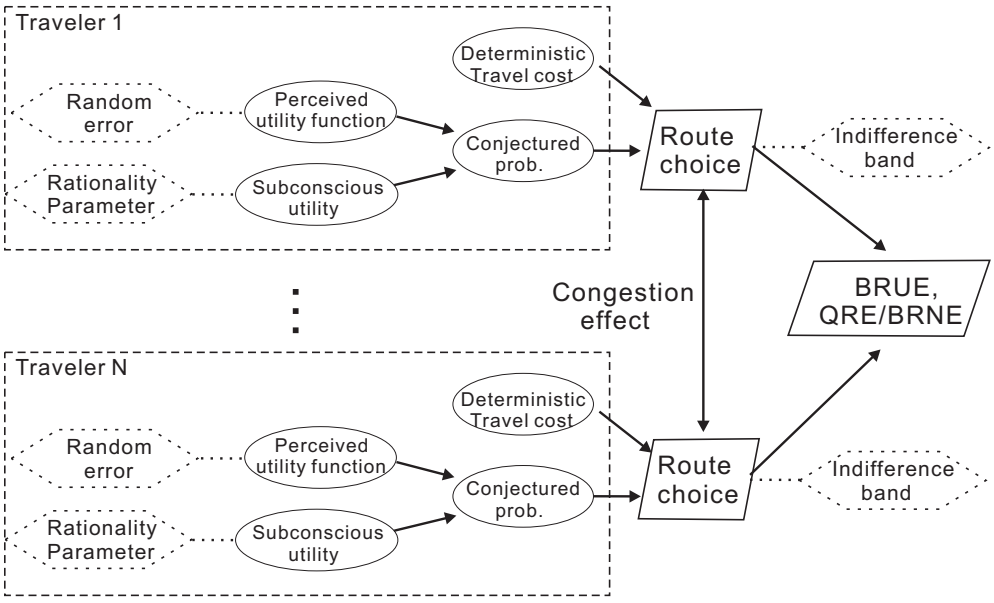

Figure 2.1: Boundedly rational game-theoretical framework in route choice

2.3.2 Static user equilibria

Wardrop's first principle says that people will take the path with the least disutility (i.e., travel time, monetary cost, etc). A Wardrop user equilibrium (UE) is reached when no one can improve his travel cost by unilaterally changing routes. At UE, all utilized routes have the minimum travel cost while all unutilized routes have higher travel costs. In other words, the following conditions hold at an equilibrium $\mathbf{f}^*$:

$$C_r^w(\mathbf{f}^*) - \pi^w \begin{cases} = 0, \text{if } f_r^{w*} > 0, \\ \geqslant 0, \text{if } f_r^{w*} = 0. \end{cases} , \forall r \in \mathcal{P}^w, \forall w \in \mathcal{W}, \tag{2.3.1}$$

where π^w is the minimum travel cost connecting OD pair w, i.e., $\pi^w = \min_{j \in \mathcal{P}^w} C_j^w(\mathbf{f})$.

Under bounded rationality, at equilibrium, "every driver uses an acceptable path, where a path is acceptable if the difference between its travel cost and that of the shortest or least-cost path is no larger than a pre-specified threshold value" (Lou et al. 2010). In other words, no one can reduce his travel cost by a threshold by unilaterally switching routes. This threshold depends on network users' behavior and varies among different OD pairs, which needs to be obtained through behavioral surveys and experiments.

Given an indifference band, BRUE is shown to be non-unique (Lou et al. 2010). Lou et al. (2010) proposed a path-based BRUE formulation and a link-node based formulation for congestion pricing. The link-node based BRUE is shown to be more restrictive than the path-based one. Di et al. (2013) developed a nonlinear complimentariy condition for one path-based BRUE:

$$\tilde{C}_r^w(\mathbf{f}^*) - \tilde{\pi}^w \begin{cases} = 0, \text{if } f_r^{w*} > 0, \\ \geqslant 0, \text{if } f_r^{w*} = 0. \end{cases} , \forall r \in \mathcal{P}^w, \forall w \in \mathcal{W}. \tag{2.3.2}$$

where,

$\tilde{C}_r^w(\mathbf{f}^*)$: the indifference travel cost, computed by $\tilde{C}_r^w(\mathbf{f}^*) = C_r^w(\mathbf{f}^*) + \rho_r^w$;

$\tilde{\pi}^w$: the shortest indifference travel cost, equal to the minimum travel cost plus the indifference band connecting OD pair w, i.e., $\tilde{\pi}^w = \min_{j \in \mathcal{P}^w} C_j^w(\mathbf{f}) + \varepsilon^w$;

$\boldsymbol{\rho}$: an indifference vector and $\boldsymbol{\rho} = (\rho_r^w)_{r \in \mathcal{P}}^{w \in W}$, where $0 \leqslant \rho_r^w \leqslant \varepsilon^w$. ρ_r^w represents the deviation of route r's actual cost from the shortest indifference travel cost, i.e.,

$$\rho_r^w \triangleq \begin{cases} \tilde{\pi}^w - C_r^w(\mathbf{f}), \text{ if } C_r^w(\mathbf{f}) \leqslant \min\limits_{j \in \mathcal{P}} C_j^w(\mathbf{f}) + \varepsilon^w, \\ 0, \text{ o.w.} \end{cases}$$

The above condition implies that, under bounded rationality, all chosen paths have the same shortest indifference travel cost, equal to $\min_{j \in \mathcal{P}^w} C_j^w(\mathbf{f}) + \varepsilon^w$. The unused paths should have equal or larger indifference path costs. Denote $\mathcal{F}_{BRUE}^{\boldsymbol{\varepsilon}}$ as the $\boldsymbol{\varepsilon}$-BRUE path flow solution set, including all the BRUE path flow patterns. There exists little literature on constructing the BRUE set because it is shown to be non-convex (Lou et al. 2010) and thus its mathematical properties are intractable.

Di et al. (2013) developed a systematic methodology of constructing this set in transportation networks with fixed demands connecting multiple OD pairs. With the increase of the indifference band, the path set that contains boundedly rational equilibrium flows will be augmented. Accordingly, the critical values of indifference bands to augment these path sets can be identified by solving a family of mathematical programs with equilibrium constraints (MPEC) sequentially. For a network with single OD pair, given a sequence of finite critical points $\varepsilon_k^*, k = 1, \cdots, K$, with $\varepsilon_0^* = 0, \varepsilon_{K+1}^* = \infty$, a BRUE solution set is the union of $K+1$ subsets:

$$\mathcal{F}_{BRUE}^{\varepsilon} = \bigcup_{k=0}^{K} \mathcal{F}_k^{\varepsilon_k^*}. \tag{2.3.3}$$

where $\mathcal{F}_k^{\varepsilon_k^*}, k = 0, \cdots, K$ is the k^{th} subset with associated critical indifference band ε_k^*.

Di et al. (2014a) studied the topological properties of the BRUE set and showed that generally the BRUE set is compact and non-convex. Given affine linear link performance functions, all the subsets are convex and the BRUE set is connected (Di et al. 2014b).

2.3.3 Boundedly rational Nash equilibria with finite players

Game theory models finite players' strategic decisions in a conflict but cooperative environment. Nash equilibrium is said to be achieved if no player can improve his payoff by chaning strategies. On the other hand, Wardrop user equilibrium is reached when no traveler can improve his travel cost by unilaterally switching routes. Therefore Wardrop user equilibrium considers infinitesimal travelers in a non-cooperative Nash game. Haurie and Marcotte (1985) showed that Nash equilibrium converges to Wardrop user equilibrium when the number of players goes to infinity. However, there exist few studies on modeling boundedly rational route choices with game theory and establishing relationship between boundedly rational Nash equilibrium and BRUE. Therefore we would like to examine the literature on boundedly rational game theory.

Through repeated game experiments with finite players, researchers realized that the perfect Nash equilibrium cannot be usually obtained. To explain these anomalies, bounded rationality is then incorporated into a non-cooperative mixed-strategy game in the form of inaccurate perception of payoff or cost functions. McKelvey and Palfrey (1995) assumed that game players are utility maximizers whose perception of utility functions is subject to noise. Chen et al. (1997) argued that players only know their subconscious utilities attached to each alternative instead of utility functions. Zhao (1994) suggested that the cost function should be represented by a fuzzy function. The associated equilibrium is "quantal response equilibrium" (QRE) (McKelvey and Palfrey 1995), "boundedly rational Nash equilibrium" (BRNE) (Chen et al. 1997) or "ϵ-equilibrium" (Zhao 1994) respectively. In the following, we will mainly introduce the seminal work proposed by McKelvey and Palfrey (1995).

In a finite game $(\mathcal{M}, S, U)$, among $\mathcal{M} = \{1, \cdots, N\}$ total players, player n has a set of pure strategies $S^n = \left\{s_n^1, \cdots, s_n^{J_n}\right\}$. Each player knows strategy sets available to himself and to others. The probability of player n taking strategy s_n^r is $p_n^r \triangleq p_n(s_n^r) \geqslant 0$,

and $\sum_{s_n^j \in S^n} p_n(s_n^j) = 1$. Denote $\mathbf{p}_n = \{p_n^r\}_{n\in\mathcal{M}}^{r\in J_n}$.

Player n does not know other players' utility functions but is aware of others' choice probability. Denote $p^{-n} = \{p_k^r\}_{k\in\mathcal{M},k\neq n}^{r\in J_k}$ as the conjectured mixed strategy adopted by players other than n. (s_n^r, p^{-n}) is the strategy pair where player n adopts the pure strategy s_n^r and conjectures that all other players adopt their components of p. Therefore, the expected utility of the rth pure strategy of player n, denoted as V_r^n, is a function of the strategy pair, i.e., $V_n^r = V_n^r(s_n^r, p^{-n})$.

As V_n^r depends on others' choice probabilities, let $\bar{V}_n^r$ be the expected utility over all possible choices of all players other than n. Assume player n's utility for each strategy is subject to random error and is defined as:

$$U_n^r = \bar{V}_n^r + \zeta_n^r, \tag{2.3.4}$$

where $\zeta_n = (\zeta_n^1, \cdots, \zeta_n^{J_n})$ is the perceived utility error vector for player n with i.i.d. Gumbel distribution.

One example of the expected utility function $\bar{V}_n^r$ is to assume that it depends on the total number of players choosing alternative r (Seim 2006), i.e.,

$$\bar{V}_n^r(s_n^r, p^{-n}) = \theta X_n^r(s_n^r) + N_r(p^{-n}), \tag{2.3.5}$$

where,

$X_n^r(\cdot)$: a utility mapping only depending on player n's strategy s_n^r;

N_r: the total number of players choosing alternative r, depending on others' choices.

Player n will take strategy r if $U_n^r \geqslant U_n^j, \forall j = 1, \cdots, J_n, j \neq r$. The probability that player n selects strategy r is:

$$p_n^r = P(U_n^r > U_n^j) = \frac{e^{\alpha \bar{V}_n^r}}{\sum_{j=1}^{J_n} e^{\alpha \bar{V}_n^j}}, j \neq r,$$

where α is the scale parameter for ζ_n^r. It also represents the rationality level of each player. When varying α from zero to infinity, the player's choice behavior varies from "placing equal probability over all alternatives" to "fully rational utility maximization".

Every player has the same equilibrium conjecture of others' path choices, i.e., $\mathbf{p}_n = \mathbf{p}_k = \mathbf{p}_*$. Therefore a statistical version of Nash equilibrium can be then defined as follows:

Definition 2.3.1. In a finite game $(\mathcal{M}, S, U)$, a quantal response equilibrium (QRE) is any $\pi = (\pi^1, \cdots, \pi^{J_n}) \in S$ such that $\forall n \in \mathcal{M}, 1 \leqslant r \leqslant J_n$,

$$\pi_*(\alpha) = \left\{ \pi \in S : \pi_n^r = \frac{e^{\alpha \bar{V}_n^r(\pi)}}{\sum_{j=1}^{J_n} e^{\alpha \bar{V}_n^j(\pi)}}, \forall n, r \right\}. \tag{2.3.6}$$

McKelvey and Palfrey (1995) showed that QRE exists but is generally non-unique. However, it is unique when α is restricted to be sufficiently small. As α goes to infinity, there always exists one subsequence of $\pi_*(\alpha)$ which converges to a unique Nash equilibrium.

Chen et al. (1997) argued that the mathematical interpretations of choice behavior by introducing noise into the utility function cannot manifest human being's bounded rationality. Accordingly, a boundedly rational Nash equilibrium model (BRNE) is developed based on the assumption that the player does not know his utility function, instead, he knows utility values associated with each alternative. This latent utility is called "subconscious utility" and BRNE is one extension of QRE.

2.3.4 Threshold discrete choice model

Aforementioned studies mainly focus on modeling boundedly rational route choice behavior and parameters associated with bounded rationality are assumed to be known. The main goal of the behavioral research is to "estimate parameters we need for fitting theoretical models incorporating known/believed laws to particular situations where we wish to make predictions" (Simon 1982). Therefore BR parameter estimation is a critical component of the BR research.

The discrete choice model is a common tool to estimate parameters. Within the framework of the discrete choice modeling, the random utility maximization model (RUM) is adopted in modeling and predicting drivers' route choice behavior among a set of finite paths. Provided perception errors are Gumbel distribution, RUM can be expressed in the form of a multinomial logit model. The logit model assumes paths are independent of each other and has independence from irrelevant alternatives (IIA) property. In reality, however, many paths overlap with each other and are thus not independent. To overcome this limitation, various RUM models were proposed:

C-logit (Cascetta et al. 1996), path-size logit (Ben-Akiva and Ramming 1998), nested logit (Jha et al. 1998), cross-nested logit (Vovsha and Bekhor 1998), multinomial probit (Cascetta 1989; Daganzo et al. 1977; Jotisankasa and Polak 2006) and mixed logit or multinomial probit with logit kernel (Ben-Akiva and Bolduc 1996). However, all these models still assume utility maximization.

Within disturbed networks, for example, real-time information becomes available or a new traffic plan (toll, addition/removal of roads) is implemented, travelers adjust their behavor accordingly based on previous experiences. Habit plays a critical role when travel choices are made repeatedly. Therefore, utility maximization is unrealistic and a threshold representing habitual choice behavior should be introduced to characterize habit.

Stimulus-response model

Stimulus-response theory, popular in psychology, economics and biology, provides an efficient tool of quantifying human being's behavioral response by varying stimulus of specific intensities. In psychology and economics, the stimulus-response studies focus on the change in decision-makers' preference or choice in response to the change in utilities of alternatives. Biologists are interested in the dose-response study, which is the impact of toxic levels on an organ or a tissue.

A large body of literature in psychology, economics and biology (Cox 1987; Krishnan 1977) indicated that the occurrence of a response depends on the intensity of a stimulus and there exists a threshold under which no response is manifest. This threshold is called "just noticeable difference" (Weber's law) or "minimum perceivable difference" (Krishnan 1977), which represents bounded rationality. If the response is discrete, such as people's choice or preference, several biological experiments (Clark 1933; Hemmingsen 1933) verify that no response occurs unless the logarithm of stimulus exceeds some threshold. When the response is qualitative, such as perceived loudness/brightness or dose quantity, Weber's law reveals that the response intensity is proportional to the logarithm of the stimulus. When making route choice decisions, the response is normally discrete, so we will review stimulus and quantal response models.

Denote X as the stimulus and ε as the threshold. The threshold varies over subjects and its distribution is normal with mean μ and variance σ, i.e., $\varepsilon \sim N(\mu, \sigma)$.

Then the probability of response can be calculated from the probit model (Clark 1933; Hemmingsen 1933):

$$P(\text{response}) = P(\log(X) > \varepsilon) = \int_{-\infty}^{\frac{\log(X)-\mu}{\sigma}} \frac{1}{\sqrt{2}\pi} \exp\left(-\frac{t^2}{2}\right) dt. \tag{2.3.7}$$

If the distribution of the threshold follows logistic distribution with location parameter μ and scale parameter s, then the probability of response is:

$$P(\text{response}) = \frac{1}{1 + \exp\left(-\frac{\log(X)-\mu}{s}\right)}. \tag{2.3.8}$$

The distribution of the threshold, including mean μ and variance σ (for probit model), or mean μ and scale s (for logit model), can be estimated by employing the maximum likelihood method.

Threshold mode choice model

One application of the stimulus-response theory is to study the impact of the transportation planning policy change on people's choice behavior. Cantillo et al. (2006, 2007) proposed discrete choice models with state dependence (due to inertias, Cantillo et al. 2006) and serial correlation (due to persistence of unobservable attributes across a sequence of choices, Cantillo et al. 2007). Travelers will not switch to a new mode unless its utility is greater than that of the current mode plus a threshold, which is a function of the difference between two experienced mode utilities.

Denote the utility of the alternative A_r as $U_{nt}^r = V_{nt}^r(X_n, Z_{nt}, \theta_{nt}) + \zeta_{nt}^r$, where ζ_{nt}^r is the error term. The traveler n picks a choice r on day t based on a multinomial logit model. Assume a change happens to some attribute attached to an alternative mode on day $t+1$. Assume travelers make stable mode choice right after the change is made. Due to inertia, the probability of switching from the current choice $A_{nt} = r$ to $A_{n,t+1} = r', r' \neq r$ is equivalent to:

$$U_{n,t+1}^{r'} - U_{n,t+1}^{r} \geqslant I_{n,t+1}^{r'r}, \tag{2.3.9a}$$

$$U_{n,t+1}^{r'} - U_{n,t+1}^{j} \geqslant I_{n,t+1}^{r'r} - I_{n,t+1}^{jr}, \forall j \in \mathcal{P}_{nt}, j \neq r. \tag{2.3.9b}$$

where,

$I_{n,t+1}^{r'r}$: the inertia variable, represented by a random utility function depending on the

utility difference, i.e., $I^{r'r}_{n,t+1} = \gamma_n(V(X_n, Z_{nt}, \theta_{nt}), V^r_{nt} - V^{r'}_{nt})$;
γ_n: an unknown coefficient varies randomly among individuals;
$V(\cdot)$: the utility function;
X_n: individual characteristics for traveler n;
Z_{nt}: trip features for traveler n on day t;
θ_{nt}: a vector of parameter needed to be estimated;
V^r_{nt}: the deterministic utility for the alternative r.

A multinomial logit model is formulated to calculate choice probabilities of each alternative and transition probabilities. The maximum likelihood estimation approach is used to estimate parameters and inertial variables. Two sets of data were collected in Cagliari, Italy: the RP data in terms of people's mode choices among car, bus and train; the SP data requiring the choice between a new train service and the current mode choice. Estimation results showed that a misspecified model without inertia and serial correlation may lead to biases and errors when a newly implemented policy has a substantial impact.

2.4 Boundedly rational dynamic traffic assignment

2.4.1 A unifying framework for dynamic travel choice process

Making travel decisions is a repeated learning process and three stages are usually considered during dynamic decision-making processes (illustrated in Figure (2.2)). These stages are indicated in rectangles and enclosed in a big box with dotted borders because they are unobservable. Individual's socioeconomic characteristics, available information and their route choices are indicated by solid parallelograms, representing observable inputs or outputs. Before making decisions, travelers are assumed to have some knowledge of networks from previous experiences. Salient information and new experiences may trigger travelers' update mechanism. Then adaptation to switch departure time, route or mode is made based on certain learning principle, which will provide more information to the next decision-making process. Due to the existence of habit, there exists a threshold at each stage to capture more realistic behavior, indicated in dotted hexagons.

Dynamical travel choices can be studied on a daily basis or within a day. According

to different time scales, a dynamic process can be represented by a day-to-day model or a within-day model. In this section, we will first review analytical models of day-to-day and within-day dynamics and then introduce parameter estimation for each stage.

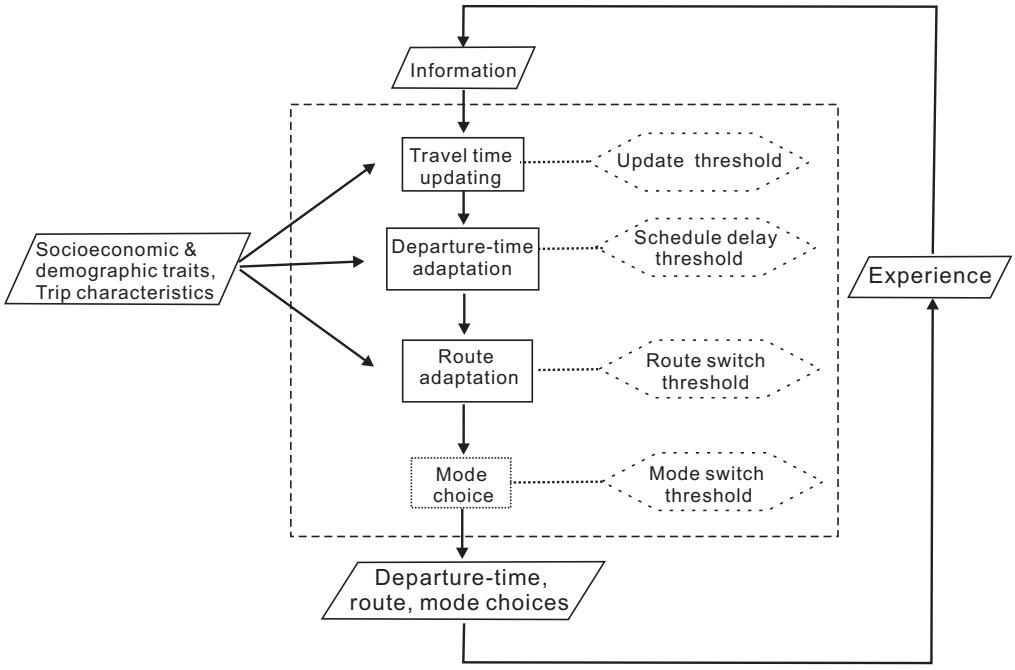

Figure 2.2: Boundedly rational travel learning process

One thing worth of note is that, the mode choice is indicated in a dotted box because there does not exist literature combining departure-time and route choices with mode choice, partly because people may not switch mode as frequently as they adjust departure-time and route. However, we should bear in mind that a multi-modal BR travel behavior process can be modeled within this framework. Moreover, destination choice can be also considered in this framework especially when non-work trips are modeled.

2.4.2 Day-to-day traffic dynamic

Day-to-day traffic dynamical systems model drivers' route choice adjustment in response to temporary changes of a traffic network based on previous experienced travel costs. There are two classes of traffic dynamics in the existing literature: (1)

deterministic user equilibrium dynamical systems (Friesz et al. 1994; He et al. 2010; Nagurney and Zhang 1997; Smith 1979), adopting various route choice update mechanism, such as proportional-switch adjustment (Smith 1979), tatonnement adjusting process (Friesz et al. 1994), dynamical projection (Nagurney and Zhang 1997) or link-based adjustment (He et al. 2010); (2) stochastic day-to-day dynamics (Cascetta 1989; Davis and Nihan 1993; Watling 1999), assuming drivers follow logit or probit model. Provided certain regulation conditions, these dynamical systems converge to different types of equilibria: the deterministic user equilibrium dynamical systems stabilizes to user equilibrium (UE) and the stochastic day-to-day dynamics' equilibrium is characterized by a stationary distribution with stochastic user equilibrium (SUE) as its mean. In this section, we will discuss how BR is embedded into these two types of traffic dynamics.

Deterministic day-to-day dynamic

The adjustment processes (Friesz et al. 1994; He et al. 2010; Nagurney and Zhang 1997) assume: on each day, the flow pattern tends to move from the current pattern $\mathbf{f}$ towards the target pattern $\mathbf{u}$, based on current day's path costs $C(\mathbf{f})$ or link costs $c(\mathbf{x})$ (Friesz et al. 1994; He et al. 2010; Nagurney and Zhang 1997). He (2010) proposed a general framework of existing day-to-day dynamics:

$$\dot{\mathbf{f}} = \lambda(\mathbf{u} - \mathbf{f}), \tag{2.4.1a}$$

$$\mathbf{u} = \mathrm{Pr}_{\Omega}(\mathbf{f} - \gamma C(\mathbf{f})), \tag{2.4.1b}$$

where,

$\mathbf{f}$: the path or the link flow vector;

$\dot{\mathbf{f}}$: the path or the link flow change;

$\mathbf{u}$: target flow pattern;

λ: a positive constant determining the flow changing rate;

$\mathbf{u} - \mathbf{f}$: a flow changing direction;

Ω: the feasible path or link flow set;

$\mathrm{Pr}_{\Omega}(\mathbf{f}-\gamma C(\mathbf{f}))$: projection operator, projecting $\mathbf{f}-\gamma C(\mathbf{f})$ onto Ω, where γ is a coefficient.

The aforementioned day-to-day dynamics mainly focus on traffic evolution from disequilibrium to equilibrium within a fixed network. When the topology of a network

is changed, such as a disrupted or restored network, travelers may behave differently from when the network is stable and the existing perfectly rational day-to-day dynamics will not work. He and Liu (2012) proposed a prediction-correction process to describe travelers' reaction within a disrupted network while Guo and Liu (2011) developed a boundedly rational route choice dynamic to capture travelers' route choices in face of a restored network. As the dynamic proposed by Guo and Liu (2011) involves bounded rationality, we will briefly discuss this model.

Under certain regularity assumptions (Cantarella and Cascetta 1995), the existing perfectly rational day-to-day dynamics have an unique fixed point. Therefore they converge to the same UE flow pattern if a network first disrupts and is then restored to the original level. This cannot capture irreversible response to the network change in Minnesota (Guo and Liu 2011). It was observed that, although the new bridge has higher capacity than the collapsed one, under similar demand level and almost identical network topology, the traffic flow across the bridge decreased significantly. Perfectly rational day-to-day dynamics will predict the same amount of traffic flow across the bridge. By allowing drivers' perception errors to vary in a presumed bound, a link-based boundedly rational day-to-day dynamic (Guo and Liu 2011) successfully explained the flow reduction phenomenon because traffic evolves from one fixed point towards another within the BRUE solution set.

In the link-based boundedly rational day-to-day dynamic (Guo and Liu 2011), Equation (2.4.1b) is replaced with the following:

$$\mathbf{u} = \mathrm{Pr}_{\Omega^{br}(c(\mathbf{x}))}(\mathbf{x}), \tag{2.4.2}$$

where $\mathbf{x}$ is the link flow and $\Omega^{br}(c(\mathbf{x}))$ is the acceptable link flow pattern induced by $\mathbf{x}$.

The acceptable set induced by path cost $c(\mathbf{x})$ is defined as:

$$\mathcal{P}^{br}(c(\mathbf{x})) \triangleq \{r \in \mathcal{P} : C_r(\mathbf{f}) \leqslant \min_{j \in \mathcal{P}^w} C_j(\mathbf{f}) + \varepsilon\}. \tag{2.4.3}$$

where $\mathbf{f}$ is the path flow vector.

According to (2.4.3), $\mathcal{P}^{br}(c(\mathbf{x}))$ can be computed in the following steps: based on the current link cost $c(\mathbf{x})$, the path cost $C(\mathbf{f})$ can be calculated for OD pair w. Find the shortest path, the 2^{nd} shortest path, $\cdots$, until the p^{th} shortest path which has the cost difference from the shortest one less than ε, while the $(p+1)^{th}$ shortest path with the

cost difference from the shortest one greater than ε. Then these p paths are acceptable paths.

After the acceptable path set $\mathcal{P}^{br}(c(\mathbf{x}))$ is known, assign the demand to those acceptable paths for each OD pair, then $\Omega^{br}(c(\mathbf{x}))$ can be mathematically expressed as:

$$\Omega^{br}(c(\mathbf{x})) \triangleq \{\mathbf{x} \in \mathcal{X} : \mathbf{x} = \Delta\mathbf{f}, \sum_{p \in \mathcal{P}^{br}(c(\mathbf{x}))} f_p^w = d^w, \forall w \in \mathcal{W}\}. \tag{2.4.4}$$

The fixed point of this dynamic is the BRUE instead of the unique UE. Therefore the stability property of this dynamic is more difficult to address. Its stability is defined as: the perturbation of a fixed point will make the system to converge to a fixed point within the set. The new fixed point can be the same or different from the initial one. Rigorous proofs of the stability property of the BR dynamic were presented in Di et al. (2014b).

Stochastic day-to-day dynamic

The existing deterministic day-to-day dynamics mainly model path choices based on the previous day's experience, while the existing stochastic day-to-day dynamics have the capability of capturing both travel time update and route adaptation illustrated in Figure (2.2). In the following, we will first give a general expression of the stochastic day-to-day dynamic and then present how it can be relaxed to incorporate BR at each stage.

Denote the expected state vector of the stochastic day-to-day dynamic as $\begin{bmatrix}\mathbf{g}_t \\ \mathbf{f}_t\end{bmatrix}$. Then the expected states of a stochastic day-to-day dynamic can be defined in a compact form:

$$\begin{bmatrix}\mathbf{g}_t \\ \mathbf{f}_t\end{bmatrix} = h\left(\begin{bmatrix}\mathbf{g}_{t-1} \\ \mathbf{f}_{t-1}\end{bmatrix}\right), \tag{2.4.5}$$

where,

$h(\cdot)$: a nonlinear mapping which will be specified later;

$\mathbf{g}_t$: the perceived travel cost vector on day t;

$\mathbf{f}_t$: the path flow on day t.

The mapping $h(\cdot)$ defines a nonlinear Markov process. It is continuously differentiable with respect to the state if link cost functions are continuous. If all eigenvalues

of the Jacobian matrix of $h(\cdot)$ are within a unit circle (Cantarella and Cascetta 1995), the dynamic will converge to a stationary flow distribution.

The mapping $h(\cdot)$ can be further specified according to two stages defined by Cantarella and Cascetta (1995). Cantarella and Cascetta (1995) built a unifying theory of both day-to-day and within-day traffic dynamics, including learning/forecasting mechanism and users' choice behavior. In the following, we will introduce how to define $h(\cdot)$ in these two stages.

Travelers update their perceived travel costs based on a weighted average of the previous day's perceived travel cost and the experienced cost (Cantarella and Cascetta 1995). Mathematically,

$$\mathbf{g}_t = \lambda \mathbf{g}_{t-1} + (1-\lambda) C(\mathbf{f}_{t-1}), 0 < \lambda < 1. \tag{2.4.6}$$

In reality, travelers may be salient to the travel cost difference between the previous day's perceived travel cost and the experienced cost if its value is within a threshold. Therefore, Wu et al. (2013) revised the cost update mechanism defined in Equation (2.4.6) as follows:

$$\mathbf{g}_t = \begin{cases} \lambda \mathbf{g}_{t-1} + (1-\lambda) C(\mathbf{f}_{t-1}), \text{ if } |\mathbf{g}_{t-1} - C(\mathbf{f}_{t-1})| \geqslant \varepsilon, \\ C_{t-1}, \text{ o.w.} \end{cases} \tag{2.4.7}$$

This travel time updating along with a logit route choice model is applied to model travelers' day-to-day evolution within urban railway networks and this updating model better captures the day-to-day dynamic (Wu et al. 2013). Due to boundedly rational cost updating, this dynamic is not continuously differentiable with respect to its state any more. Its convergence and stability properties, unaddressed by Wu et al. (2013), are more challenging to identify and remain unanswered.

For users' choice behavioral modeling, the expected path choice dynamic can be defined as a logit model $\mathbf{f}_t = \mathbf{d}P(\mathbf{g}_t)$, where $P(\cdot)$ is a logit probability. More generally (Cantarella and Cascetta 1995),

$$\mathbf{f}_t = P(\mathbf{g}_{t-1}, C(\mathbf{f}_{t-1}))\mathbf{f}_{t-1}, \tag{2.4.8}$$

where $P(\cdot)$ is a transition probability matrix, depending on previous day's perceived and actual costs.

The transition matrix $P(\cdot)$ can be further decomposed into two parts (Cantarella and Cascetta 1995): reconsidering previous day's choice and choosing today's path. Then the probability of choosing a path is the probability of reconsidering the previous day's choice (switching choice) times the conditional probability of choosing that path given that the previous day's choice is reconsidered (path choice). BR can be embedded into calculating both switching choice and path choice. The representation of BR in these two choices along with the methodology of estimating parameters will be introduced in Section (2.4.5).

2.4.3 Within-day traffic dynamic

Dynamic traffic assignment (DTA) models traveler's temporal travel choice change. Peeta and Ziliaskopoulos (2001) classified existing dynamic traffic assignment models into four methodological groups: discrete-time mathematical programming, continuous-time optimal control, variational inequality and simulation-based. To the best of our knowledge, bounded rationality has been only embedded into the third and the forth categories in existing literature, which will be explained in the following.

Variational inequality

Szeto and Lo (2006) indicated that a DTA model with a physical queue paradigm may not even converge. To solve this anomaly, a tolerance-based principle is proposed that a route carrying flow at a time interval has a travel cost which is less than an acceptable tolerance from the shortest travel cost.

Based on this principle, a nonlinear complementarity problem was formulated and a heuristic day-to-day route-swapping algorithm was developed to solve dynamic user optimal (DUO). To analyze the existence and uniqueness of the solution, a theoretical gap was defined as the minimum of the largest difference between the travel times of all used routes and the shortest OD travel times. DUO exists if and only if the theoretical gap falls within the acceptable tolerance. Therefore, existence of the dynamic equilibrium depends on both network topology and route swapping behavior. Furthermore, there exist multiple dynamical equilibria.

Simulation

Various DTA simulators, such as DYNASMART (Jayakrishnan et al. 1994a), DynaMIT (Ben-Akiva et al. 1997) and RouteSim (Ziliaskopoulos and Waller 2000), are employed to compute dynamic user equilibrium (DUE). Simulation cannot obtain analytical properties of DUE but it satisfies FIFO (First In First Out) and circumvents holding-back of vehicles. DTA simulators usually include three components (Cantarella and Cascetta 1995): demand/supply model, learning/forecasting mechanism and choice behavior. BR principle can be introduced into learning/forecasting mechanism and choice models, which will be discussed in detail in Section (2.4.5).

2.4.4 Boundedly rational dynamical game with finite players

In Section 2.3.3, a game-theoretical approach is introduced to model boundedly rational decisions. When the game is played repeatedly, Chen et al. (1997) proposed a boundedly rational dynamical game and established the connection between static and dynamic game. Supposing that the subconscious utility a player has depends on that player's beliefs about others' strategies, when the player repeatedly play the game, this belief can be obtained by the observed choices of other players in the past. So a dynamical adjustment process using fictitious play is modeled where each player plays the game based on others' historic strategies.

Assume N players start with an arbitrary mixed strategy and then adjust their strategies over time based on the observed play. The empirical distribution of player n is $\bar{P}_{nt} = (\bar{P}^1_{nt}, \cdots, \bar{P}^{J_n}_{nt})$, which can be calculated as:

$$\bar{P}_{nt} = \frac{1}{t} \sum_{\tau=0}^{t-1} \hat{p}_{n\tau}. \tag{2.4.9}$$

where $\hat{p}_{n\tau}$ is the actual choice probability of player n at time τ.

The subjective utilities are calculated based on empirical distributions prior to taking action. Travelers are myopic when making choice adjustment. It is shown that both players' beliefs about others' strategies and actual choices converge in probability to a boundedly rational Nash equilibrium (BRNE).

2.4.5 Boundedly rational learning behavior estimation

In this section, we will discuss how BR is embedded into travel time updating and choice adaptation stages and how the BR parameters are estimated from observed choices.

In the repeated learning process illustrated in Figure (2.2), as a result of habit, commuters will not update their travel time perception if the perceived one minus the predicted one is within a threshold. Moreover, they will not adjust their departure time unless the difference between the preferred arrival time and the actual arrival time exceeds a bound (Chen and Mahmassani 2004; Hu and Mahmassani 1997; Jayakrishnan et al. 1994a; Mahmassani and Chang 1987; Mahmassani and Jayakrishnan 1991; Mahmassani and Liu 1999; Srinivasan and Mahmassani 1999; Yanmaz-Tuzel and Ozbay 2009). This bound for lateness and earliness are different and people are usually more sensitive to lateness. In addition, commuters will not switch routes if the difference between perceived travel time and experienced one exceeds a bound (Akiva 1994).

Travel time perception updating

Jha et al. (1998) assumed that individuals update their travel time whenever new traffic information is obtained or new travel time is perceived. This assumption is unreasonable due to the existence of updating costs. Chen and Mahmassani (2004) and Jotisankasa and Polak (2006) proposed that only salient information impacts travelers. Travelers do not update travel time if the difference between the perceived travel time $\hat{C}_{nt}$ and the experienced travel time C_{nt} exceeds some threshold. Let y_{nt}^{time} denote a travel time update indicator for traveler n at the end of day t, which equals to 1 if traveler n updates travel time after day t, and 0 otherwise:

$$y_{nt}^{time} = \begin{cases} 0, \text{if } \hat{C}_{nt} - C_{nt} \leqslant \varepsilon_{nt}^{time,o}, C_{nt} - \hat{C}_{nt} \leqslant \varepsilon_{nt}^{time,u}, \\ 1, \text{o.w.} \end{cases} \tag{2.4.10}$$

where $\varepsilon_{nt}^{time,o}, \varepsilon_{nt}^{time,u}$ denote travel time overestimation and underestimation thresholds for user n on day t respectively. If ε_{nt}^{time} is treated as a fraction instead of an absolute value, then travel time updating only happens if $|\hat{C}_{nt} - C_{nt}| \leqslant \varepsilon_{nt}^{time}\hat{C}_{nt}$. In this case, overestimation and underestimation share the same fractional threshold.

If travel time is random, Chen and Mahmassani (2004) proposed another updating mechanism that a traveler would not update travel time perception until his confidence in all path travel times was below a desired level, i.e., $\alpha_{nt}^r \leqslant \frac{1}{\sigma_n \bar{C}_{nt}^r}, r \in \mathcal{P}$, where α_{nt}^r is traveler's confidence in path r's travel time, σ_n is the variance of the perceived travel time over a segment of unit travel time, and $\bar{C}_{nt}^r$ is the mean perceived travel time of path r.

Overestimation and underestimation thresholds are random variables depending on individual characteristics and trip features. Therefore they can be expressed as:

$$\epsilon_{nt}^{time,o} = V_o^{time}(X_n, Z_{nt}, \theta_{nt}) + \zeta_{nt}^{time,o}, \tag{2.4.11a}$$

$$\epsilon_{nt}^{time,u} = V_u^{time}(X_n, Z_{nt}, \theta_{nt}) + \zeta_{nt}^{time,u}. \tag{2.4.11b}$$

where,

$V_o^{time}(\cdot), V_u^{time}(\cdot)$: deterministic utility functions for overestimation and underestimation;

X_n: individual characteristics for traveler n;

Z_{nt}: trip features for traveler n on day t;

θ_{nt}: parameters for traveler n on day t;

ζ_{nt}: error terms for traveler n on day t, is either ζ_{nt}^o or ζ_{nt}^u.

The probability of updating can be calculated by a multinomial logit or a multinomial probit model. If the traveler decides to update travel time, there are three classes of models in travel time updating: weighted average (Nakayama et al. 2001), adaptive expectation (Nakayama et al. 2001) and Bayesian (Jha et al. 1998; Jotisankasa and Polak 2006). If myopic factor is considered, updating is reduced to $\hat{C}_{nt} = C_{n,t-1}$, i.e., the perceived travel time on day t is equal to the experienced travel time on day $t-1$.

Departure-time and route choice adaptation

After travel time is updated, drivers adjust their departure-time and route choices based on certain rules. There are two classes of research on modeling choice adaptation: the first one is based on utility maximization (Chen and Mahmassani 2004; Jotisankasa and Polak 2006) and the second one is based on bounded rationality. We will only focus on boundedly rational departure-time and route choice adaptation.

To study the impact of advanced travel information on people's behavior, Mahmassani and his colleagues conducted a series of experiments and showed that people were boundedly rational when choosing routes repeatedly with information. These experiments were run on an interactive simulator-DYNASMART, incorporating pre-trip departure time, route choices and en-route path switching decisions. Subjects, as travelers, picked departure time pre-trip based on the previous days' travel experiences and chose paths en-route at each node based on available information.

Let y_{nt}^{dep} denote a departure time switching indicator for traveler n on day t, which equals to 1 if traveler n switches departure time on day $t+1$, and 0 otherwise. Traveler n will not adjust his departure time unless the schedule delay (i.e., preferred arrival time minus actual arrival time) exceeds some threshold. Early and late arrivals have distinct indifference bands, denoted as $\varepsilon_{nt}^{dep,e}, \varepsilon_{nt}^{dep,l}$ respectively, representing tolerable schedule delay. Then,

$$y_{nt}^{dep} = \begin{cases} 0, \text{if } T_{nt}^{*} - T_{nt} \leqslant \varepsilon_{nt}^{dep,e}, T_{nt} - T_{nt}^{*} \leqslant \varepsilon_{nt}^{dep,l} \\ 1, \text{o.w..} \end{cases} \tag{2.4.12}$$

where T_{nt}^{*}, T_{nt} denote preferred arrival time and actual arrival time for traveler n on day t respectively.

Similarly, let y_{njt}^{route} denote a route switching indicator for traveler n at the intermediate junction node j on day t, which equals to 1 if traveler n switches his initial route or route en-route at node j after day t, and 0 otherwise. Travelers do not change pre-trip route or path en-route unless the trip time saving (the difference between predicted travel time of the current path and that of the best path from this node to destination) remains within his route indifference band:

$$y_{njt}^{route} = \begin{cases} 0, \text{if } C_{njt} - C_{njt}^{b} \leqslant \varepsilon_{njt}^{route} C_{njt}, \\ 1, \text{o.w.} \end{cases} \tag{2.4.13}$$

where,

C_{njt}, C_{njt}^{b}: the trip times of the chosen and the best path for traveler n from node j to destination on day t respectively;

$\varepsilon_{njt}^{route}$: the relative indifference band, as a fraction of C_{njt}.

The aforementioned indifference bands vary among the population over time and thus are random. They are influenced by individual characteristics (e.g., age, gender,

myopia) and real-time information.

When travel time is assumed to be random, Yanmaz-Tuzel and Ozbay (2009) applied another learning mechanism, stochastic learning automata (SLA), to study drivers' departure-time choice adaptation in response to a toll change on New Jersey Turnpike (NJTPK). Travelers have three options to depart for work: pre-peak, peak and post-peak. Each driver's departure time choice is assumed to be automated by a stochastic learning automaton which generates a sequence of actions based on drivers' past experiences and interactions with the environment. The driver will not update his or her departure time if the experienced utility falls within a confidence interval from that of the desired arrival time. Then the transition probability of the departure-time choice is updated based on a linear reward-penalty reinforcement learning scheme. Learning parameters introduced in the reinforcement scheme are estimated from drivers' departure time choices observed from NJTPK toll data. This model successfully mimics NJTPK users' day-to-day travel behavior.

Estimation of departure-time and route choices

There are two schemes of estimating departure time and route choices under real-time information: joint estimation based on joint probability and hierarchical estimation based on conditional probability.

When estimating joint decisions of departure time and routes under real-time information, y_{nt}^{dep} and y_{njt}^{route} are assumed to follow a multivariate normal distribution. Then the probability of switching both departure time and route is computed by a multinomial probit model.

Departure-time and route choices can be also estimated by a hierarchical model (Jha et al. 1998): the probability of selecting departure interval i and path j on day t by individual n is based on a conditional probability instead of a joint probability: $P_{nt}^{i,j} = P_{nt}^{i} \times P_{nt}^{j|i}$, where, P_{nt}^{i} is the probability of selecting departure interval i and $P_{nt}^{j|i}$ is the conditional probability of selecting route j given the traveler n has selected departure interval i. These two probabilities can be calculated by logit models respectively.

Given specifications for utility functions $V(\cdot)$, repeated observations of departure time and route switching decisions made by N Commuters over T days can be modeled as a multinomial logit or a multinomial probit function. The maximum likelihood

estimation is adopted to estimate parameters in utility functions.

2.5 Boundedly rational cognitive process

In static traffic assignment, the traditional 'perfect rationality'(PR) route choice paradigm (Wardrop 1952) makes three assumptions regarding human being's cognitive processes:

- Each traveler is able to enumerate all alternative paths connecting his origin-destination pair in a transportation network;
- Each traveler has access to information of all path costs;
- Each traveler is capable of picking the one with the least disutility.

The above assumptions are too restrictive in reality. First of all, due to the large size of available paths in real traffic networks and people's limited computational ability, it is impossible to identify all feasible paths connecting each origin-destination pair. Secondly, accessing information of all paths is unrealistic due to the following reasons: (a) No information provider can offer all path costs; (b) The costly information acquisition process prevents travelers from obtaining all information. In addition, there are many factors affecting path costs, such as travel time, travel distance, the number of traffic lights and turns, weather, scenery, and so on. Some of these factors cannot be directly measured from the field or are difficult to measure; (c) Human beings have limited cognitive capabilities and are unable to discern two alternatives with similar utilities, not mentioning finding the best routes in their minds.

In summary, a complicated cognitive process is involved in route choice. Though previous two categories of BR models can describe static and dynamic boundedly rational route choice behavior, the cognitive process leading to such behavior has not been fully explored.

2.5.1 A unifying framework for boundedly rational cognitive processes

Figure (2.3) summarizes four types of cognitive processes (mental map formation, route generation, information acquisition and alternative comparison) before making route

choices. These cognitive processes are indicated in rectangles and enclosed in a big box with dotted borders because they are unobservable. Individual's socioeconomic characteristics, available information and their route choices are indicated by solid parallelograms, representing observable inputs or outputs. Bounded rationality thresholds can be embedded into each process, represented by dotted hexagons. In this section, we will review how BR is modeled and estimated within each cognitive process.

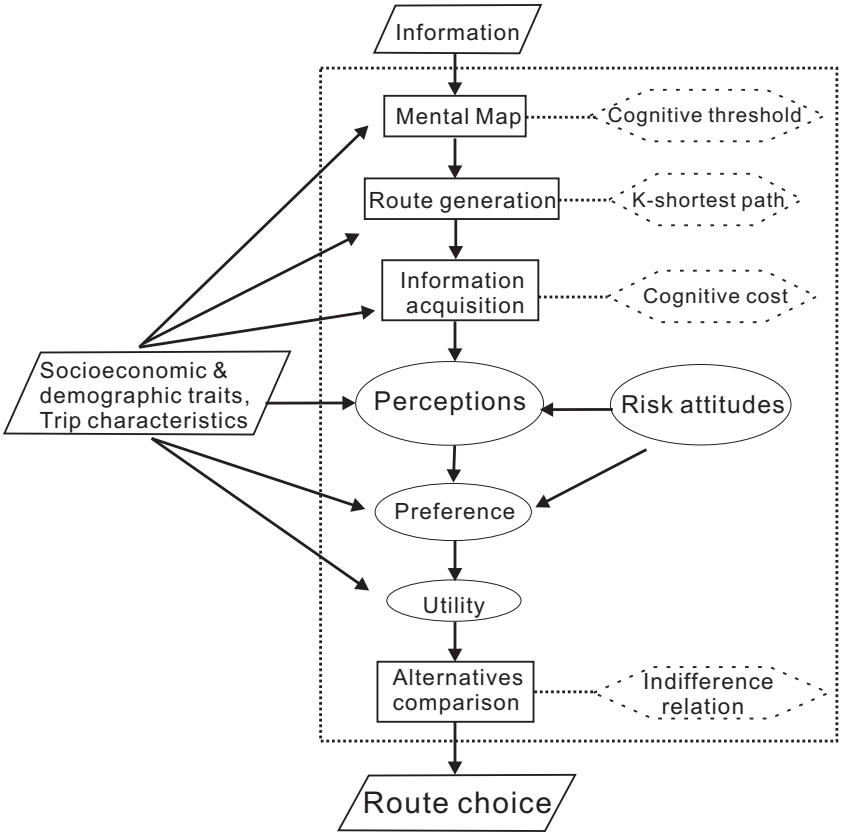

Figure 2.3: Boundedly rational cognitive processes with random utility

2.5.2 Boundedly rational network recognition and route generation

The route choice behavior process can be decomposed into three stages (Hato and Asakura 2000; Hiraoka et al. 2002; Ridwan 2004): network recognition; alternative generation and elimination; behavior decision. Bounded rationality is introduced into the first two stages. The model proposed by Hato and Asakura (2000) will be

mainly discussed.

At the first stage, each traveler has a perception value for each link. Perception value, denoted as Cog_n^{ij} for link ij, is a random variable depending on individual characteristics and link attributes. A link cannot be recognized unless its perception value exceeds a threshold ε_n. Mathematically, link ij can be recognized if $P(Cog_n^{ij} > \varepsilon_n) > 0.5$. A logit model can be used to identify the mental map in a traveler's mind.

At the second stage, routes are generated from the mental map based on some path generation algorithm, such as K-shortest path, labeling approach (Ben-Akiva et al. 1984), parametric least-generalized cost path algorithm (Mahmassani et al. 2005), doubly stochastic choice set generation (Bovy and Fiorenzo-Catalano 2007) or pareto paths generation (Wang et al. 2009). K-shortest path algorithm, widely used in path set generation, searches for the first K paths with the least path costs. This algorithm relaxes the requirement of obtaining the shortest paths and reduces computational burdens, which reflects the BR principle.

Given a path set, travelers extract attributes of each generated path. Each path has many attributes, but only partial attributes are evaluated. Assume each path attribute is attached with a reference value ε_k, which is a random error with i.i.d. Gumbel distribution. For example, the distance of the alternative path should be within 1.33 times the shortest distance and the number of left or right turns cannot exceed 5 times. Then those inferior paths are eliminated if the probability of one attribute V_k^r of path r exceeding ε_k, i.e., $P(V_k^r > \varepsilon_k) > 0.5$.

At the third stage, based on the extracted routes, the utility theory (Hato and Asakura 2000) or the inductive rule-based theory (Ridwan 2004) is assumed for route choice behavior and traffic assignment is conducted. Hato and Asakura (2000) showed that the chosen routes estimated by the BR model matched the stated preference survey better than the model with full network.

2.5.3 Path information search

When the BR principle is used to model travelers' route choice behavior, some researchers argued that travelers do not take the shortest paths because they are not capable of perceiving actual travel costs due to limited cognitive capacities, or it is too costly to search information over all alternative paths (Gao et al. 2011). Therefore,

Gao et al. (2011) proposed a cognitive cost model to capture people's route choices in complex contexts with costly information acquisition.

In cognitive cost model, the path travel time is assumed to be random. Before searching, travelers only know the mean and the variance. If they decide to search information, travelers will know the exact travel time of the searched path; however, search consumes cognitive cost. Therefore search action is the trade-off between travel benefit and cognitive cost. Accordingly, the probability of choosing path r given a choice set $\mathcal{P}_n$ for traveler n is mainly composed of two parts:

$$P(r|\mathcal{P}_n) = P(r|\mathcal{P}_n, \text{no search})P(\text{no search}) + P(r|\mathcal{P}_n, \text{search}). \tag{2.5.1}$$

If traveler n decides to search information, the probability of choosing path r given a choice set $\mathcal{P}_n$ is further decomposed into the sum of three parts:

$$P(r|\mathcal{P}_n, \text{search}) = \sum_s \sum_{t=1}^{T_n^s} P(r|t, \mathcal{P}_n, H_n^s)P(t|H_n^s)P(H_n^s), \tag{2.5.2}$$

where,
$P(H_n^s)$: the probability of individual n belonging to search class s;
$P(t|H_n^s)$: the probability of searching path information till stage t given class H_n^s;
$P(r|t, \mathcal{P}_n, H_n^s)$: the probability of choosing path r given information is searched till stage t. Logit models are used to calculate all three probabilities.

In the following, we will mainly introduce the methodology of computing $P(t|H_n^s)$, because it involves cognitive process modeling. To reflect that a traveler chooses a satisfying route due to information availability, cognitive constraints and time limit, Gao et al. (2011) adapted a directed cognition model (Gabaix et al. 2006) proposed in economics.

Let $\mu_{nt}^{rs}, \sigma_{nt}^{rs}$ be mean and standard deviation of path travel cost r for individual n from class s at stage t respectively. They are random variables at stage t when search is conducted till $t-1$. At stage t, traveler n decides to continue search or stop. To compute $P(t|H_n^s)$, the utilities associated with these two actions are defined as:

$$V(\text{go at } t|H_n^s) = \theta_{cost}^s + \theta_{benefit}^s B_{nt}^s(go),$$
$$V(\text{stop at } t|H_n^s) = \theta_{benefit}^s B_{nt}^s(stop),$$

where,

$B^s_{nt}(go)$: the expected maximum benefit of searching at stage t, computed in Equation (2.5.4a);

$B^s_{nt}(stop)$: the benefit of stopping search at stage t, computed in Equation (2.5.4b);

$\theta^s_{cost}, \theta^s_{benefit}$: cost and benefit coefficients, which need to be estimated.

If search stops at stage t, there is no search cost and thus $V(\text{stop at } t|H^s_n)$ does not contain the term θ^s_{cost}. On the other hand, when search is conducted, a higher benefit will be obtained. $B^s_{nt}(go)$ and $B^s_{nt}(stop)$ are defined as follows:

$$B^s_{nt}(go) = \int_{\mu^{rs}_{nt},\sigma^{rs}_{nt}} \ln \sum_{r\in\mathcal{P}_n} \exp\left[V^{rs}_{nt}(\mu^{rs}_{nt},\sigma^{rs}_{nt})\right] f(\mu^{rs}_{nt},\sigma^{rs}_{nt}) d\mu^{rs}_{nt} d\sigma^{rs}_{nt}, \tag{2.5.4a}$$

$$B^s_{nt}(stop) = \ln \sum_{r\in\mathcal{P}_n} \exp\left(V^{rs}_{n,t-1}\right), \tag{2.5.4b}$$

where,

$V^{rs}_{nt}(\mu^{rs}_{nt},\sigma^{rs}_{nt})$: the utility of choosing path r for individual n from class s at stage t, which is a linear function of travel time's mean and standard deviation;

$f(\mu^{rs}_{nt},\sigma^{rs}_{nt})$: the joint distribution of path travel time means and standard deviations given the search operation.

Gao et al. (2011) estimated route choice parameters from simulated revealed preference data among three alternative routes from home to workplace. The estimation results showed that a model with information acquisition gave more accurate parameter estimates than those without.

2.5.4 Minimum perceivable difference model

Most discrete choice models assume implicitly the existence of a preferable ordering over alternatives even if the difference in utilities is negligible. Psychological experiments (Guilford 1954) showed that people may be indifferent to two alternatives with similar utilities.

Ridwan (2004) defined three fuzzy preference relations for two alternatives: strict preference; indifference; incomparability. A fuzzy choice function was proposed capturing the fuzziness feature of choices to calculate their rankings. Krishnan (1977) proposed a minimum perceivable difference (MPD) model describing travelers' mode

choices among two alternatives with two relations: strict preference and indifference. Denote U_i as the utility of alternative $A_i, i = 1, 2$. It can be expressed as the sum of a deterministic component V_i and a random component e_i: $U_i = V_i + e_i$. Denote ε as an indifference threshold. The ordering over two alternatives and its associated probability can be defined as follows:

1. $A_1 \succ A_2$ if $U_1 > U_2 + \varepsilon$, A_1 will be chosen with probability 1;
2. $A_2 \succ A_1$ if $U_2 > U_1 + \varepsilon$, A_2 will be chosen with probability 1;
3. $A_1 \sim A_2$ if $|U_1 - U_2| \leqslant \varepsilon$, A_1 and A_2 will be chosen with probability θ and $1 - \theta$ respectively.

Denote the probability of preferring A_1 and A_2 as π_1 and π_2 respectively, and the probability of being indifferent to A_1 and A_2 by π_{12}. Given the distribution of e_1 and e_2, the above preferring probability can be computed based on utility maximization. The probabilities of choosing A_1 and A_2 are:

$$\begin{aligned} P(A_1) &= \pi_1 + \theta\pi_{12}, \\ P(A_2) &= \pi_2 + (1-\theta)\pi_{12}. \end{aligned}$$

where θ is the probability of choosing A_1 given A_1 and A_2 have the indifference relation.

Given choices made by N individuals, the likelihood function is: $L = \prod_{n=1}^{N} P(A_1^{(n)})P(A_2^{(n)})$. The maximum likelihood method is used to estimate parameters as follows:

$$\begin{aligned} \min \quad & -log(L) \\ s.t. \quad & \varepsilon \geqslant 0, && \text{(2.5.5a)} \\ & 0 \leqslant \theta \leqslant 1. && \text{(2.5.5b)} \end{aligned}$$

The estimated threshold ε is the by-product of the above program. The shortcoming of the model is that only two alternatives are considered and it becomes complicated or impossible to implement when multiple alternatives are involved.

Chapter 3

Empirical analysis of boundedly rational route choice behavior

3.1 Introduction

The I-35W Mississippi River bridge plays a critical role in transporting commuters to downtown Minneapolis and the University of Minnesota. Its collapse in 2007 forced 140,000 daily users (Guo and Liu 2011; Zhu et al. 2010) to switch to other parallel bridges or to cancel their trips. Accordingly, the I-94 Bridge was restriped with one more lane to relieve traffic pressure across the river. A year later, a replacement I-35W bridge was rebuilt over the same location and the extra lanes on I-94 were closed. The addition of the bridge offered commuters another option to cross the river. Surprisingly, only 100,000 daily trips on average were observed on the new bridge (He and Liu 2012; Zhu 2011). According to Zhu (2011), the total travel demand in the Minneapolis-St. Paul metropolitan area dropped slightly in 2008 due to the economic crisis, but not enough to explain this fall-off. In contrast, daily trips on the I-94 Bridge returned to the original level before the I-35W bridge collapsed. Therefore, we assume that variation in travel demands is not the main reason for the significant traffic reduction on the replacement bridge.

To further understand the aforementioned phenomenon, two major GPS-based studies, including 143 commuters whose route choices might be affected by the addition of the new link were conducted (Carrion and Levinson 2012; Zhu 2011; Zhu and Levinson

2012). These commuters' trips were tracked by GPS two to three weeks before and eight to ten weeks after the reopening of the new I-35W bridge. Each commuter's day-to-day commuting routes and associated travel time could be drawn from GPS data. By comparing route choices before and after the new bridge was rebuilt, it is posited that commuters' "stickiness of driving habit" Zhu (2011) prevented them from taking the new bridge and thus resulted in a traffic flow drop on the new bridge. There may also be perception errors at work. Moreover, Zhu (2011) further calculated travel time differences between the routes actually taken and the shortest time routes from GPS data. Fewer than 40% of commuters took the shortest paths, though 90% of subjects took routes which were within 5 minutes of the shortest paths and almost no commuter chose a route 20 minutes longer than the shortest path.

Utilizing the same GPS dataset, Carrion and Levinson (2012) modeled the time a commuter consistently left his current bridge choice for other alternative bridges and found that commuters chose routes based on a specific threshold and might abandon a route if its travel time exceeded the margin. This threshold depended on the social-demographics of subjects and varied day-to-day.

Previous studies focused on estimating indifference bands from laboratory experiment data. For example, Mahmassani and Chang (1987) estimated indifference bands by utilizing laboratory experiment data. By comparing commuter departure time and route choice switch behavior in laboratory experiments with field surveys in Dallas and Austin, Texas, Mahmassani and Jou (2000) showed that boundedly rational route choice modeling observed from experiments provided a valid description of actual commuter daily behavior. However, whether laboratory experimental experiences can represent actual commuter daily behavior still remains unclear.

Other studies incorporated given values of the thresholds into their route choice models, such as 20% of the mean travel time or 0.5 times the mean travel time of certain previous trips (Carrion and Levinson 2012; Yanmaz-Tuzel and Ozbay 2009; Zhu and Levinson 2012). These thresholds were obtained from experience or assumptions and served as inputs of specific route choice behavior models. Therefore the adoption of a given value may not be valid.

People do not choose routes irrationally. Yet, the empirical evidence argues that travelers do not always select the shortest travel time paths, but the chosen routes are

within some threshold from the shortest ones. This chapter examines the phenomenon of boundedly rational route choice behavior with GPS travel data collected in Minneapolis in 2008 (Carrion and Levinson 2012; Zhu 2011; Zhu and Levinson 2012). The disruption and the rebuilding of the I-35W bridge in Minneapolis provides us a rare opportunity to use GPS travel survey data to study route choices in response to the change in road network's topology. This study offers the first empirical estimation of bounded rationality parameters from GPS data.

The rest of the chapter is organized as follows: The next Section focuses on the theoretical background of route choice. In Section 3.3, we discuss the details of the GPS data and present two categories of commuters of interest. Trip distribution among bridges over the Mississippi River is also presented. In Section 3.4, travel time saving by taking the new I-35W bridge is calculated based on a speed map pooled from GPS commuting trips. In Section 3.5, the boundedly rational route choice model is presented and we will show that subjects who used the old I-35W bridge display different behavioral patterns compared to those who never used the old bridge. Accordingly, in Section 3.6, indifference bands for old-users and non-users are estimated separately using GPS travel survey data.

3.2 Theoretical Background

3.2.1 Boundedly rational route choice behavior

In practice, most transportation planning software packages employ route choice algorithms based on Wardrop's first principle Wardrop (1952) that people take the shortest path(s) when traffic assignment is performed. In the academic literature, route choice is often considered within the framework of random utility maximization (RUM), each driver is assumed to take the route with the maximum utility among a set of finite paths. Each path is attached with several attributes, including travel time, distance, overlap with other paths, reliability, the number of traffic lights and turns, weather, scenery and so on. Provided perception errors are Gumbel or normal distribution, stochastic user equilibrium model can be expressed in the form of a multinomial logit or probit model.

One critique of both Wardrop's first principle and RUM is the assumption that people are "utility maximizers" (where utility is either travel time (Wardrop) or a bundle

of factors including travel time (RUM)). Alternative hypotheses that are empirically based posit that people actually make decisions by strategies (Simon 1982), heuristics (Conlisk 1996), elimination by aspects (Tversky 1972), norms (Conlisk 1996) and/or rules (Nakayama et al. 2001; Lotan 1997), rather than solving an optimization.

Therefore people do not always choose the alternative with the maximum utility. Evidence from revealed route choice behavior finds after evaluating habitual routes, only 59% of respondents from Cambridge, Massachusetts (Bekhor et al. 2006), 30% from Boston (Ramming 2001), and 86.8% from Turin, Italy (Prato and Bekhor 2006) chose paths with the shortest distance or shortest travel time. According to GPS studies, 90% of subjects in the Minneapolis-St. Paul region took paths one-fifth longer than average commute time (Zhu 2011) and a high percentage of commuting routes were found to differ considerably from the shortest paths in Nagoya, Japan (Morikawa et al. 2005) and Lexington, Kentucky (Jan et al. 2000). All findings above revealed that people do not usually take the shortest paths and the utilized paths generally have higher costs than shortest ones.

To relax the unrealistic assumption that only the shortest paths are used, several route choice behavior models were proposed (Zhang 2011). This chapter examines one alternative of the existing route choice behavior theories, i.e., bounded rationality. It says that people do not always select the shortest paths, but the chosen routes are within some threshold from the shortest ones.

As opposed to 'rationality as optimization', Herbert Simon, in 1957, proposed that people are boundedly rational in their decision-making processes (Simon 1957). This is either because people lack accurate information, or they are incapable of obtaining an optimized decision due to complexity of the situation. They tend to seek a satisfactory choice solution instead. Since then, bounded rationality has been studied extensively in economics and psychology. Bounded rationality in decision-making may also result from habit and inertia. People "place higher value on an opportunity if it is associated with the status quo" (Samuelson and Zeckhauser 1988), because it can provide significant energy saving to cognitive thinking. A large amount of empirical evidence finds that habit plays a significant role in behavior in stable situations (Bamberg and Schmidt 2003).

In travel behavior study, a series of experiments was conducted in the 1990s to empirically validate bounded rationality (Hu and Mahmassani 1997; Jayakrishnan et al. 1994a; Mahmassani and Chang 1987; Mahmassani and Jayakrishnan 1991; Mahmassani and Liu 1999; Srinivasan and Mahmassani 1999). These experiments were run on an interactive simulator – DYNASMART, incorporating pre-trip departure time, route choices and en-route path switching decisions. Subjects, as travelers, picked departure time pre-trip based on previous days' travel experiences and chose paths en-route at each node based on available information. The experimental results showed that, in the repeated learning process, as a result of habit, commuters would not adjust their departure time unless the difference between preferred arrival time and actual arrival time exceeded a bound (Chen and Mahmassani 2004; Hu and Mahmassani 1997; Jayakrishnan et al. 1994a; Mahmassani and Chang 1987; Mahmassani and Jayakrishnan 1991; Mahmassani and Liu 1999; Srinivasan and Mahmassani 1999). This bound for lateness and earliness differed and people were usually more sensitive to lateness.

Bounded rationality was also found in mode choices. Cantillo et al. (2006, 2007) indicated that there existed a threshold when the impact of the transportation planning policy change was evaluated on choice behavior. Travelers would not switch to a new mode unless its utility was greater than that of the current mode plus a threshold, which was a function of the difference between two experienced mode utilities. Then a discrete choice model with thresholds was applied to simulated SP/RP datasets to estimate and predict mode choice. The prediction results showed that a model without considering inertia overestimated benefits of transport investments substantially.

3.2.2 Threshold stimulus-response models

The existence of a threshold in choice behavior has also long been explored in other fields and the model describing this behavior is called "threshold stimulus-response" model. The stimulus-response model, popular in biology, psychology and economics, provides an efficient method of quantifying behavioral response by varying stimulus of specific intensities.

Biologists are interested in dose-response, which explores the impact of toxic levels on an organ or a tissue. In psychology and economics, stimulus-response studies focus

on the change in decision-makers' preferences or choices in response to the change in utilities of alternatives. The occurrence of a response depended on the intensity of a stimulus and there existed a threshold under which no response was manifest (Cox 1987; Krishnan 1977). This threshold was named "just noticeable difference" by Weber or "minimum perceivable difference" by Krishnan (1977).

When the response is qualitative, such as dose quantity, Weber's law revealed that the response intensity is proportional to the logarithm of the stimulus. If the response is discrete, such as choices or preferences, several biological experiments (Clark 1933; Hemmingsen 1933) verified that no response occurred unless the logarithm of stimulus exceeded some threshold. Several models, such as the threshold dose-response models (Cox 1987), minimum perceivable difference model (Krishnan 1977), and biological probit or logit model (Krishnan 1977), were proposed to estimate the threshold. These models will be briefly discussed subsequently.

- Dose-response models (Cox 1987) assumed that the probability of response is zero if the amount of dosage is below a threshold parameter and follows logit or probit model if it is more than the threshold. Cox (1987) showed that the threshold model fit data better than traditional logit or probit model.

- The minimum perceivable difference model (Krishnan 1977) assumed indifference between two alternatives if the difference of their values falls within a threshold. Therefore, a third relation (i.e., indifference) other than 'greater than' or 'less than' was introduced. The threshold parameter was estimated via maximum likelihood method.

- In the biological probit or logit model (Krishnan 1977), the threshold is assumed to be a random variable with normal or logistic distribution and therefore a probit or a logit regression can be used to estimate distribution related parameters. The biological probit model was shown to predict responses more accurately than the logit model.

This chapter employs threshold stimulus-response framework to model route choice behavior and estimate associated thresholds.

3.3 Route choice observations

GPS studies (Zhu 2011) provide the following data for 143 subjects:

- Each subject's home and work locations;
- Each subject's day-to-day commuting routes;
- Each subject's day-to-day travel time.

Most subjects use more than one path and switch routes from time to time. Therefore we define a "commonly chosen route" as the route a commuter uses most frequently during the study period. The commonly chosen route from the beginning of the study period up to September 18, 2008 (the day when the replacement I-35W bridge was opened) is the "before-route", and the one from September 18, 2008 until the end of the study is the "after-route".

Remark.

1. The same routes are defined as the ones which overlap at least 95% in length and start within a 600 m (approximately 4 city blocks) radius from home and end in a 600 m radius from the work location.

2. For each commuter, his or her experienced travel time on a path varies from day to day due to uncertainty in traffic conditions. Therefore "average travel time" on a before-route or on an after-route for a commuter is computed as the mean of day-to-day GPS measured travel time on that route when he or she uses it.

3.3.1 Subject classification

A "crosser" is the commuter whose home and work locations are on different sides of the river. Specifically, a crosser's commuting route options may be enlarged by the addition of the new bridge. Otherwise the subject is a "non-crosser". In general a non-crosser's route options are not enlarged by the existence of the new bridge. (Note: some individuals, nominally non-crossers, but in fact "double-crossers", may have crossed the river twice on certain routes from home to work, those individuals have been removed from the analysis, as the sample size was too small. ("Triple-crossers" etc. were not observed.))

The addition of the new bridge may or may not save crossers' average travel time. Denote $C_b^{(n)}, C_a^{(n)}$ as average travel times experienced by commuter n before and after the reopening of the new bridge. When the average travel time on the after-route minus that on the before-route is less than zero, i.e., $C_a^{(n)} - C_b^{(n)} < 0$, we say that the addition of the new bridge saves commuter n's travel time, or else it does not.

Table (3.1) shows the number of crossers and non-crossers. The "Change" column refers to those commuters who change their routes after the addition of the bridge, i.e., their before-routes and after-routes are different. Or else they belong to the "No change" column. The "Save time" row refers to those whose average travel time on after-routes is shorter than that on before-routes.

Table 3.1: Statistics of crossers and non-crossers

Type		Change	No change	Total (excluding missing data)	Subjects with incomplete observations	Total (including missing data)
		C1	C2	C3=C1+C2	C4	C5=C3+C4
Non-crosser	Save time	5	16	21	0	30
	Save no time	0	9	9		
Crosser	Save time	47	31	78	19	113
	Save no time	2	14	16		
Total		54	70	124	19	143

Remark. There are 19 crossers whose route choice observations before the addition of the bridge were missing, therefore they are classified as "Subjects with incomplete observations" in column $C4$.

When the addition of the new bridge saves crossers' commuting time, a crosser chooses either to change to the new bridge or not. Thus we further divide those crossers into the following two categories:

- A "Switcher" is a crosser who switches to the new I-35W bridge as his or her after-route given his or her travel time can be shortened by the new bridge;
- A "Stayer" is a crosser whose travel time can be improved by the new bridge but stays on his or her before-route, i.e., the before-route and the after-route are the same.

Figure (3.1) illustrates examples of a non-crosser, a switcher, a stayer and a crosser with no time saving. The I-35W bridge is indicted by the purple line. In Figure (3.1a), the non-crosser's before-route and after-route are the same because he does not need to cross the river and thus his route is not influenced by the new bridge. In Figure (3.1b-3.1c), the switcher uses two different routes before the bridge was rebuilt and after, while the stayer uses the same route which is not via the I-35W bridge. In Figure (**??**), taking the new bridge cannot improve the crosser's travel time, so he stays on the same route.

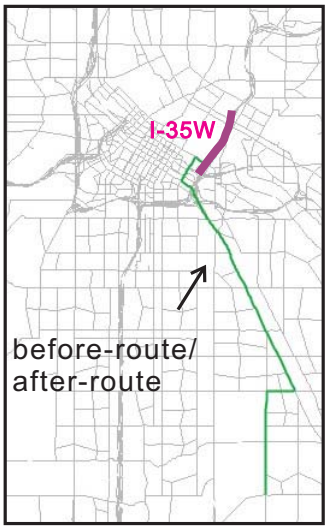

(a) Non-crosser

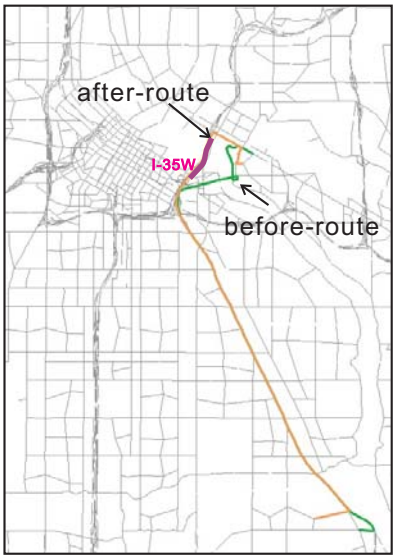

(b) Switcher

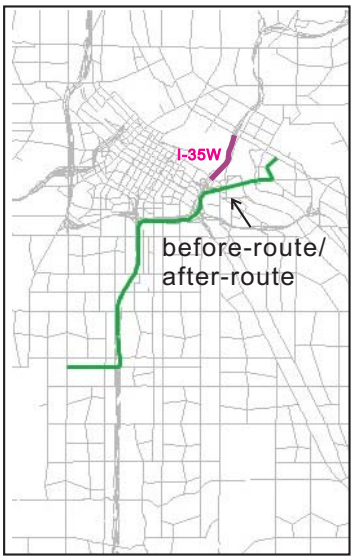

(c) Stayer

Figure 3.1: Examples of subjects

In this study, only 47 switchers and 31 stayers are considered. So there are 78 subjects of interest.

3.3.2 Bridge usage analysis for switchers and stayers

Figure (3.2) shows eleven bridges, indicated by red with names next to them, used by subjects across the Mississippi River before and after the new bridge's reopening. The background is the TLG network (generated and maintained by Metropolitan Council and The Lawrence Group) which encompasses the entire seven-county Minneapolis-St. Paul Metropolitan Area.

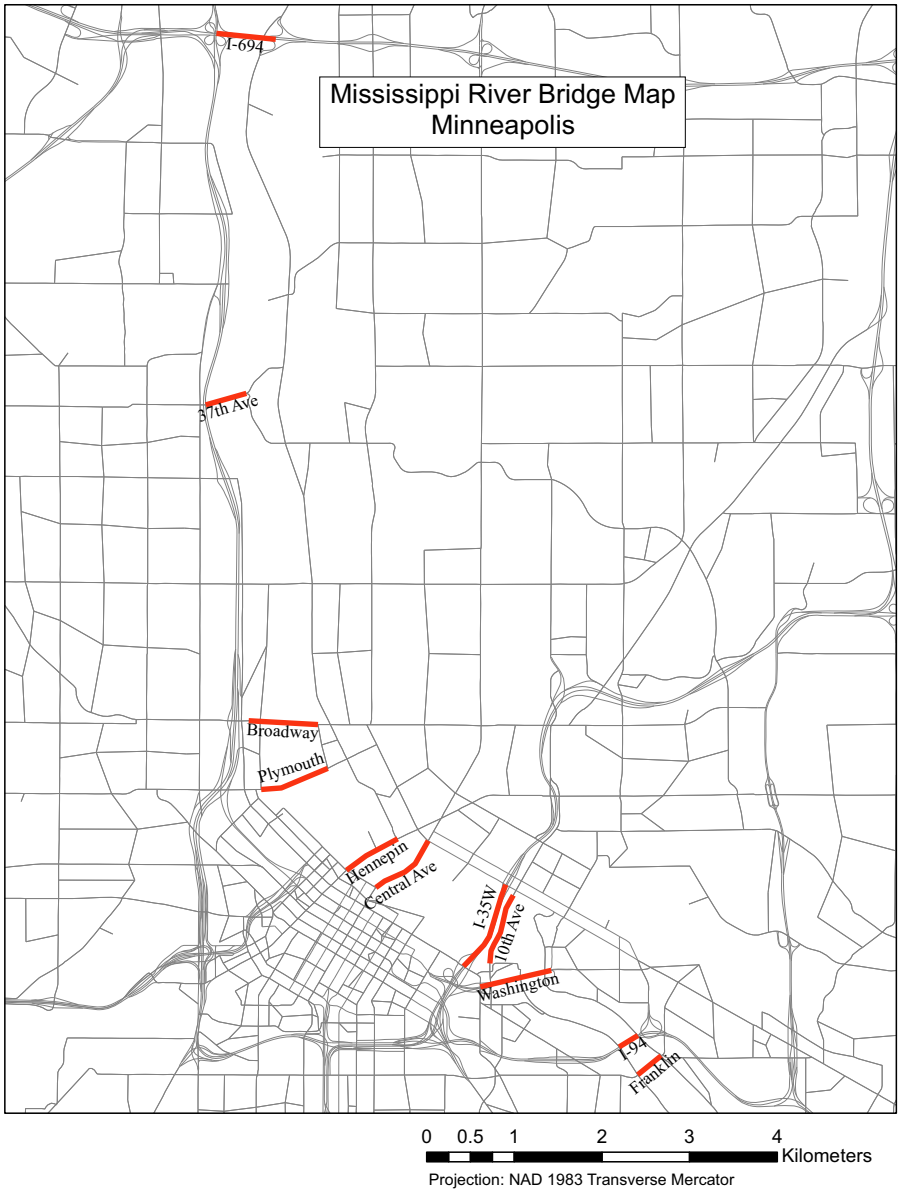

Figure 3.2: Bridges over the Mississippi River

Seventy-eight subjects made 2,167 morning commuting trips during the study period. Most subjects use more than one bridge to cross the river. The bridge used by the most trips is the "most frequently used bridge".

Figure (3.3) illustrates trip distribution among bridges. Before the new bridge was

built, Washington, 10th Avenue and I-94 are the three most used bridges in the sample. After its reopening, the I-35W bridge is the main bridge carrying 64% of observed cross-river trips in the sample.

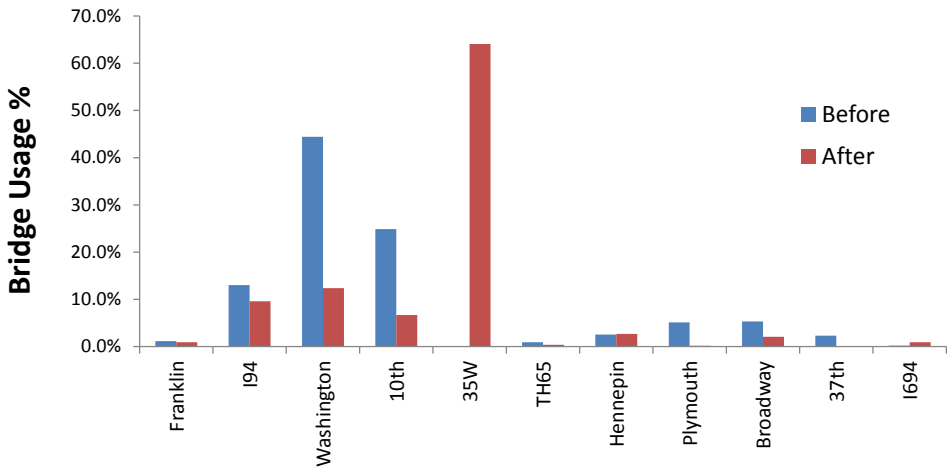

Figure 3.3: Cross-river trip distribution among bridges for study subjects

For 47 switchers, we further calculate the percentage of switchers who changed from their frequently used bridges to the I-35W bridge. Switchers originally on the 10th Avenue Bridge provide the highest portion of switching to the I-35W bridge and those originally on the Washington Ave Bridge follows. This is reasonable because the 10th Avenue Bridge and the Washington Ave Bridge are the nearest to the I-35W bridge.

We also compute the duration it took subjects to settle on a bridge after the reopening, i.e., from September 18, 2008 until the day when the subject have been taking the *most frequently used bridge* for at least two times consecutively (Carrion and Levinson 2012). Zero day for switchers means they immediately use the new bridge on September 18, 2008; while zero day for stayers means they stick to their before-routes regardless of the addition of the bridge. On average, it took 3.0 days for 78 subjects to stabilize their bridge choices. The number of days for switchers to stabilize is slightly longer than that for stayers and it has larger variation. Interested readers can refer to Carrion and Levinson (2012) which employed duration analysis to analyze how many days it took commuters to use the current bridge choice.

Table 3.2: Descriptive statistics of duration of bridge stabilization

	Mean	Std	Median	Min	Max
Switcher	3.2	6.0	0	0	27
Stayer	2.7	5.7	0	0	20
Total	3.0	5.8	0	0	27

3.4 Travel time saving calculation

In this study, we assume that travel time saving is the only stimulus for commuters to switch to the new bridge disregard of travel time reliability and other factors.

To obtain the travel time savings brought by taking the new I-35W bridge, we need to identify routes via the new bridge. For switchers, the after-route is the route via the new bridge. Stayers, on the other hand, never use the new bridge and therefore a route via I-35W bridge for each stayer should be first identified.

The speed map was pooled from $6,059$ commuting trips out of $25,157$ total trips. Only links with more than 5 observations before and after the new bridge's reopening were included. The average link speed was estimated from GPS data of all probe vehicles passing this link during the experiment period. This map covers a high portion of the freeway system and a fairly high portion of arterial roads, especially trunk highways and downtown streets.

Based on the speed map, each link's average travel time can be computed. Then estimated travel times of a route is the sum of average travel times of all links along that route. Consequently, the shortest paths via I-35W bridge is identified for stayers, named "new-after-route". Provided a new-after-route, the travel time saving for each stayer can be estimated from the speed map.

Remark. Subjects' commuting times are not the same, to make sure the following comparison is performed under the same benchmark, travel time saving proportion instead of absolute travel time saving will be used. Denote $\triangle^{(n)}$ as the travel time saving proportion by taking the new bridge for commuter n. It is computed as $\triangle^{(n)}= \frac{C_a^{(n)}-C_b^{(n)}}{C_b^{(n)}}$,

where $C_b^{(n)}, C_a^{(n)}$ are estimated travel times experienced by commuter n before and after the reopening of the new bridge.

Table (3.3) summarizes the statistics of estimated travel time saving by using the new bridge among switchers and stayers:

Table 3.3: Estimated time saving statistics

Statistics		Switcher	Stayer	Total
Distribution	Counts	47	31	78
	Percentage (%)	60.3	39.7	100.0
Average Travel Time (minute)	Before	16.4	19.2	17.5
	After	14.5	18.2	16.0
	Difference	1.9	1.0	1.5
Average Travel Time Saving Percentage (%)	Average	13.0	5.4	10.0
	Minimum	2.6	0.4	0.4
	Maximum	34.4	25.2	34.4
	Median	10.5	3.5	7.9

3.5 Route switching analysis

3.5.1 Old-users and non-users

Subjects have different time saving by taking the new bridge which varies from 2.6% to 34.4% for switchers and from 0.4% to 25.2% for stayers. This wide range of time saving overlap between switchers and stayers results partially from drivers' heterogeneity.

Among 78 subjects, 44 used the old I-35W bridge regularly before it collapsed and 34 were not the regular old bridge users. Old bridge users are pre-disposed to use the new bridge while non-users may not use it even it could save substantial travel time. Therefore, old-users and non-users should display different route choice behavior in response to the addition of the new bridge.

In the following, we will further divide switchers and stayers based on whether they are "old-users" or "non-users". Denote y as the indicator of stayer (i.e., $y = 0$) or

switcher (i.e., $y = 1$) and U as the indicator of non-user (i.e., $U = 0$) or old-user (i.e., $U = 1$). The frequency of stayers and switchers for non-users and old-users are summarized in Table (3.4).

Table 3.4: Contingency table of subjects' categories

	Non-user (U=0)	Old-user (U=1)	Total
Stayer (y=0)	23	8	31
Switcher (y=1)	11	36	47
Total	34	44	78

Figure (3.4) illustrates the boxplot of estimated time saving proportion statistics for two groups (non-user and old-user). The dots are data which are outside third quartile and represent outliers. Overall the mean and the median travel time savings for switchers are higher than those of stayers. The mean travel time savings for non-users are slightly higher than those for old-users.

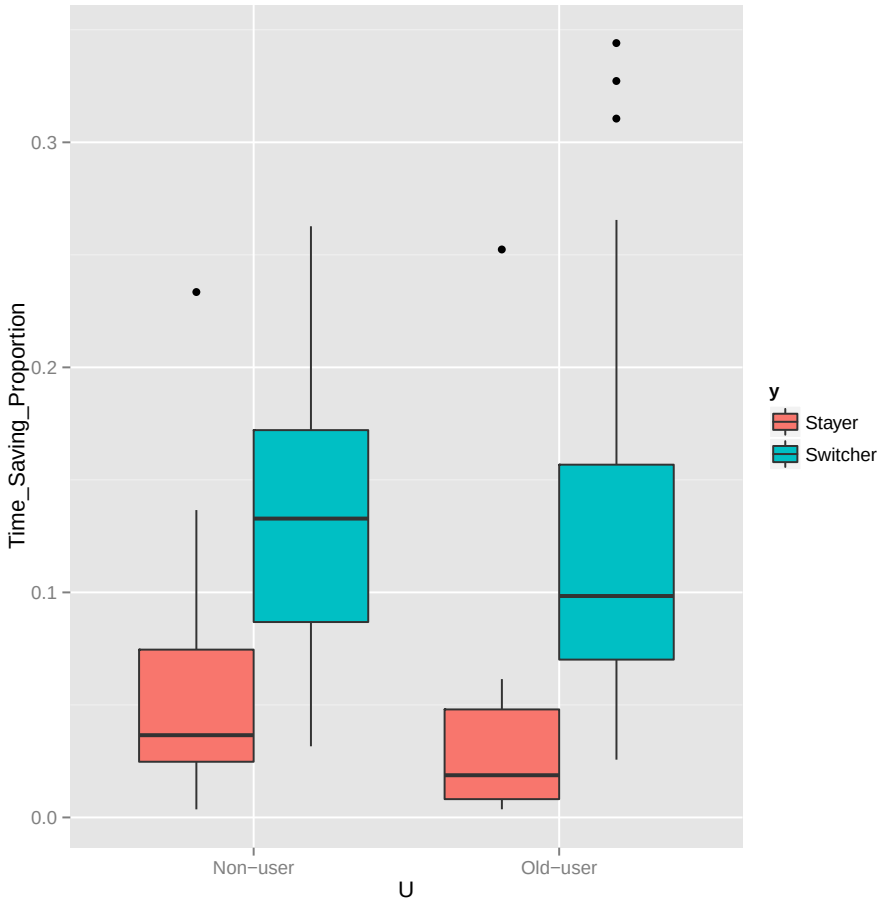

Figure 3.4: Boxplot of travel time saving proportions

3.5.2 Factors contributing to route switching

The path set for traveler $n, n = 1, \cdots, 78$ on day t before addition of the I-35W bridge is $\mathcal{P}_{nt}$. The chosen route for traveler n at time t is denoted as $A_{nt} = r$. Assume at time $t + 1$, the I-35W bridge was rebuilt. The new route due to addition of the I-35W bridge is r'_{nt}. Accordingly, the new path set enlarged by addition of the I-35W bridge is $\tilde{\mathcal{P}}_{nt} = \{\mathcal{P}, r'_{nt}\}$. Therefore, the probability of switching to the new route and the

probability of staying on the current route are computed respectively as follows:

$$P(y^{(n)} = 1) = P(A_{n,t+1} = r'_{nt} | A_{nt} = r_{nt}, U_n), \tag{3.5.1a}$$

$$P(y^{(n)} = 0) = P(A_{n,t+1} = r_{nt} | A_{nt} = r_{nt}, U_n). \tag{3.5.1b}$$

where $U_n = 1$ represents that commuter n is an old-user.

$P(A_{n,t+1} = r'_{nt} | A_{nt} = r_{nt}, U_n)$ depends on the time saving by taking the new route r'_{nt} and whether commuter n has used this bridge before. Assume the log ratio of switching over staying is a linear function of time saving and commuter's group, thus a logit model is formulated:

$$\log \frac{P(y^{(n)} = 1)}{P(y^{(n)} = 0)} = \beta_0 + \beta_1 * \log(\triangle^{(n)}) + \beta_2 U_n, \tag{3.5.2}$$

where $\beta_0, \beta_1, \beta_2$ are regression coefficients and need to be estimated from the data. We use logarithm of time saving proportions here because time saving percentage varies between 0% and 100% and rescaling will facilitate parameter estimation.

Given 78 subjects' choices of switching or staying along with their characteristics, we have $\{y_1, \cdots, y_{78}\}$ and the predictors are $\log(\triangle^{(n)}), n = 1, \cdots, 78$ and $U_n, n = 1, \cdots, 78$. The likelihood function is: $L = \prod_{n=1}^{78} P(y^{(n)} = 1) P(y^{(n)} = 0)$. The maximum likelihood method (i.e., logit regression) is conducted to estimate parameters β_0, β_1 and results are as follows:

	Estimate	Std. Error	t-value	Pr($>\|t\|$)
(Intercept)	4.15	1.27	3.27	0.001 **
$\log(\triangle)$	1.85	0.48	3.828	0.000 ***
U	2.73	0.73	3.74	0.000 ***

** Statistically significant at .5% level

*** Statistically significant at .1% level

All three parameters are significantly different from zero at 0.5% significance level. The goodness-of-fit measure by using Chi Square test gives p-value of $1.9e-5$.

$\beta_1 = 1.85$ indicates that the log ratio of switching versus staying, i.e., $\log\left(\frac{P(y=1)}{P(y=0)}\right)$, increases by 1.85 if there is one unit increase in the logarithm of time saving brought by a new route. $\beta_2 = 2.73$ indicates that the log ratio of switching versus staying for an old-user is 2.73 times higher than that for a non-user.

Given a certain time saving, old-users have higher probability of switching than non-users. Therefore these two groups display different route switching characteristics in response to the addition of a new link.

3.6 Indifference band estimation

When the network topology remains the same for a long enough period of time, the traffic flow pattern stabilizes and therefore travelers' route choice decisions are usually stable (Zhu and Levinson 2012), implying that they do not switch. Major network disruptions force travelers to search for new routes. Network restorations allow travelers to stay on the old route or switch to new routes, without any requirement they change.

Several assumptions are made regarding boundedly rational route switching in this analysis:

- The network stabilized at an equilibrium before the new bridge was rebuilt;
- A commuter will decide to switch to the new bridge based on the principle of bounded rationality.
- A new equilibrium is reached at the end of our GPS study period.

For old-users and non-users, subjects have different time saving ranges by taking the new bridge. We divide this time saving range into $I = 11$ bins ($i = 1, \cdots, 11$) respectively. The total number of switchers and stayers for each bin can be calculated. Figure (3.5) illustrates the distribution of switchers and stayers for each bin for old-users. Figure (3.5a) show the frequencies within each bin. As the time saving increases, generally speaking, the percentage of stayers gradually decreases to zero (with only one outlier). Similar analysis can be applied to non-users shown in Figure (3.5b).

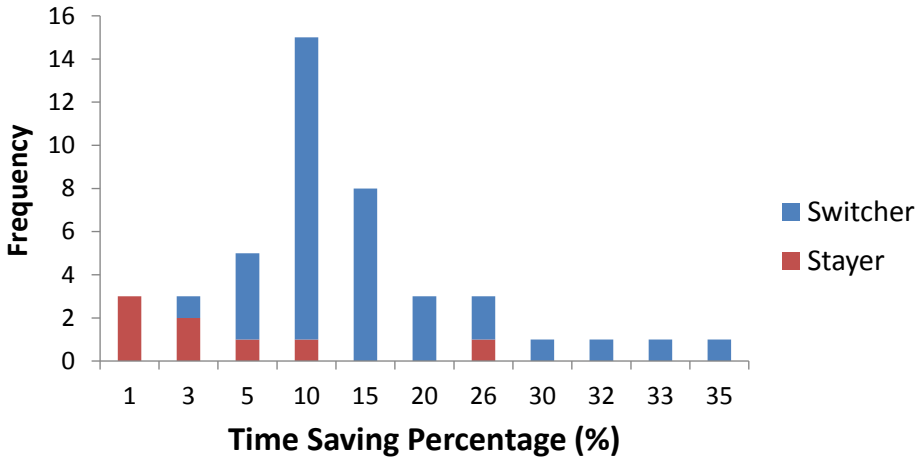

(a) Old-users

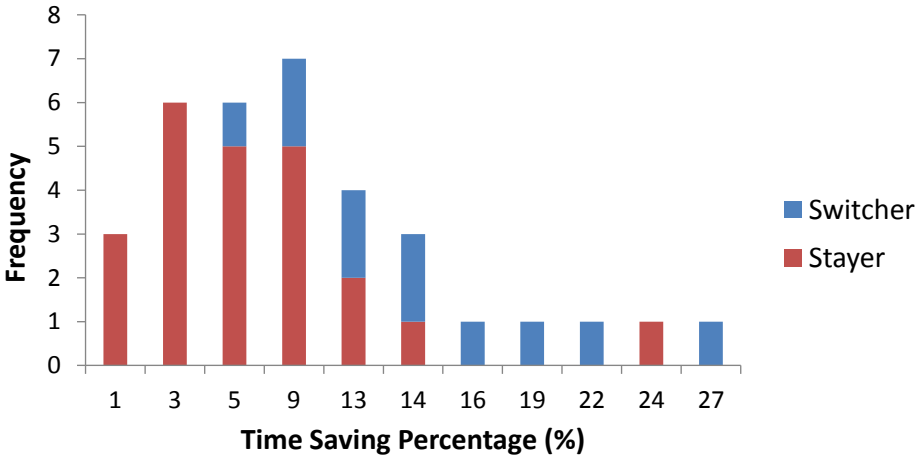

(b) Non-users

Figure 3.5: Travel time saving distribution

If travel time were the only factor which impacting route choice, classical perfect rationality cannot explain this phenomenon. Because if this were the case, everybody should immediately switch as long as the time saving is greater than zero. This may be caused by stickiness of the driving habit (Zhu and Levinson 2012). Therefore we propose that travelers are boundedly rational in route switching. Accordingly a travel time saving threshold, termed 'indifference band', is defined to capture this driving

inertia. The boundedly rational user equilibrium is reached when no traveler can reduce his travel time by an indifference band by unilaterally changing routes.

3.6.1 Unsupervised learning

According to Figure (3.5), when time saving is higher than 10%, everybody tends to use the new bridge (regardless of the outlier). Thus an estimate of the indifference band for old-users is 10%. Accordingly, when the new bridge can save at least 10% travel time, 17 out of 18 subjects (i.e., the number of old-users whose time saving is greater than 10%) switched, which can capture behavioral change of 94% subjects. Similarly, an estimate of the indifference band for non-users is 14%, meaning when the new bridge saves at least 14% travel time, 4 out of 5 non-users switched and the estimation accuracy is 80.0%.

This method belongs to unsupervised learning and its disadvantage is that outlier is not considered.

3.6.2 Logit regression model formulation

In this section, we assume that the indifference band is a deterministic constant for old-users and non-users respectively. However, commuters may not perceive travel time accurately.

As indicated in the stimulus-response model, several biological experiments (Clark 1933; Hemmingsen 1933) verified that no response occurs unless the logarithm of stimulus exceeds some threshold. In our context, the new bridge serves as a stimulus and travelers decide to choose it or not in response. Therefore, the logarithm of time saving, denoted as $\log(\triangle^{(n)})$ will be adopted.

Travel time savings is estimated from GPS data and speed map. However, drivers may perceive it with some error (Parthasarathi et al. 2013). Denote $\hat{\triangle}^{(n)}$ as the logarithm of commuter n's perceived travel time saving, which is random:

$$\hat{\triangle}^{(n)} = \beta \log(\triangle^{(n)}) + \eta, \tag{3.6.1}$$

where η is a standard normal random variable, i.e., $\eta \sim N(0,1)$ with cumulative distribution function $\Phi_\eta(x)$.

Commuters will not switch routes unless the logarithm of the perceived travel time saving is greater than the logarithm of the indifference band, i.e.,

$$y^{(n)} = \begin{cases} 1, \text{ if } \hat{\triangle}^{(n)} > \log(\varepsilon^*); \\ 0, \text{ if } \hat{\triangle}^{(n)} \leqslant \log(\varepsilon^*). \end{cases} \tag{3.6.2}$$

where,

$y^{(n)}$: a binary indicator for commuter n. It equals one if commuter n switches to the new bridge and zero otherwise;

ε^*: the indifference band.

Therefore the probability of switching for commuter n is then computed as:

$$\begin{aligned} P(y^{(n)} = 1 |\ \triangle_n, U_n) &= P(\hat{\triangle}^{(n)} > \log(\varepsilon^*) |\ \triangle_n, U_n) = P(\beta \log(\triangle^{(n)}) + \eta > \log(\varepsilon^*) |\ \triangle_n, U_n) \\ &= P(\eta > \log(\varepsilon^*) - \beta \log(\triangle^{(n)}) |\ \triangle_n, U_n) \\ &= 1 - \Phi_\eta(\beta_0 + \beta_1 \log(\triangle^{(n)})) \end{aligned} \tag{3.6.3}$$

where $\beta_0 = \log(\varepsilon^*)$, $\beta_1 = -\beta$.

Using probit regression, coefficients are estimated separate for old-users and new-users (Table 3.5):

Table 3.5: Probit regression coefficients

	Estimate	Std. Error	t-value	Pr($>\|t\|$)
Old-users				
(Intercept)	-2.42	1.00	-2.42	0.016 *
log($\triangle$)	-1.08	0.38	-2.81	0.005 **
Non-users				
(Intercept)	-3.51	0.91	-3.84	0.000 ***
log($\triangle$)	-0.92	0.30	-3.06	0.002 **

* Statistically significant at 5% level

** Statistically significant at 1% level

*** Statistically significant at 0.1% level

To illustrate, the mean indifference band for old-users is $\varepsilon^* = \exp(-2.42) = 8.9\%$ with the 97.5% confidence interval as $[1.1\%, 53.8\%]$. $\beta_1 = -1.08$ indicates that the log ratio of switching versus staying, i.e., $\log\left(\frac{P(y=1)}{P(y=0)}\right)$, increases by 1.08 if there is one unit increase in the logarithm of time saving brought by a new route.

Estimation

To estimate the number of switchers and stayers given $\triangle$, we divide the time saving range ($0 \sim 35\%$ for old-users and $0 \sim 27\%$ for non-users respectively) into bins with 1% increment, denoted as the j^{th} bin ($j = 1, \cdots, 35$ for old-users and $j = 1, \cdots, 27$ for non-users). For each $\triangle_j$, $P(y^{(n)} = 1|\ \triangle_j^{(n)}, U_n)$ can be computed according to Equation (3.6.3). The expected number of switchers for the j^{th} bin can be computed as:

$$\hat{N}_{switcher}^{(j)} = N^{(j)} P(y = 1|\ \triangle = \triangle_j, U) \tag{3.6.4}$$

where,
$N^{(j)}$: the number of observations (i.e., switchers plus stayers) for the j^{th} bin;
$\triangle_j$: the critical time saving thresholds for the j^{th} bin.

Note that we also divide the range into $I = 11$ bigger bins (each bin is denoted as the i^{th} bin) when we calculate frequencies of switchers and stayers in Figure (3.5). Then we can aggregate the total expected number of switchers and stayers within the j^{th} bin for each $i^{th}, i = 1, \cdots, 11$ bin. Figures (3.6-3.7) illustrate frequency and cumulative distribution of switchers and stayers from estimation and observation respectively.

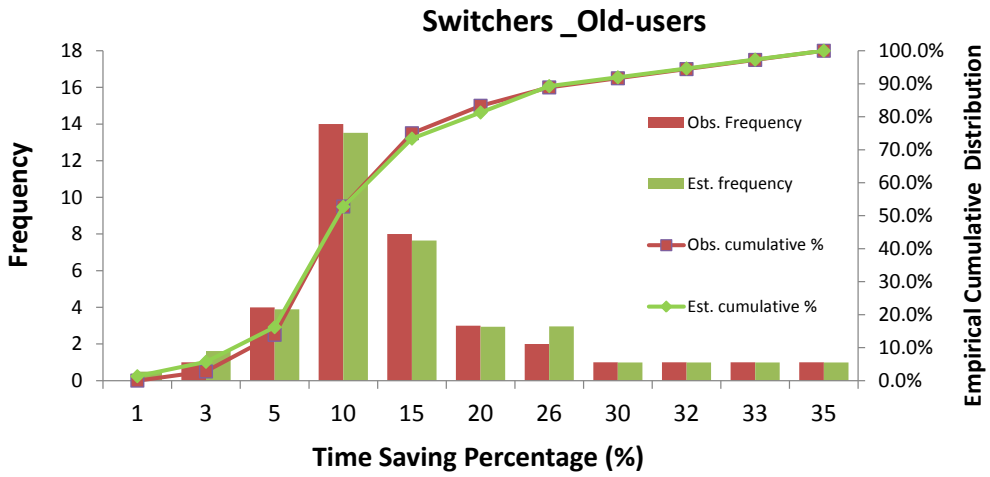

(a) Switchers among old-users

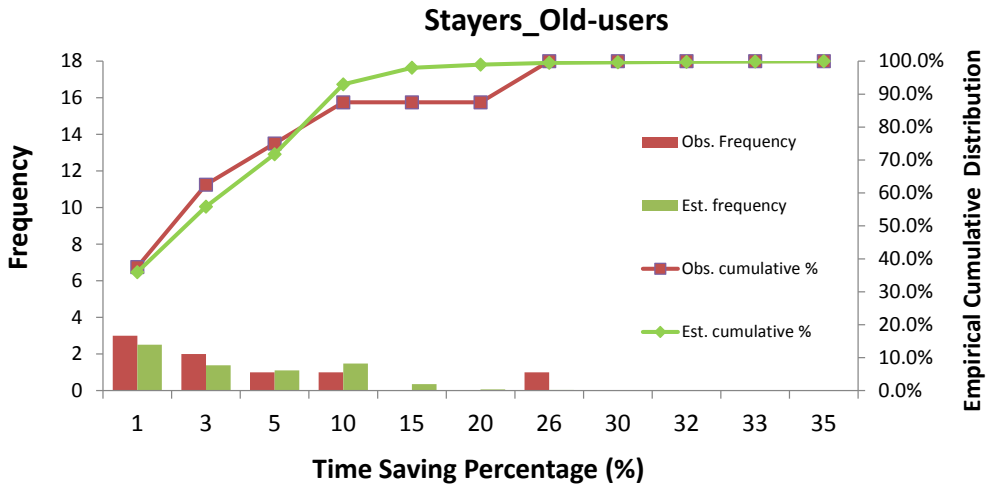

(b) Stayers among old-users

Figure 3.6: Frequency and cumulative distribution for old-users

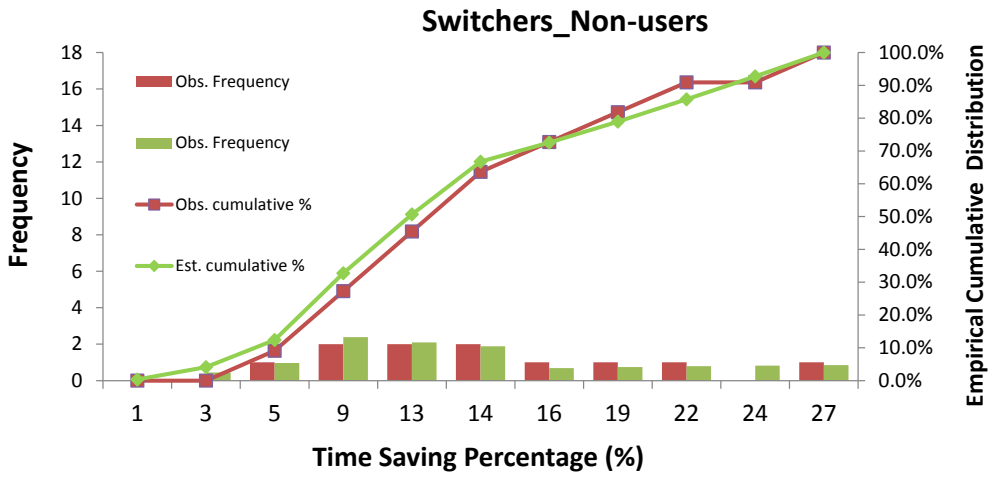

(a) Switchers among non-users

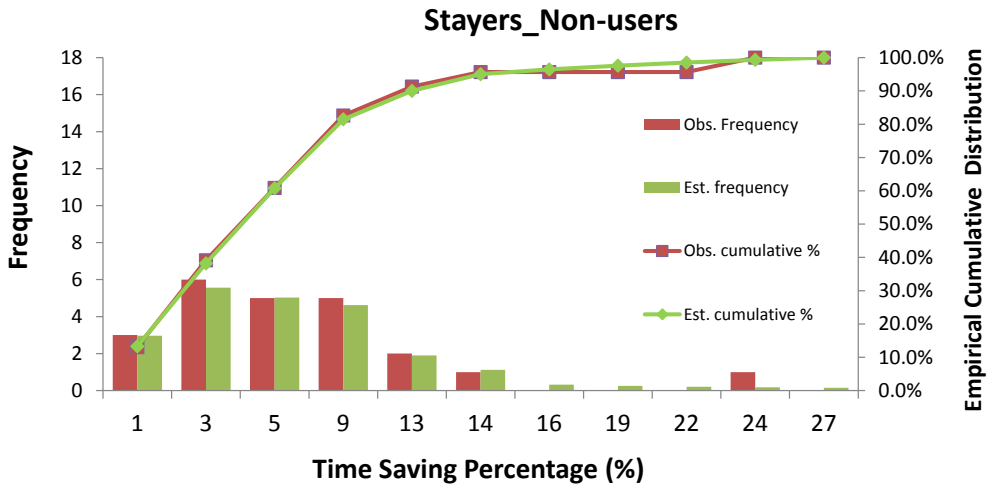

(b) Stayers among non-users

Figure 3.7: Frequency and cumulative distribution for non-users

Define the mean square error as $MSE = \frac{1}{N}\sum_{i=1}^{I}\left(\hat{N}^{(i)}_{switcher} - N^{(i)}_{switcher}\right)^2$, where $\hat{N}^{(i)}_{switcher}$ is the estimated number of switchers for the j^{th} bin and $N^{(i)}_{switcher}$ is the observed number of switchers, N is the total number of subjects. MSE is 17.4% for old-users and 11.5% for non-users respectively. The estimated frequency and cumulative percentage of switchers match the observed ones well and indicates that the proposed

model can capture the switching pattern in data.

Chapter 4

Boundedly rational user equilibrium (BRUE)

4.1 Introduction

When the BR assumption is used to model drivers' route choice behavior, there are two aspects regarding the boundedly rational route choice process. Some studies suggested that travelers do not take the shortest paths because they are not capable of perceiving actual travel costs due to limited cognitive capacity, or it is too costly to search information about all alternative paths (Gabaix et al. 2006; Gao et al. 2011).

On the other hand, some studies assumed that all path cost information is available to travelers through some information system, but they will not switch to shorter paths due to existence of inertia, which was quantified by a term named 'indifference band' (Mahmassani and Chang 1987). A series of experiments were conducted by Mahmassani and his colleges to validate this BR behavioral assumption and calibrate values of indifference bands (Hu and Mahmassani 1997; Jayakrishnan et al. 1994a; Mahmassani and Chang 1987; Mahmassani and Jayakrishnan 1991; Mahmassani and Liu 1999; Srinivasan and Mahmassani 1999). These experiments were conducted on an interactive simulator-DYNASMART, incorporating pre-trip departure time, route choices and en-route path switching decisions. Subjects, as travelers, could change paths en-route at each node and also adjust their departure-time choices the next day based on previous days' travel experiences. Travelers were assumed to follow

the BR behavioral rule in decision-making processes, i.e., they would only switch routes when improved trip time exceeded some indifference bands. The values of these indifference bands depended on individual characteristics and network performances. Lu and Mahmassani (2008) further studied the impact of congestion pricing on drivers' behavior within the boundedly rational behavioral framework.

In this chapter, we assume that travelers can perceive travel costs accurately but some indifference bands exist due to inertia to switch routes. When traffic flow patterns stabilize to some equilibrium, called 'boundedly rational user equilibrium' (BRUE), travelers can take any route whose travel time is within an indifference band of the shortest path cost (Guo and Liu 2011; Lou et al. 2010). Indifference bands vary among origin-destination (OD) pairs. By introducing one parameter (i.e., indifference band) for each OD pair, the BR framework relaxes the restrictive PR assumption that travelers only take the shortest paths at equilibrium.

According to Ben-Akiva et al. (1984), travelers' route choice behavior is regarded as a two-stage process: path set generation (i.e., a path choice set is generated between origin and destination according to route characteristics) and traffic assignment (i.e., traffic demands are mapped to these generated paths based on certain traffic assignment criteria). Accordingly, we will first study how to generate boundedly rational path sets first and then assign traffic demands to these paths based on BRUE conditions. The BRUE solution set is constructed by using networks with fixed demand. Obtaining the BRUE solution set and exploring fundamental mathematical properties of BRUE will serve as a building block for BRUE related applications, such as BR-related congestion pricing and other network design problems.

Following the two-stage route choice process, the rest of the chapter is organized as follows: In Section 4.2, the ε-BRUE is defined and formulated as a nonlinear complementarity problem (NCP). In Section 4.3, a BRUE-related acceptable path set is defined and its structure is studied. In Section 4.4, how to obtain acceptable path set is presented. In Section 4.5, we will construct BRUE path flow solution set based on the acceptable path set. Some examples are given to illustrate structure of the BRUE path flow solution set.

4.2 Definition of ε-BRUE and nonlinear complementarity formulation

The traffic network is represented by a directed graph that includes a set of consecutively numbered nodes, $\mathcal{N}$, and a set of consecutively numbered links, $\mathcal{L}$. Let $\mathcal{W}$ denote the origin-destination (OD) pair set connected by a set of simple paths (composed of a sequence of distinct nodes), $\mathcal{P}^w$, through the network. The traffic demand for OD pair w is d^w. Let f_i^w denote the flow on path $i \in \mathcal{P}^w$ for OD pair w, then the path flow vector is $\mathbf{f} = \{f_i^w\}_{i\in\mathcal{P}^w}^{w\in\mathcal{W}}$. The feasible path flow set is to assign the traffic demand on the feasible paths: $\mathcal{F} \triangleq \{\mathbf{f} : \mathbf{f} \geqslant \mathbf{0}, \sum_{i\in\mathcal{P}} f_i^w = d^w, \forall w \in \mathcal{W}\}$. Denote x_a as the link flow on link a, then the link flow vector is $\mathbf{x} = \{x_a\}_{a\in\mathcal{L}}$. Each link $a \in \mathcal{L}$ is assigned a cost function of the link flow, written as $c(\mathbf{x})$. Let $\delta_{a,i}^w = 1$ if link a is on path i connecting OD pair w, and 0 if not; then $\Delta \triangleq \{\delta_{a,i}^w\}_{a\in\mathcal{L},i\in\mathcal{P}}^{w\in\mathcal{W}}$, denotes the link-path incidence matrix. Therefore $f_i^w = \sum_a \delta_{a,i}^w x_a$, and it can be rewritten in a vector form as $\mathbf{x} = \Delta\mathbf{f}$. Denote $C_i^w(\mathbf{f})$ as the path cost on path i for OD pair w, then the path cost vector $C(\mathbf{f}) \triangleq \{C_i^w(\mathbf{f})\}_{i\in\mathcal{P}}^{w\in\mathcal{W}}$. So $C(\mathbf{f}) = \Delta^T c(\mathbf{x})$ under the additive path cost assumption.

In this chapter, we assume the link cost is separable, continuous and linear with respect to its own link flow, i.e., $c(\mathbf{x}) = H\mathbf{x}$, where H is the Jacobian matrix of the link cost. Then the path cost can be computed as: $C(\mathbf{f}) = \Delta^T c(\mathbf{x}) = \Delta^T H\Delta\mathbf{f} \triangleq A\mathbf{f}$, where $A = \Delta^T H\Delta$.

4.2.1 Definition

Mahmassani and Chang (1987) defined a BRUE flow vector as the one 'whenever all users' perceived travel costs on their selected routes are constrained within their respective indifference bands'. Following this line, we define $\boldsymbol{\varepsilon}$-BRUE as follows.

Definition 4.2.1. For a given nonnegative vector $\boldsymbol{\varepsilon} = (\varepsilon^w)_{w\in\mathcal{W}}, \varepsilon^w \geqslant 0$, a feasible path flow vector $\mathbf{f} \in \mathcal{F}$ is said to be a $\boldsymbol{\varepsilon}$-boundedly rational user equilibrium (BRUE) path flow pattern, denoted by $\mathbf{f}_{BRUE}^{\varepsilon}$, if

$$f_i^w > 0 \Rightarrow C_i^w(\mathbf{f}) \leqslant \min_{j\in\mathcal{P}} C_j^w(\mathbf{f}) + \varepsilon^w, \forall i \in \mathcal{P}, \forall w \in \mathcal{W} \tag{4.2.1}$$

This definition says that, for a one path flow pattern which is a boundedly rational user equilibrium, travelers only pick any route that is within a given indifference band ε of the shortest path.

Remark.

- Equation (4.2.1) gives a necessary condition judging whether a flow pattern is BRUE, and is equivalent to the following condition:

$$C_i^w(\mathbf{f}) > \min_{j\in\mathcal{P}^w} C_j^w(\mathbf{f}) + \varepsilon^w \Rightarrow f_i^w = 0,$$

But the inverse is not always true:

$$f_i^w = 0 \nRightarrow C_i^w(\mathbf{f}) > \min_{j\in\mathcal{P}^w} C_j^w(\mathbf{f}) + \varepsilon^w.$$

In other words, an unused path may have lower cost than a used one, which will never happen in the UE setting. Therefore, if $C_i^w(\mathbf{f}) \leqslant \min_{j\in\mathcal{P}^w} C_j^w(\mathbf{f}) + \varepsilon^w$, then $f_i^w \geqslant 0$.

- When $\varepsilon = 0$, the BRUE definition is reduced to:

$$\mathcal{F}_{BRUE}^0 \triangleq \mathcal{F}_{UE} = \{\mathbf{f}\in\mathcal{F} : f_i^w > 0 \Rightarrow C_i^w(\mathbf{f}) = \min_{j\in\mathcal{P}} C_j^w(\mathbf{f}), \forall i\in\mathcal{P}, \forall w\in\mathcal{W}\}; \tag{4.2.2}$$

The path flow set satisfying the above definition is called the UE path flow set. Based on the UE path flow set $\mathcal{F}_{UE}$, the UE shortest path set $\mathcal{P}_{UE}$ can be defined as:

$$\mathcal{P}_{UE} = \{i\in\mathcal{P} : C_i^w(\mathbf{f}) = \min_{j\in\mathcal{P}} C_j^w(\mathbf{f}), \forall \mathbf{f}\in\mathcal{F}_{UE}\}. \tag{4.2.3}$$

We should note that the UE shortest path from $\mathcal{P}_{UE}$ may carry flow or may have no flow on it.

- Some literature (Mahmassani and Chang 1987; Mahmassani and Stephan 1988; Mahmassani and Liu 1999) assumed that the indifference band is a relative value instead of an absolute value adopted here: the cost difference between cost of the utilized path and that of the shortest path is within a fraction of the shortest cost. Though the indifference band is presented differently in the above literature, the methodologies of constructing the BRUE set remain the same.

Usually the $\boldsymbol{\varepsilon}$-BRUE is non-unique. Denote a set containing all path flow patterns satisfying Definition (4.2.1) as the $\boldsymbol{\varepsilon}$-BRUE path flow solution set:

$$\mathcal{F}^{\boldsymbol{\varepsilon}}_{BRUE} \triangleq \{\mathbf{f} \in \mathcal{F} : f_i^w > 0 \Rightarrow C_i^w(\mathbf{f}) \leqslant \min_{j \in \mathcal{P}} C_j^w(\mathbf{f}) + \varepsilon^w, \forall i \in \mathcal{P}, \forall w \in \mathcal{W}\}; \quad (4.2.4)$$

Proposition 4.2.1. *If the link cost function is continuous, the $\boldsymbol{\varepsilon}$-BRUE solution ($\boldsymbol{\varepsilon} \geqslant 0$) is non-empty.*

Proof. First, Patriksson (1994) showed that, when the link cost function is continuous, UE exists.

Let $\mathbf{f} \in \mathcal{F}_{UE}$ be the UE path flow pattern, when $\boldsymbol{\varepsilon} \geqslant 0$,

$$f_i^w > 0 \Rightarrow C_i^w(\mathbf{f}) = \min_{j \in \mathcal{P}} C_j^w(\mathbf{f}) \leqslant \min_{j \in \mathcal{P}} C_j^w(\mathbf{f}) + \varepsilon^w, \forall i \in \mathcal{P}, \forall w \in \mathcal{W}$$

So $\mathbf{f}$ is also a $\boldsymbol{\varepsilon}$-BRUE ($\boldsymbol{\varepsilon} \geqslant 0$), i.e., $\mathbf{f} \in \mathcal{F}^{\boldsymbol{\varepsilon}}_{BRUE}$. Then $\mathcal{F}_{UE} \subseteq \mathcal{F}^{\boldsymbol{\varepsilon}}_{BRUE}$. In other words, UE must be contained in the BRUE set. Given the continuous link cost function, at least one BRUE flow pattern exists, and therefore $\mathcal{F}^{\boldsymbol{\varepsilon}}_{BRUE} \neq \emptyset$. □

Note. $\mathcal{F}_{UE}$ may be non-unique if the link cost function is not strictly monotone. In spite of its non-uniqueness, it is still contained in the ε-BRUE set.

4.2.2 BRUE-NCP formulation

Given the continuous link cost function, the $\boldsymbol{\varepsilon}$-BRUE must exist. The next question is, how we can compute equilibrium solutions. Since UE is a special case of BRUE, we will start with UE. Based on the Wardrop's first principle, UE can be solved from a nonlinear complementarity problem (NCP). For all $i \in \mathcal{P}^w$ and all $w \in \mathcal{W}$:

$$0 \leqslant f_i^w \perp C_i^w(\mathbf{f}) - \pi^w \geqslant 0, \quad (4.2.5a)$$

$$0 \leqslant \pi^w \perp d^w - \sum_{i \in \mathcal{P}} f_i^w \geqslant 0. \quad (4.2.5b)$$

where π^w is the shortest path cost for tOD pair w. $\perp$ is the orthogonal sign representing the inner product of two vectors is zero.

Similarly, BRUE can be formulated as a NCP as well, but some changes should be made.

Proposition 4.2.2 (BRUE NCP). *Given $\varepsilon^w (w \in \mathcal{W})$, and some $\boldsymbol{\rho} = (\rho_i^w)_i^w$, where $0 \leqslant \rho_i^w \leqslant \varepsilon^w$. A feasible path flow vector $\mathbf{f} \in \mathcal{F}$ is a $\boldsymbol{\varepsilon}$-BRUE path flow pattern if and only if it solves the following NCP, $\forall i \in \mathcal{P}^w, \forall w \in \mathcal{W}$:*

$$(NCP(\boldsymbol{\rho})) \qquad 0 \leqslant f_i^w \perp C_i^w(\mathbf{f}) + \rho_i^w - \pi^w \geqslant 0, \tag{4.2.6a}$$

$$0 \leqslant \pi^w \perp d^w - \sum_{i \in \mathcal{P}} f_i^w \geqslant 0. \tag{4.2.6b}$$

where the physical meaning of π^w is the maximum path cost within the band ε^w for OD pair w.

Proof. In the fixed-demand case, (4.2.6b) is reduced to the nonnegative constraint on $\pi^w \geqslant 0$.

(1) To prove the necessary part, let $\mathbf{f}$ be a feasible flow pattern and let $(\boldsymbol{\rho}, \boldsymbol{\pi})$ be a pair such that Equation (4.2.6) holds, then $0 \leqslant \rho \leqslant \varepsilon, \pi^w \geqslant 0$ for all $w \in W$ and $i \in P^w$.

Moreover, $C_i^w(\mathbf{f}) + \rho_i^w - \pi^w \geqslant 0$ and $0 \leqslant \rho_i^w \leqslant \varepsilon^w$ indicate that

$$\pi^w \leqslant C_i^w(\mathbf{f}) + \rho_i^w \leqslant C_i^w(\mathbf{f}) + \varepsilon^w,$$

thus,

$$\pi^w \leqslant \min_{j \in \mathcal{P}} C_j^w(\mathbf{f}) + \varepsilon^w.$$

For $f_i^w > 0$, (4.2.6a) holds iff $C_i^w(\mathbf{f}) + \rho_i^w - \pi^w = 0$, i.e.,

$$f_i^w > 0 \Rightarrow C_i^w(\mathbf{f}) = \pi^w - \rho_i^w \leqslant \pi^w \leqslant \min_{j \in \mathcal{P}} C_j^w(\mathbf{f}) + \varepsilon^w,$$

which satisfies Definition (4.2.1), so $\mathbf{f}$ is a $\boldsymbol{\varepsilon}$-BRUE path flow pattern.

(2) To prove the sufficient part, suppose $\mathbf{f}$ is a BRUE flow pattern. For $i \in P^w$ and $w \in W$, define

$$\pi^w \triangleq \min_{j \in \mathcal{P}} C_j^w(\mathbf{f}) + \varepsilon^w \geqslant 0. \tag{4.2.7}$$

and

$$\rho_i^w \triangleq \begin{cases} \pi^w - C_i^w(\mathbf{f}), \text{ if } C_i^w(\mathbf{f}) \leqslant \min_{j \in \mathcal{P}} C_j^w(\mathbf{f}) + \varepsilon^w; \\ 0, \text{ if } C_i^w(\mathbf{f}) > \min_{j \in \mathcal{P}} C_j^w(\mathbf{f}) + \varepsilon^w; \end{cases} \tag{4.2.8}$$

Equation (4.2.6) holds automatically for any BRUE flow pattern. It suffices to show that $0 \leqslant \rho_i^w \leqslant \varepsilon^w, \pi^w \geqslant 0$. Since $\mathbf{f}$ is a BRUE flow pattern, it follows that, by

Definition (4.2.1), if $f_i^w \geqslant 0$, $C_i^w(\mathbf{f}) \leqslant \min_{j\in\mathcal{P}} C_j^w(\mathbf{f}) + \varepsilon^w$; if $C_i^w(\mathbf{f}) > \min_{j\in\mathcal{P}} C_j^w(\mathbf{f}) + \varepsilon^w$, then $f_i^w = 0$.

When $f_i^w \geqslant 0$, then $C_i^w(\mathbf{f}) \leqslant \min_{j\in\mathcal{P}} C_j^w(\mathbf{f}) + \varepsilon^w$,

$$C_i^w(\mathbf{f}) \leqslant \min_{j\in\mathcal{P}} C_j^w(\mathbf{f}) + \varepsilon^w = \pi^w,$$

which yields $\rho_i^w \geqslant 0$ from (4.2.8). Again, by (4.2.8),

$$\rho_i^w = \pi^w - C_i^w(\mathbf{f}) = \min_{j\in\mathcal{P}} C_j^w(\mathbf{f}) + \varepsilon^w - C_i^w(\mathbf{f}) \leqslant \varepsilon^w,$$

showing that $\rho_i^w \leqslant \varepsilon^w$. So $0 \leqslant \rho_i^w \leqslant \varepsilon^w$ if $f_i^w > 0$.

When $C_i^w(\mathbf{f}) > \min_{j\in\mathcal{P}} C_j^w(\mathbf{f}) + \varepsilon^w$, i.e., $f_i^w = 0$, then $\rho_i^w = 0$ by (4.2.8).

In summary, $0 \leqslant \rho_i^w \leqslant \varepsilon^w$ and $\pi^w \geqslant 0$ for $i \in P^w$ and $w \in W$. □

Remark.

- Comparing the UE-NCP with the BRUE-NCP formulation, there is one additional term ρ_i^w in BRUE-NCP, we call it 'indifference function.' If $C_i^w(\mathbf{f}) \geqslant \min_{j\in\mathcal{P}} C_j^w(\mathbf{f}) + \varepsilon^w$, then $\rho_i^w = 0$; if $C_i^w(\mathbf{f}) = \min_{j\in\mathcal{P}} C_j^w(\mathbf{f})$, then $\rho_i^w = \varepsilon^w$.
- The meaning of π^w is different in the two settings. Regarding UE, π^w is the shortest travel time; while in BRUE, its value is equal to the shortest travel cost plus ε^w (see Equation (4.2.7)). π^w is a function of the flow pattern, so we call it the 'maximum path cost' for a specific BRUE flow pattern. For some flow pattern, there may not exist a path with the exact cost of π^w. If some flow pattern happens to have a path with the cost of π^w, this path may or may not carry flows.

From BRUE NCP (4.2.6) and its proof, we have another conclusion:

Corollary 1. *If $\mathbf{f} \in \mathcal{F}_{BRUE}^{\varepsilon}$, there must exist at least one vector pair $(\boldsymbol{\rho}, \boldsymbol{\pi})$ satisfying NCP (4.2.6). Moreover, one value of $(\boldsymbol{\rho}, \boldsymbol{\pi})$ is determined by (4.2.7) and (4.2.8).*

By substituting one indifference function $\rho \in \mathbb{R}_+^n$ into the BRUE-NCP, one BRUE path flow pattern can be obtained. The BRUE-NCP formulation provides an approach of solving one BRUE solution. In the following we will show how to construct complete BRUE solution sets out of a specific solution.

4.3 Monotonically non-decreasing acceptable path set

In the last section, we show that when the indifference band is zero, BRUE is equivalent to UE flow pattern and travelers will only take shortest paths. When the indifference band gradually increases, some paths which are too costly to take under UE may be utilized under BRUE. In this section, we will discuss the relationship between the indifference band and the number of utilized paths.

4.3.1 Monotonically non-decreasing property

All feasible paths for one particular BRUE flow pattern can be classified into three categories:

Definition 4.3.1. Given a ε-BRUE flow pattern $\mathbf{f} \in \mathcal{F}^{\varepsilon}_{BRUE}$, the total feasible paths could have three statuses: acceptable, zero-acceptable and unacceptable. The acceptable path carries flow while its cost is within the shortest one plus a band; the zero-acceptable path is acceptable in terms of the cost but carries no flow; and the unacceptable path is longer than the shortest cost plus the band.

$$a^{\varepsilon}(\mathbf{f}) = \{i \in \mathcal{P} : f_i > 0, C_i^w(\mathbf{f}) \leqslant \min_{j\in\mathcal{P}} C_j^w(\mathbf{f}) + \varepsilon^w, \forall w\}; \tag{4.3.1a}$$

$$0^{\varepsilon}(\mathbf{f}) = \{i \in \mathcal{P} : f_i = 0, C_i^w(\mathbf{f}) \leqslant \min_{j\in\mathcal{P}} C_j^w(\mathbf{f}) + \varepsilon^w, \forall w\}; \tag{4.3.1b}$$

$$u^{\varepsilon}(\mathbf{f}) = \{i \in \mathcal{P} : f_i = 0, C_i^w(\mathbf{f}) > \min_{j\in\mathcal{P}} C_j^w(\mathbf{f}) + \varepsilon^w, \forall w\}. \tag{4.3.1c}$$

There are three properties of the above three path sets:

Proposition 4.3.1. *(1) Given one BRUE flow pattern* $\mathbf{f}$*, the union of paths at these three status is the feasible path set:* $a^{\varepsilon}(\mathbf{f}) \cup 0^{\varepsilon}(\mathbf{f}) \cup u^{\varepsilon}(\mathbf{f}) = \mathcal{P}$*;*

(2) Given one BRUE flow pattern $\mathbf{f}$*, we can always find at least one path which is acceptable or zero-acceptable:* $a^{\varepsilon}(\mathbf{f}) \cup 0^{\varepsilon}(\mathbf{f}) \neq \emptyset$*;*

(3) Given one BRUE flow pattern $\mathbf{f}$*, if* $\varepsilon \geqslant \max_{j\in\mathcal{P}} C_j^w(\mathbf{f}) - \min_{j\in\mathcal{P}} C_j^w(\mathbf{f})$*, all feasible paths are either acceptable or zero-acceptable:* $u^{\varepsilon}(\mathbf{f}) = \emptyset$*.*

Proof. (1) It is obvious from the definition.

(2) Since the shortest path $i = \arg\min_{j\in\mathcal{P}} C_j^w(\mathbf{f})$ always exists, so $i \in a^\varepsilon(\mathbf{f}) \cup 0^\varepsilon(\mathbf{f}) \subseteq \mathcal{P}$.

(3) $\max_{j\in\mathcal{P}} C_j^w(\mathbf{f}) - \min_{j\in\mathcal{P}} C_j^w(\mathbf{f}) \leqslant \varepsilon$ implies $C_i^w(\mathbf{f}) \leqslant \min_{j\in\mathcal{P}} C_j^w(\mathbf{f}) + \varepsilon, \forall i \in \mathcal{P}$, thus no path is unacceptable, i.e., $u^\varepsilon(\mathbf{f}) = \emptyset$. □

Definition (4.3.1) divides all the feasible paths for one BRUE flow pattern into three classes. Each status notation indicates dependency of path status on ε and a specific BRUE flow pattern. The following proposition will discuss the relationship between the path status and the value of ε.

Proposition 4.3.2. *Given* $\mathbf{f} \in \mathcal{F}^{\boldsymbol{\varepsilon}}_{BRUE}$, *if* $0 \leqslant \varepsilon < \varepsilon'$, *then* $a^\varepsilon(\mathbf{f}) \subseteq a^{\varepsilon'}(\mathbf{f}), 0^\varepsilon(\mathbf{f}) \subseteq 0^{\varepsilon'}(\mathbf{f})$.

Proof. It suffices to show that, if an arbitrary path i is acceptable or zero-acceptable under the indifference band ε, it is also acceptable or zero-acceptable when the indifference band is $\varepsilon' > \varepsilon$. $\forall i \in a^\varepsilon(\mathbf{f})$, we know $f_i > 0$, and

$$C_i^w(\mathbf{f}) \leqslant \min_{j\in\mathcal{P}} C_j^w(\mathbf{f}) + \varepsilon^w < \min_{j\in\mathcal{P}} C_j^w(\mathbf{f}) + \varepsilon' \implies i \in a^{\varepsilon'}(\mathbf{f}).$$

Therefore $a^\varepsilon(\mathbf{f}) \subseteq a^{\varepsilon'}(\mathbf{f})$. Similarly $0^\varepsilon(\mathbf{f}) \subseteq 0^{\varepsilon'}(\mathbf{f})$. □

Proposition (4.3.2) says that, for a ε-BRUE flow pattern, the status of a path depends on the value of ε. Since its total feasible paths are fixed, those unused paths under smaller ε can be utilized with bigger ε. Therefore, the bigger ε is, the more paths are acceptable or zero-acceptable, and the less paths are unacceptable.

In the following, we will discuss the impact of the value of ε on the size of the ε-BRUE flow set.

Proposition 4.3.3 (**Monotonically non-decreasing flow set**). *If* $0 \leqslant \varepsilon < \varepsilon'$, *then* $\mathcal{F}^{\boldsymbol{\varepsilon}}_{BRUE} \subseteq \mathcal{F}^{\varepsilon'}_{BRUE}$.

Proof. It suffices to show that $\forall \mathbf{f} \in \mathcal{F}^{\boldsymbol{\varepsilon}}_{BRUE} \implies \mathbf{f} \in \mathcal{F}^{\varepsilon'}_{BRUE}$.

$$\begin{aligned}
\forall \mathbf{f} \in \mathcal{F}^{\varepsilon}_{BRUE} \quad &\implies \quad \{f_i^w > 0 \Rightarrow C_i^w(\mathbf{f}) \leqslant \min_{j\in\mathcal{P}} C_j^w(\mathbf{f}) + \varepsilon \\
&< \quad \min_{j\in\mathcal{P}} C_j^w(\mathbf{f}) + \varepsilon', \forall i \in \mathcal{P}, \forall w \in \mathcal{W}\} \\
&\implies \quad \mathbf{f} \in \mathcal{F}^{\varepsilon'}_{BRUE} \implies \mathcal{F}^{\varepsilon}_{BRUE} \subseteq \mathcal{F}^{\varepsilon'}_{BRUE}.
\end{aligned}$$

□

Proposition (4.3.3) indicates that when ε increases, more flow patterns will be included in the ε-BRUE flow set.

When the ε-BRUE flow set exists and is non-unique, each flow pattern has different combination of acceptable, zero-acceptable and unacceptable paths. A 'largest ε-acceptable path set' contains all acceptable paths for every flow pattern in the ε-BRUE flow set, mathematically:

$$\mathcal{P}_l^{\varepsilon} = \bigcup_{\mathbf{f} \in \mathcal{F}_{BRUE}^{\varepsilon}} a^{\varepsilon}(\mathbf{f}). \tag{4.3.2}$$

The largest ε-acceptable path set shares the similar property as the ε-BRUE flow set has:

Proposition 4.3.4 (Monotonically non-decreasing path set). *If $0 \leqslant \varepsilon < \varepsilon'$, $\mathcal{P}_l^{\varepsilon} \subseteq \mathcal{P}_l^{\varepsilon'}$, where $\mathcal{P}_l^{\varepsilon}$ is defined in (4.3.2).*

Proof.

$$\begin{aligned} \mathcal{P}_l^{\varepsilon} &= \bigcup_{\mathbf{f} \in \mathcal{F}_{BRUE}^{\varepsilon}} a^{\varepsilon}(\mathbf{f}) \subseteq \bigcup_{\mathbf{f} \in \mathcal{F}_{BRUE}^{\varepsilon'}} a^{\varepsilon}(\mathbf{f}) \text{ (Proposition (4.3.3))} \\ &\subseteq \bigcup_{\mathbf{f} \in \mathcal{F}_{BRUE}^{\varepsilon'}} a^{\varepsilon'}(\mathbf{f}) \text{ (Proposition (4.3.2))} = \mathcal{P}_l^{\varepsilon'}. \end{aligned}$$

□

When ε varies from zero to infinity, the minimum number of paths the largest ε-acceptable path set contains is the UE shortest paths when $\varepsilon = 0$, i.e., $\mathcal{P}_{BRUE}^{0} \triangleq \mathcal{P}_{UE}$. The maximum number of paths the largest ε-acceptable path set contains is all feasible paths, meaning all feasible paths will be utilized if the indifference band is too large. Then we have the following corollary:

Corollary 2. $\mathcal{P}_{UE} \subseteq \mathcal{P}_l^{\varepsilon} \subseteq \mathcal{P}$.

Given ε, the largest ε-acceptable path set (defined in Equation (4.3.2)) is a set of all acceptable paths under the ε-BRUE set. It is possible that some acceptable paths for one ε-BRUE flow pattern are not acceptable for other flow patterns; vice versa. This necessitates the exploration of the interior structure of the ε-acceptable path set. Proposition (4.3.4) provides us with one approach of analyzing its structure by varying values of ε.

The path set is a set of finite paths, while ε is treated as a continuous parameter for the time being. Starting with the UE path set when $\varepsilon = 0$, provided the topology of a network and the link cost functions, $\mathcal{P}_{UE}$ can be determined by some established algorithms, e.g., column generation algorithm (Patriksson 1994), gradient projection algorithm (Jayakrishnan et al. 1994b), or maximum entropy algorithm (Bell and Iida 1997). According to Proposition (4.3.4), when ε is gradually increased, more paths will be included. We should be able to identify those acceptable paths one by one until all alternative paths are included. This offers theoretical foundation for deriving different combinations of acceptable paths by varying ε subsequently.

4.3.2 Definition of ε-acceptable path set

It is assumed that there are n alternative paths for OD pair w, i.e., $\mathcal{P} = \{1, \cdots, n\}$ and $|\mathcal{P}| = n$, where $|\mathcal{P}|$ is the cardinality of set $\mathcal{P}$. Among these n paths, there are p shortest paths at the UE, i.e., $\mathcal{P}_{UE} = \{1, \cdots, p\}$ and $|\mathcal{P}_{UE}| = p \leqslant n$.

Definition 4.3.2. Assuming there exists a unique sequence of finite critical points $\varepsilon_j^{*w}, (j = 1, \cdots, J)$, with $\varepsilon_0^* = 0, \varepsilon_{J+1}^* = \infty$, dividing the nonnegative real line into $(J+1)$ intervals: $[0, \infty) = [0, \varepsilon_1^*) \cup [\varepsilon_1^*, \varepsilon_2^*) \cdots \cup [\varepsilon_J^*, \infty) = \bigcup_{j=0}^{J} [\varepsilon_j^*, \varepsilon_{j+1}^*)$. A sequence of critical points are defined as:

$$
\begin{aligned}
\varepsilon_1^* &\triangleq \inf_{\varepsilon>0}\{\mathcal{P}_{UE} \subset \mathcal{P}_l^{\varepsilon}\};\\
&\vdots\\
\varepsilon_j^* &\triangleq \inf_{\varepsilon>0}\{\mathcal{P}_l^{\varepsilon_{j-1}^*} \subset \mathcal{P}_l^{\varepsilon}\};\\
&\vdots\\
\varepsilon_J^* &\triangleq \inf_{\varepsilon>0}\{\mathcal{P}_l^{\varepsilon} = \mathcal{P}\}.
\end{aligned}
\tag{4.3.3}
$$

The largest $\boldsymbol{\varepsilon}$-acceptable path set will remain the same until ε reaches these values, i.e., for $\varepsilon_j^* \leqslant \varepsilon_1 < \varepsilon_2 < \varepsilon_{j+1}^*$, $\mathcal{P}_l^{\varepsilon_j^*} = \mathcal{P}_l^{\varepsilon_1} = \mathcal{P}_l^{\varepsilon_2} \subset \mathcal{P}_l^{\varepsilon_{j+1}^*}$.

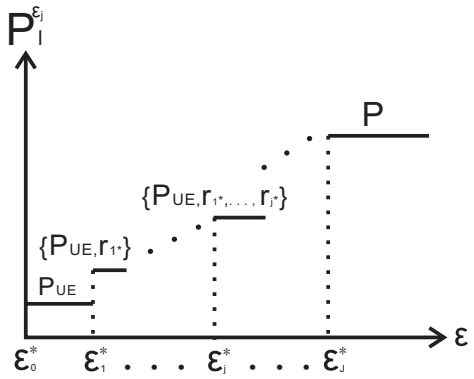

Figure 4.1: Monotonically non-decreasing property illustration

A 'newly added path' is defined as the path which is unacceptable under ε_{j-1}^* but acceptable when $\varepsilon = \varepsilon_j^*$:

$$r_j^* \triangleq \{i \in \mathcal{P} : i \in \mathcal{P}_l^{\varepsilon_j^*}, i \notin \mathcal{P}_l^{\varepsilon_{j-1}^*}\}, \tag{4.3.4}$$

Given the current acceptable path set $\mathcal{P}_l^{\varepsilon_{j-1}^*}$, after newly acceptable paths are identified, the updated acceptable path set is:

$$\mathcal{P}_l^{\varepsilon_j^*} \triangleq \mathcal{P}_l^{\varepsilon_{j-1}^*} \bigcup r_j^*. \tag{4.3.5}$$

Remark. There may exist two or more paths added at the same time, so r_j^* should be treated as a path set.

Provided a fixed indifference band ε, $\varepsilon_I^* \leqslant \varepsilon < \varepsilon_{I+1}^*$. Let $K = \min\{I, J\}$. The ε-acceptable path set is defined as:

$$\mathcal{P}^{\varepsilon} = \{\mathcal{P}_{UE}, \mathcal{P}_l^{\varepsilon_1^*}, \cdots, \mathcal{P}_l^{\varepsilon_K^*}\}. \tag{4.3.6}$$

In other words, the ε-acceptable path set is composed of K acceptable path sets with $\mathcal{P}_{UE} \subset \mathcal{P}_l^{\varepsilon_1^*} \subset \cdots \subset \mathcal{P}_l^{\varepsilon_K^*} \subseteq \mathcal{P}$.

4.4 Generation of the ε-acceptable path set

In the last section, we introduced a BR-related path set: the largest ε-acceptable path set. In this section, we will explore how to generate this path set. Definition (4.3.3) says

that, the largest ε-acceptable path set includes more paths when ε increases to some critical values. Thus, a mathematical program with equilibrium constraint (MPEC) can be developed to solve these critical values:

$$
\begin{aligned}
\text{(MPEC)} \qquad & \min \qquad \varepsilon_j \\
& s.t. \\
& 0 \leqslant f_i \perp C_i(\mathbf{f}) + \rho_i - \pi \geqslant 0, \forall i \in \mathcal{P}, && \text{(4.4.1a)} \\
& \sum_{r \in \mathcal{P}} f_r = d, && \text{(4.4.1b)} \\
& d - \sum_{j \in \mathcal{P}_l^{\varepsilon^*_{j-1}}} f_j > 0, && \text{(4.4.1c)} \\
& 0 \leqslant \rho_i \leqslant \varepsilon_j, \forall i \in \mathcal{P}, && \text{(4.4.1d)} \\
& f_i + C_i(\mathbf{f}) + \rho_i - \pi > 0, \forall i \in \mathcal{P}. && \text{(4.4.1e)}
\end{aligned}
$$

(4.4.1a-4.4.1b) is to guarantee that the path flow pattern is a feasible BRUE; (4.4.1c) tries to push a small amount of flow from the acceptable path set $\mathcal{P}_l^{\varepsilon^*_{j-1}}$ to some newly acceptable path if ε is increased a little bit; (4.4.1d) sets bounds for the indifference function; (4.4.1e) ensures strict complementarity condition in (4.4.1a) (Cottle et al. 2009).

If MPEC (4.4.1) is solvable, optimal solutions $(\mathbf{f}^*, \boldsymbol{\rho}^*, \pi^*, \varepsilon_j^*)$ will be obtained. The newly added path r_j^* can be derived from $\mathbf{f}^*$. It is the path that is excluded from $\mathcal{P}_l^{\varepsilon^*_{j-1}}$ but begins to carry a very small amount of flow in $\mathbf{f}^*$.

(4.4.1c) and (4.4.1e) are inequalities without equal sign, which defines an open set causing non-attainability of the optimal solution. So we introduce a parameter $0 < \delta \leqslant 1$ such that $d - \sum_{r \in \mathcal{P}_l^{\varepsilon^*_{j-1}}} f_r \geqslant \delta d$ and $f_i + C_i(\mathbf{f}) + \rho_i - \pi \geqslant \delta$. We call this modified version as 'δ-MPEC', and we will solve this version in practice by giving δ a very small value

($\delta = 0.01$ works well). Rewrite the δ-MPEC in a compact form:

$$
\begin{aligned}
(\delta\text{-MPEC}) \qquad & \min \qquad \varepsilon_j \\
s.t. \qquad & \mathbf{1}^T\mathbf{f} = d, && \text{(4.4.2a)}\\
& -\mathbf{v}^T\mathbf{f} \geqslant (\delta - 1)d, && \text{(4.4.2b)}\\
& \varepsilon_j\mathbf{1} - \boldsymbol{\rho} \geqslant \mathbf{0}, && \text{(4.4.2c)}\\
& \mathbf{f} + C(\mathbf{f}) + \boldsymbol{\rho} - \boldsymbol{\pi} \geqslant \delta, && \text{(4.4.2d)}\\
& \boldsymbol{\rho}, \pi, \varepsilon_j \geqslant \mathbf{0}, && \text{(4.4.2e)}\\
& \mathbf{f} \geqslant \mathbf{0}, && \text{(4.4.2f)}\\
& C(\mathbf{f}) + \boldsymbol{\rho} - \pi\mathbf{1} \geqslant \mathbf{0}, && \text{(4.4.2g)}\\
& \mathbf{f}^T(C(\mathbf{f}) + \mathbf{f}^T\boldsymbol{\rho} - \pi\mathbf{1}) = \mathbf{0}. && \text{(4.4.2h)}
\end{aligned}
$$

where $\mathbf{v}$ is an vector of the same dimension with the path flow vector, with the i^{th} component equal to one if $f_i \in \mathcal{P}^{\varepsilon_{j-1}^*}$ and zero otherwise. $\mathbf{1}$ is a vector of 1.

In practice, this MPEC problem can be solved by GAMS software (General Algebraic Modeling System, see Rosenthal and Brooke 2007).

4.4.1 Solving critical points sequentially

When ε_1^* is achieved, we include the corresponding path r_1^* into the UE shortest path set and get $\mathcal{P}_l^{\varepsilon_1^*}$. Next we are interested in finding the critical point ε_2^* based on current $\mathcal{P}_l^{\varepsilon_1^*}$. We can solve the above MPEC again by replacing $\mathcal{P}_l^{\varepsilon_1^*}$ in (4.4.1b) with $\mathcal{P}_l^{\varepsilon_2^*}$, and ε_2^* will be obtained. Similarly, $\varepsilon_3^*, \cdots$, are able to be computed sequentially. This procedure will not stop until all feasible paths are included into the BRUE acceptable set or the critical value reaches the given ε.

The above procedure provides a method of obtaining the critical points and the order of adding new paths to the acceptable path sets. We will illustrate how to implement this procedure on a small network in the following.

Example 4.4.1. A four-link network connects one OD pair in parallel with demand 2. The link cost for each link is 1, $x_2 + 1.5$, $x_3 + 3$, $x_4 + 3$. The UE is $x_1 = 2, x_2 = x_3 = x_4 = 0$. Four paths are numbered as path $1, 2, 3, 4$.

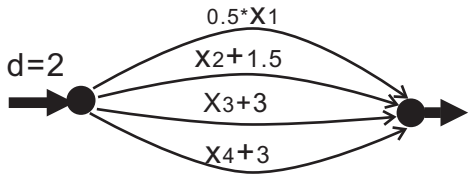

Figure 4.2: Single-OD pair network illustration

Solving MPEC, we have $\varepsilon_0^* = 0, \varepsilon_1^* = 0.5, \varepsilon_2^* = 2, \varepsilon_3^* = \infty$. There are three cases for the largest ε-acceptable path sets:

(1) $0 \leqslant \varepsilon < 0.5$: $\mathcal{P}_l^{\varepsilon} = \{1\}, \mathbf{f} = [2, 0, 0, 0]$;

(2) $0.5 \leqslant \varepsilon < 2$: $\mathcal{P}_l^{\varepsilon} = \{1, 2\}, \mathbf{f} = [2, 0, 0, 0]$;

(4) $\varepsilon \geqslant 2$: $\mathcal{P}_l^{\varepsilon} = \{1, 2, 3, 4\}, \mathbf{f} = [2, 0, 0, 0]$.

If ε is calibrated from empirical data as 1.5, then $\mathcal{P}_l^{1.5} = \{1, 2\}$. Therefore, $\mathcal{P}^{1.5} = \{\{1\}\{1, 2\}\}$.

4.4.2 ε-acceptable path set for multiple OD pairs

For a network with total W OD pairs, let ε_j^{*w} be the critical point for OD pair $w \in \mathcal{W}$, $j = 0, 1, \cdots, J^w$. Then $\varepsilon_j^* \triangleq \left\{\varepsilon_j^{*w}\right\}$ is a set of critical points for all OD pairs, assuming $\varepsilon_0^{*w} = 0, w \in \mathcal{W}$.

Given $\varepsilon = (\varepsilon^1, \cdots, \varepsilon^W)$, if $\varepsilon_{n_{K_1}}^1 \leqslant \varepsilon^1 < \varepsilon_{n_{K_1+1}}^1, \cdots, \varepsilon_{n_{K_W}}^W \leqslant \varepsilon^W < \varepsilon_{n_{K_W+1}}^W$, then the largest ε-acceptable set for multiple OD pairs is the union of the largest ε-acceptable set for each OD path pair:

$$\mathcal{P}_l^{\varepsilon} = \mathcal{P}_l^{(\varepsilon^1, \cdots, \varepsilon^w, \cdots, \varepsilon^W)} = \mathcal{P}_l^{\varepsilon_{n_{K_1}}^{*1}} \bigcup \cdots \bigcup \mathcal{P}_l^{\varepsilon_{n_{K_W}}^{*W}}. \tag{4.4.3}$$

where $\mathcal{P}_l^{\varepsilon_{n_{K_w}}^{*w}}$ is the largest $\varepsilon_{n_{K_w}}^{*w}$-acceptable set for OD pair w and can be solved by MPEC (4.4.1).

The ε-acceptable path set is composed of multiple largest $\varepsilon_{n_{K_w}}^{*w}$-acceptable sets when varying ε_j^{*w} among every critical point across all OD pairs:

$$\mathcal{P}^{\varepsilon} = \mathcal{P}^{(\varepsilon^1, \cdots, \varepsilon^w, \cdots, \varepsilon^W)} = \left\{\mathcal{P}_l^{(\varepsilon^1, \cdots, \varepsilon_j^{*w}, \cdots, \varepsilon^W)}\right\}_{\varepsilon_j^{*w}}, w \in \mathcal{W}, j = 0, 1, \cdots, J^w. \tag{4.4.4}$$

Now we will discuss how to solve each critical point for every OD pair. Regarding one OD pair $\nu \in \mathcal{W}$, the same approach of computing $\varepsilon_j^{*\nu}$ as mentioned in Equation (4.4.1) can be adopted. The only difference is, to compute path costs needs the information of path flows across all OD pairs. So path flows $\mathbf{f}^w, w \in \mathcal{W}, w \neq \nu$ are parameters when Equation (4.4.1) for ν is calculated. In other words, $\varepsilon_j^{*\nu}$ is a function of $\mathbf{f}^w, w \neq \nu$. But we only want those $\mathbf{f}^w, w \neq \nu$ such that $\varepsilon_j^{*\nu}$ which can be achieved. So accordingly, we modify Equation (4.4.1) to accommodate this distinction. For any OD pair ν and the $j^{th}, j = 1, \cdots, J^w$ the critical point ε_j^{ν} can be computed as:

$$\begin{aligned}
&\min \qquad \varepsilon_j^{\nu} \\
&s.t. \\
&0 \leqslant f_i^{\nu} \perp C_i^{\nu}(\mathbf{f}) + \rho_i^{\nu} - \pi^{\nu} \geqslant 0, \forall i \in \mathcal{P}^{\nu}, && \text{(4.4.5a)} \\
&\sum_{j \in \mathcal{P}^w} f_j^w = d^w, \forall w \in \mathcal{W}, && \text{(4.4.5b)} \\
&d^{\nu} - \sum_{j \in \mathcal{P}_l^{\varepsilon_{j-1}^{*\nu}}} f_j^{\nu} > 0, && \text{(4.4.5c)} \\
&0 \leqslant \rho_i^{\nu} \leqslant \varepsilon_j^{\nu}, \forall i \in \mathcal{P}^{\nu}, && \text{(4.4.5d)} \\
&0 \leqslant f_i^{\nu} + C_i^{\nu}(\mathbf{f}) + \rho_i^{\nu} - \pi^{\nu} > 0, \forall i \in \mathcal{P}^{\nu}. && \text{(4.4.5e)}
\end{aligned}$$

The algorithm of calculating $\boldsymbol{\varepsilon}$-acceptable path set for multiple OD pairs is thus summarized as follows:

1. Calculate $\varepsilon_j^{*\nu}(j = 1, \cdots, J^w, \nu \in \mathcal{W})$ from Equation (4.4.5) and obtain the ε^{ν}-acceptable path set for OD pair ν;

2. As a by-product of solving Equation (4.4.5), one feasible path flow pattern $\mathbf{f}^{*w}, w \neq \nu$ is attained simultaneously. Denote the longest used path for OD pair $w, \forall w \neq \nu$ as $p^w := \left\{ \max_{j \in \mathcal{P}^w} C_j^w(\mathbf{f}), f_i^w > 0 \right\}$ and compute $C_p^w(\mathbf{f})$. Then the $i^{th}(i = 1, \cdots, J^w)$ critical point for OD pair w is computed as: $\varepsilon_i^{*w} = C_p^w(\mathbf{f}) - \min_{j \in \mathcal{P}^w} C_j^w(\mathbf{f})$;

3. After obtaining the critical points ε_i^{*w} $(i = 1, \cdots, J^w, w \neq \nu)$, if $\varepsilon_{i-1}^{*w} < C_p^w(\mathbf{f}) - \min_{j \in \mathcal{P}^w} C_j^w(\mathbf{f}) < \varepsilon_i^{*w}$, $\mathbf{f}^{*w}(w \neq \nu)$ is also a BRUE path flow pattern. Then the path p^w is acceptable when $\varepsilon_j^{\nu} < \varepsilon_j^{*\nu}$ and $\varepsilon_i^w < \varepsilon_i^{*w}$; or else path p^w is unacceptable;

4. Combine the acceptable paths under various combinations of critical points among all OD pairs and the ε-acceptable path set $\mathcal{P}^{\varepsilon}$ is obtained.

The following example will illustrate how to construct the $\boldsymbol{\varepsilon}$-acceptable path set for multiple OD pairs.

Example 4.4.2. The topology of the test network, two OD demands and link cost functions are illustrated above each link in Figure (4.3). Red curves on the right indicate six paths, denoted by the number of links it passes along: 1-3, 1-4, 2-3, 2-4, 1, 2. The first four paths belong to OD pair 1 and the rest two belong to OD pair 2. The equilibrium path flow pattern is $f_1 = 0, f_2 = 1, f_3 = 0, f_4 = 0, f_5 = 1, f_6 = 0$.

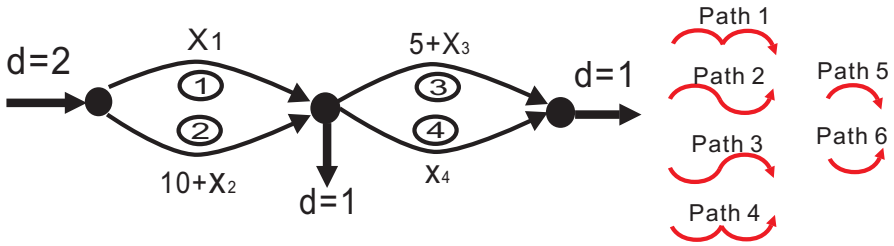

Figure 4.3: Two-OD pair network and paths illustration

Based on Equation (4.4.5), $\varepsilon_1^{*1}, \varepsilon_2^{*1}$ and ε_1^{*2} can be computed separately. The critical points for each OD pair are:

For OD pair 1,

(1) $0 \leqslant \varepsilon^1 < 4$: $\mathcal{P}^{\varepsilon^1} = \{2\}$;

(2) $4 \leqslant \varepsilon^1 < 8$: $\mathcal{P}^{\varepsilon^1} = \{\{2\}, \{1,2\}\}$;

(2) $8 \leqslant \varepsilon^1 < 12$: $\mathcal{P}^{\varepsilon^1} = \{\{2\}, \{1,2\}, \{1,2,4\}\}$;

(3) $\varepsilon^1 \geqslant 12$: $\mathcal{P}^{\varepsilon^1} = \{\{2\}, \{1,2\}, \{1,2,4\}, \{1,2,3,4\}\}$.

For OD pair 2,

(1) $0 \leqslant \varepsilon^2 < 8$: $\mathcal{P}^{\varepsilon^2} = \{5\}$;

(2) $\varepsilon^2 \geqslant 8$: $\mathcal{P}^{\varepsilon^2} = \{\{5\}, \{5,6\}\}$;

Combing two OD pairs, the overall ε-acceptable path set under different combination of critical points is:

$$\mathcal{P}^{\varepsilon} = \begin{cases} \{2,5\}, 0 \leqslant \varepsilon^1 \leqslant 4, 0 \leqslant \varepsilon^2 \leqslant 8; \\ \{\{2,5\},\{2,5,6\}\}, 0 \leqslant \varepsilon^1 \leqslant 4, \varepsilon^2 \geqslant 8; \\ \{\{2,5\},\{1,2,5\}\}, 4 \leqslant \varepsilon^1 \leqslant 8, 0 \leqslant \varepsilon^2 \leqslant 8; \\ \{\{2,5\},\{1,2,5\},\{2,5,6\},\{1,2,5,6\}\}, 4 \leqslant \varepsilon^1 \leqslant 8, \varepsilon^2 \geqslant 8; \\ \{\{2,5\},\{1,2,5\},\{1,2,4,5\}\}, 8 \leqslant \varepsilon^1 \leqslant 12, 0 \leqslant \varepsilon^2 \leqslant 8; \\ \{\{2,5\},\{1,2,5\},\{1,2,4,5\},\{2,5,6\},\{1,2,5,6\},\{1,2,4,5,6\}\}, 8 \leqslant \varepsilon^1 \leqslant 12, \varepsilon^2 \geqslant 8; \\ \{\{2,5\},\{1,2,5\},\{1,2,4,5\},\{1,2,3,4,5\}\}, \varepsilon^1 \geqslant 12, 0 \leqslant \varepsilon^2 \leqslant 8; \\ \{\{2,5\},\{1,2,5\},\{1,2,4,5\},\{2,5,6\},\{1,2,5,6\}, \\ \{1,2,4,5,6\},\{1,2,3,4,5\},\{1,2,3,4,5,6\}\}, \varepsilon^1 \geqslant 12, \varepsilon^2 \geqslant 8. \end{cases} \tag{4.4.6}$$

All acceptable path sets are also illustrated in the following figure: numbers in each block display acceptable path numbers for certain (ε^1,ε^2) pair. The left bottom block for ($\varepsilon^1 < 4$,$\varepsilon^2 < 8$) is the UE shortest path set. How to get acceptable paths for ($\varepsilon^1 \geqslant 4$,$\varepsilon^2 < 8$) in the block to its right will be explained in the following and other blocks follow the same line of reason. As described above in steps (2) and (3), one path flow pattern $f_1 = 0.001, f_2 = 0.9999, f_3 = 0, f_4 = 0, f_5 = 1, f_6 = 1$ is attained when $\varepsilon^1 = 4$ is solved from Equation (4.4.5). For OD pair 1, its path flow increases from 0 to a positive number 0.001, meaning that path 1 will start to carry flows if $\varepsilon^1 > 4$; the utilized path 5 has the cost of 2 and the unused path 6 has the cost of 10. Their cost difference is 8. When $\varepsilon^2 < 8$, only path 5 is acceptable for OD pair 2. Therefore, when $\varepsilon^1 \geqslant 4$ and $\varepsilon^2 < 8$, only paths 1,2 (connecting OD pair 1) and 5 (connecting OD pair 2) are acceptable.

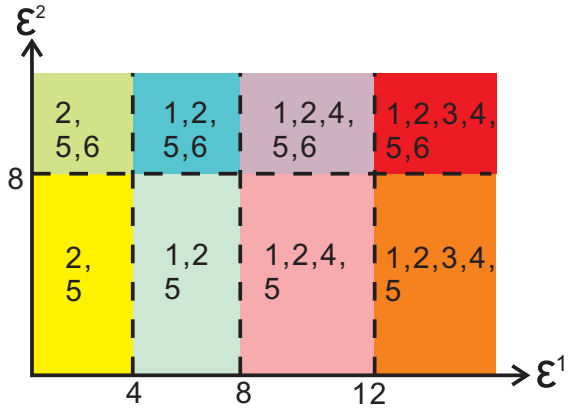

Figure 4.4: Acceptable paths for critical point pairs (ε^1,ε^2)

By far we have proposed how to solve the ε-acceptable path set for both single OD pair and multiple OD pairs. In the following we will discuss the methodology of constructing the ε-BRUE path flow set.

4.5 Construction of ε-BRUE path flow set

Generally the ε-BRUE set is non-convex (Lou et al. 2010), so it is not easy to construct it directly. If we can decompose the whole BRUE set into small subsets, which are easier to study, then constructing the whole set can be reduced to constructing each subset. Based on this idea, the key step is to explore the interior structure of the ε-BRUE set and identify these simpler subsets.

In Section (4.4), we analyze the interior structure of the ε-acceptable path set: as the indifference band gradually increases, more paths will begin to carry flows. Correspondingly, the ε-BRUE set can be decomposed into subsets as well, with only acceptable paths carrying flows for each subset. Denote the k^{th} subset as $\mathcal{F}_k^\varepsilon$ and K as the total number of largest ε-acceptable path sets. Mathematically, $\mathcal{F}_{BRUE}^\varepsilon$ is the union of $K+1$ disjoint subsets:

$$\mathcal{F}_i^\varepsilon \bigcap \mathcal{F}_j^\varepsilon = \emptyset, i, j = 0, \cdots, K, i \neq j; \tag{4.5.1a}$$

$$\mathcal{F}_{BRUE}^\varepsilon = \bigcup_{k=0}^{K} \mathcal{F}_k^\varepsilon. \tag{4.5.1b}$$

According to the largest acceptable path set defined in Equation (4.3.2), the k^{th} ε-BRUE path flow subset is defined as:

$$\begin{aligned} \mathcal{F}_0^{\varepsilon} &= \{\mathbf{f} \in \mathcal{F}_{BRUE}^{\varepsilon} : a^{\varepsilon}(\mathbf{f}) \subseteq \mathcal{P}_{UE}\}, \\ \mathcal{F}_k^{\varepsilon} &= \{\mathbf{f} \in \mathcal{F}_{BRUE}^{\varepsilon} : \mathcal{P}_l^{\varepsilon_{k-1}^*} \subset a^{\varepsilon}(\mathbf{f}) \subseteq \mathcal{P}_l^{\varepsilon_k^*}\}, k = 1, \cdots, K. \end{aligned} \tag{4.5.2}$$

where $\mathcal{P}_l^{\varepsilon_k^*}$ is the largest ε_k^*-acceptable path set defined in (4.3.5).

4.5.1 ε-BRUE path flow set for one OD pair

Equation (4.5.2) defines the k^{th} subset of the ε-BRUE path flow set. In this section, we will explore how to construct each subset. By defining a sequence of sets $\mathcal{S}_k^{\varepsilon}, k = 0, \cdots, K$ and assigning all travel demands to paths from the associated largest path set, we get:

$$\begin{aligned} \mathcal{S}_0^{\varepsilon} \triangleq \{\mathbf{f} \in \mathcal{F} : \quad & \forall \quad i \in \mathcal{P}_{UE} : f_i, f_j \geqslant 0, |C_i(\mathbf{f}) - C_j(\mathbf{f})| \leqslant \varepsilon; \\ & \forall \quad i \notin \mathcal{P}_{UE} : f_i = 0\}. \end{aligned}$$

$$\begin{aligned} \mathcal{S}_k^{\varepsilon} \triangleq \{\mathbf{f} \in \mathcal{F} : \quad & \forall \quad i \in \mathcal{P}_l^{\varepsilon_{k-1}^*} : f_i \geqslant 0; \exists i \in \mathcal{P}_l^{\varepsilon_k^*} \backslash \mathcal{P}_l^{\varepsilon_{k-1}^*} : f_i > 0; \\ & \forall \quad i, j \in \mathcal{P}_l^{\varepsilon_k^*} : |C_i(\mathbf{f}) - C_j(\mathbf{f})| \leqslant \varepsilon; \\ & \forall \quad i \notin \mathcal{P}_l^{\varepsilon_k^*} : f_i = 0\}, k = 1, \cdots, K. \end{aligned} \tag{4.5.3}$$

where $\mathcal{P}_l^{\varepsilon_k^*}$ is defined in (4.3.5).

The set $\mathcal{S}_0^{\varepsilon}$ contains all feasible path flow patterns where only the UE shortest paths carry flows and the cost difference between any two shortest paths are within the band ε. For the set $\mathcal{S}_k^{\varepsilon}, k = 1, \cdots, K$, there are two types of paths: the newly acceptable paths will carry flows and those belonging to the ε_{k-1}^*-largest acceptable paths may carry flow or not. The cost difference between any two acceptable or zero-acceptable paths are within the band ε. By definition, each subset is disjoint, i.e., $\bigcap_{k=0}^{K} \mathcal{S}_k^{\varepsilon} = \emptyset$; and it is a subset of the ε-BRUE set, i.e., $\mathcal{S}_k^{\varepsilon} \subseteq \mathcal{F}_{BRUE}^{\varepsilon}$. The following proposition will show that $\mathcal{F}_k^{\varepsilon}$ and $\mathcal{S}_k^{\varepsilon}$ are equivalent sets.

Proposition 4.5.1.

$$\mathcal{F}_k^\varepsilon = \mathcal{S}_k^\varepsilon, k = 0, \cdots, K. \tag{4.5.4}$$

where $\mathcal{F}_k^\varepsilon$ is defined in (4.5.2), $\mathcal{S}_k^\varepsilon$ is defined in (4.5.3).

Proof. (1)$\mathcal{F}_k^\varepsilon \subseteq \mathcal{S}_k^\varepsilon, k = 0, \cdots, K$.

$\forall \mathbf{f} \in \mathcal{F}_k^\varepsilon$, by definition, $a^\varepsilon(\mathbf{f}) \subseteq \mathcal{P}^{\varepsilon_k^*}$, i.e., $\forall i, j \in a^\varepsilon(\mathbf{f}), C_i(\mathbf{f}) \leqslant \min_{j \in \mathcal{P}} C_j(\mathbf{f}) + \varepsilon \leqslant C_j(\mathbf{f}) + \varepsilon \Rightarrow C_i(\mathbf{f}) - C_j(\mathbf{f}) \leqslant \varepsilon$. Similarly, $C_j(\mathbf{f}) - C_i(\mathbf{f}) \leqslant \varepsilon$. In summary, $|C_i(\mathbf{f}) - C_j(\mathbf{f})| \leqslant \varepsilon, \forall i, j \in \mathcal{P}_l^{\varepsilon_k^*} \Rightarrow \mathbf{f} \in \mathcal{S}_k^\varepsilon$.

(2)$\mathcal{S}_k^\varepsilon \subseteq \mathcal{F}_k^\varepsilon, k = 0, \cdots, K$.

When $k = 0$:

$\forall i \in a^\varepsilon(\mathbf{f}), \mathbf{f} \in \mathcal{S}_0^\varepsilon$, we need to show $i \in \mathcal{P}_{UE}$. Assume $i \notin \mathcal{P}_{UE}$, since $\mathbf{f} \in \mathcal{S}_0^\varepsilon$, then $f_i = 0$. On the other hand, because $i \in a^\varepsilon(\mathbf{f})$, $f_i > 0$, contradicted with $f_i = 0$. Thus $\forall i \in a^\varepsilon(\mathbf{f}), i \in \mathcal{P}_{UE}$, i.e., $a^\varepsilon(\mathbf{f}) \subseteq \mathcal{P}_{UE}, \forall \mathbf{f} \in \mathcal{S}_0^\varepsilon \subseteq \mathcal{F}_{BRUE}^\varepsilon \Rightarrow \mathbf{f} \in \mathcal{F}_0^\varepsilon$. So $\mathcal{F}_0^\varepsilon \subseteq \mathcal{S}_0^\varepsilon$. Combing with the result from (1), $\mathcal{F}_0^\varepsilon = \mathcal{S}_0^\varepsilon$.

When $k = 1$, similarly, $a^\varepsilon(\mathbf{f}) \subseteq \mathcal{P}^{\varepsilon_1^*}, \forall \mathbf{f} \in \mathcal{S}_1^\varepsilon$, and $\mathcal{P}_{UE} \subset a^\varepsilon(\mathbf{f})$ as $\exists i \in \mathcal{P}_l^{\varepsilon_1^*} \backslash \mathcal{P}_{UE}$: $f_i > 0$, i.e., at least one newly added path needs to carry flow. Because $\mathcal{S}_1^\varepsilon \subseteq \mathcal{F}_{BRUE}^\varepsilon \backslash \mathcal{S}_0^\varepsilon$, and $\mathcal{F}_0^\varepsilon = \mathcal{S}_0^\varepsilon$, therefore $\mathcal{P}_{UE} \subset a^\varepsilon(\mathbf{f}) \subseteq \mathcal{P}_l^{\varepsilon_1^*}, \forall \mathbf{f} \in \mathcal{F}_{BRUE}^\varepsilon \backslash \mathcal{F}_0^\varepsilon$, so $\mathbf{f} \in \mathcal{F}_1^\varepsilon$.

We can repeat this proof similarly for $k = 2, \cdots, K$. Therefore $\mathcal{S}_k^\varepsilon \subseteq \mathcal{F}_k^\varepsilon, k = 0, \cdots, K$.

In conclusion, $\mathcal{F}_k^\varepsilon = \mathcal{S}_k^\varepsilon, k = 0, \cdots, K$. □

Proposition (4.5.1) shows that by constructing each flow subset as in Equation (4.5.3), then it is equivalent to the definition of the subset in Equation (4.5.2). The union of these subsets constitutes the ε-BRUE set:

Corollary 3.

$$\mathcal{F}_{BRUE}^\varepsilon = \bigcup_{k=1}^{K} \mathcal{S}_k^\varepsilon. \tag{4.5.5}$$

where $\mathcal{S}_j^\varepsilon$ is defined in Equation (4.5.3). In summary, Proposition (4.5.4) and Corollary (3) provide the methodology of constructing the ε-BRUE set. The following example will illustrate this methodology.

Example 4.5.1. The topology of the test network, the OD demand between nodes $1 - 4$ and link cost functions are illustrated in Figure (4.5) with $\varepsilon = 15$. Red lines

display four paths: 1-3-4 (path 1),1-3-2-4 (path 2), 1-2-3-4 (path 3), 1-2-4 (path 4). The equilibrium path flow pattern is $[2, 2, 0, 2]$, i.e., path 1,2 and 4 are utilized under UE. Substituting $\mathcal{P}_l^{\varepsilon_0^*} = \{1, 2, 4\}$, path costs and demands into MPEC (4.4.2), we obtain $\varepsilon_1^* = 6.5, \mathbf{f} = [1.5, 3, 0, 1.5], C(\mathbf{f}) = [96.5, 103, 103, 96.5]$. In other words, if $\varepsilon_1^* > 6.5$, path 3 is utilized as well. Since $\varepsilon = 15 > \varepsilon_1^*$, we know $\mathcal{P}^{\varepsilon=15} = \{\{1, 2, 4\}, \{1, 2, 3, 4\}\}$.

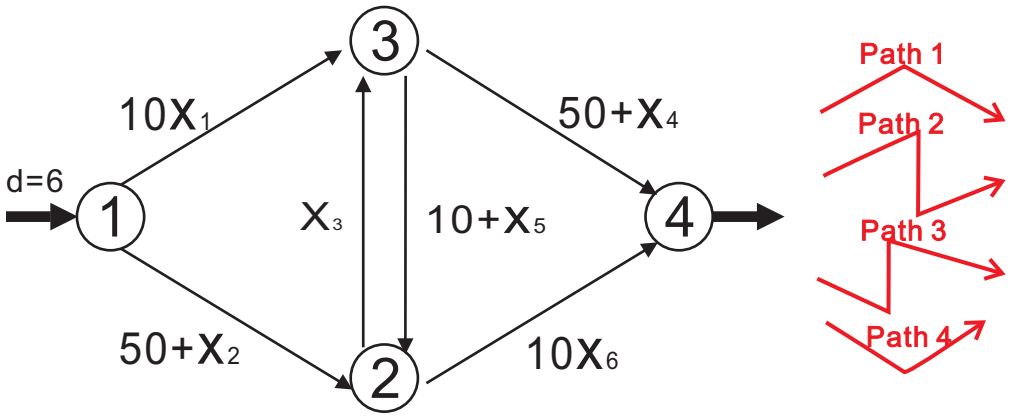

Figure 4.5: Single OD pair network illustration

Due to flow conservation of the fixed demand, its BRUE solution set can be characterized by the first three paths. The whole BRUE solution set is shown in Figure (4.6), composed of a 3-path yellow subset and a 4-path magenta subset. Each subset satisfies Equation (4.5.4):

$$\begin{aligned}
\mathcal{F}_0^{\varepsilon=15} &= \{\mathbf{f} \in \mathcal{F} : \forall i \in \{1, 2, 4\} : f_i, f_j \geqslant 0, |C_i(\mathbf{f}) - C_j(\mathbf{f})| \leqslant 15, f_1 + f_2 + f_4 = 6; f_3 = 0\}; \\
\mathcal{F}_1^{\varepsilon=15} &= \{\mathbf{f} \in \mathcal{F} : \forall i \in \{1, 2, 4\} : f_i \geqslant 0; f_3 > 0; f_1 + f_2 + f_3 + f_4 = 6; \\
&\quad \forall i, j \in \{1, 2, 3, 4\} : |C_i(\mathbf{f}) - C_j(\mathbf{f})| \leqslant 15\}.
\end{aligned}$$

Within $\mathcal{F}_0^{\varepsilon=15}$, path 3 does not carry flow, so the 3-path subset is on the bottom of the (f_1, f_2, f_3) coordinates; Within $\mathcal{F}_1^{\varepsilon=15}$, path 3 begins to carry flow and $f_3 > 0$. Either the 3-path subset or the 4-path subset is convex, but their union is not convex, which is consistent with results in Lou et al. (2010).

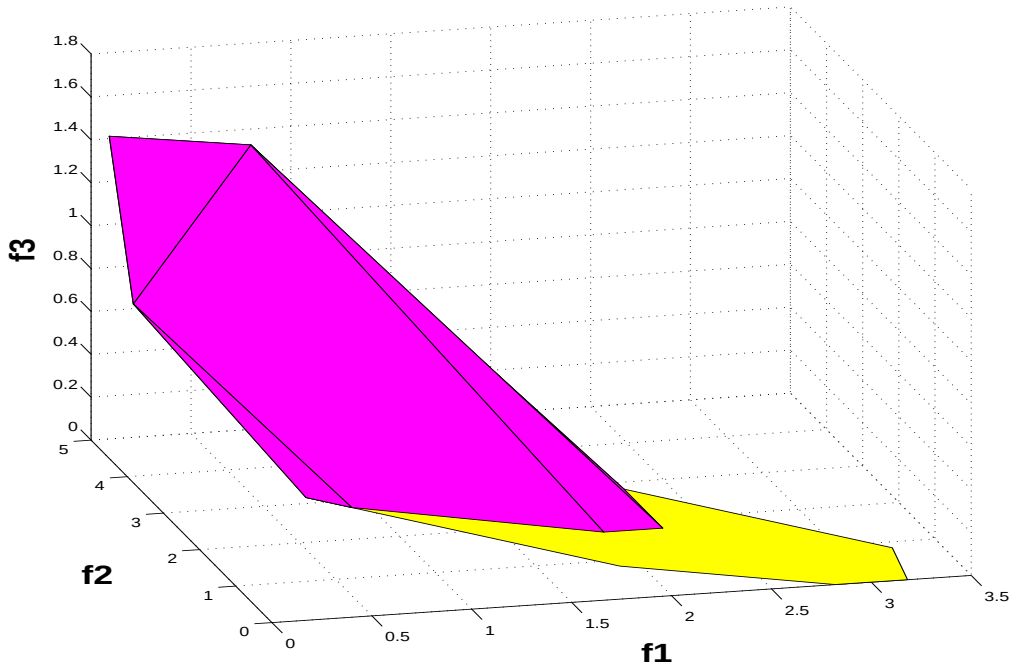

Figure 4.6: BRUE solution set illustration composed of two pieces

4.5.2 ε-BRUE path flow set for multiple OD pairs

After knowing the methodology of obtaining all acceptable paths sets for multiple OD pairs in Section (4.4.2), it is not difficulty to generalize the methodology of constructing the ε-BRUE set for a single OD pair to multiple OD pairs. For a network with multiple OD pairs, the ε-BRUE set is the union of all subsets where demands are assigned to all acceptable paths across OD pairs:

$$\mathcal{F}_{BRUE}^{\varepsilon} = \bigcup_{k=1}^{K} \mathcal{S}_k^{\varepsilon^*}, \tag{4.5.6}$$

where,

$$\begin{aligned} \mathcal{S}_1^{\varepsilon} \triangleq \{\mathbf{f} \in \mathcal{F}: \quad & \forall \quad i,j \in \mathcal{P}_{UE}: f_i^w, f_j^w \geqslant 0, |C_i^w(\mathbf{f}) - C_j^w(\mathbf{f})| \leqslant \varepsilon^w; \\ & \forall \quad i \notin \mathcal{P}_{UE}: f_i^w = 0, w \in W\}. \end{aligned}$$

$$\mathcal{S}_k^{\varepsilon} \triangleq \{\mathbf{f} \in \mathcal{F}: \quad \forall \quad i \in \mathcal{P}_l^{\varepsilon_{k-2}^*}: f_i^w \geqslant 0; \exists i \in \mathcal{P}_l^{\varepsilon_{k-1}^*} \backslash \mathcal{P}_l^{\varepsilon_{k-2}^*}: f_i^w > 0;$$
$$\forall \quad i,j \in \mathcal{P}_l^{\varepsilon_{k-1}^*}: |C_i^w(\mathbf{f}) - C_j^w(\mathbf{f})| \leqslant \varepsilon^w;$$
$$\forall \quad i \notin \mathcal{P}_l^{\varepsilon_{k-1}^*}: f_i^w = 0, w \in W\}, k = 2, \cdots, K.$$

where, K is the total number of acceptable path sets; $\mathcal{P}_l^{\varepsilon_k^*}$ is defined in Equation (4.4.3).

4.6 Topological properties of the BRUE set

After the BRUE path flow set is obtained, it is crucial to explore its topological properties to facilitate BR related applications.

4.6.1 Closedness and compactness

A closed set can guarantee that if the solution is on the boundary, it can be attained. Compactness of a set has many well-established characteristics in the field of topology. So it is essential to know whether the BRUE set is compact or not.

Heine-Borel theorem says that, if a set is closed and bounded, then it is compact. So boundedness and closedness will be established first.

Proposition 4.6.1. *$\mathcal{F}_{BRUE}^{\varepsilon}$ is bounded.*

Proof. Since $\mathcal{F}$ is bounded, and $\mathcal{F}_{BRUE}^{\varepsilon} \subset \mathcal{F}$. Thus $\mathcal{F}_{BRUE}^{\varepsilon}$ is bounded. □

Proposition 4.6.2. *$\mathcal{F}_{BRUE}^{\varepsilon}$ is closed.*

Proof. $\mathcal{F}_{BRUE}^{\varepsilon}$ defined by Inequalities (4.5.2) is closed obviously. Since the union of the closed sets are closed, so $\mathcal{F}_{BRUE}^{\varepsilon}$ is closed. □

Following the two propositions above and Heine-Borel theorem, we have:

Corollary 4. *$\mathcal{F}_{BRUE}^{\varepsilon}$ is compact.*

4.6.2 Connectedness

A topological space X is said to be connected if it cannot be represented as the union of two disjoint, nonempty, open sets. A topological space X is said to be path connected if for all $x_1, x_2 \in X$, there exists a path τ such that $\tau(0) = x_1$ and $\tau(1) = x_2$. It can be

shown that if X is path connected, it is also connected. So we will show that $\mathcal{F}^{\varepsilon}_{BRUE}$ is path-connected and therefore connected.

Proposition 4.6.3. *$\mathcal{F}^{\varepsilon}_{BRUE}$ is connected given affine linear cost functions.*

Proof. First of all, it can be shown that each subset is connected. Each subset is the solution set of a system of linear inequalities $|C_i(\mathbf{f}) - C_j(\mathbf{f})| \leqslant \varepsilon, \forall i, j \in \mathcal{P}_{UE}$ or $\mathcal{P}^k_l, k = 0, \cdots, K$, which is a polytope, so it is connected.

Secondly, we will show that $\mathcal{F}^{\varepsilon}_k, k = 0, \cdots, K-1$ and $\mathcal{F}^{\varepsilon}_{k+1}$ are connected pairwise by mathematical induction. Start with $k = 0$. The monotonic property implies that $\mathcal{P}_{UE} \subset \mathcal{P}^1_l$.

Denote $\mathbf{f}^0 \in \mathcal{F}^{\varepsilon}_0, \mathbf{f}^1 \in \mathcal{F}^{\varepsilon}_1$. Let the path $k \in \mathcal{P}^1_l \backslash \mathcal{P}_{UE}$. Then for $\mathbf{f}^0$: $f^0_k = 0, |C_k(\mathbf{f}^0) - C_i(\mathbf{f}^0)| > \varepsilon, \forall i \in \mathcal{P}_{UE}$. For $\mathbf{f}^1$: $f^1_k > 0, C_k(\mathbf{f}^1) - C_i(\mathbf{f}^1) > \varepsilon, \forall i \in \mathcal{P}_{UE}$. With continuous path cost functions, there must exist a flow pattern $\mathbf{f}^* \in \mathcal{F}^{\varepsilon}_0$ such that $f^*_k = 0, |C_k(\mathbf{f}^*) - C_i(\mathbf{f}^*)| \leqslant \varepsilon, \forall i \in \mathcal{P}_{UE}$. Then $\mathbf{f}^* \in \mathcal{F}^{\varepsilon}_1$. Consequently $\mathbf{f}^* \in \mathcal{F}^{\varepsilon}_0 \bigcap \mathcal{F}^{\varepsilon}_1 \neq \emptyset$.

As $\mathcal{F}^{\varepsilon}_0$ and $\mathcal{F}^{\varepsilon}_1$ are connected, i.e., there exist paths p_0, p_1 joining $\mathbf{f}^0$, $\mathbf{f}^1$ with $\mathbf{f}^*$ respectively. Therefore there exists a path $p = p_0 \bigcup p_1$ joining $\mathbf{f}^0$ and $\mathbf{f}^1$ through $\mathbf{f}^*$, i.e., $\mathcal{F}^{\varepsilon}_0$ and $\mathcal{F}^{\varepsilon}_1$ are path-connected and therefore connected pairwise.

Similarly, $\mathcal{F}^{\varepsilon}_k$ and $\mathcal{F}^{\varepsilon}_{k+1}, k = 1, \cdots, K-1$ are connected pairwise. In conclusion, $\mathcal{F}^{\varepsilon}_{BRUE} = \bigcup^K_{k=0} \mathcal{F}^{\varepsilon}_k$ is connected.

□

4.6.3 Non-convexity

Lou et al. (2010) illustrated the non-convexity of $\mathcal{F}^{\varepsilon}_{BRUE}$. The following validates theoretically this statement:

Proposition 4.6.4. *Given affine linear link performance function, $\mathcal{F}^{\varepsilon}_k$ is a polytope; however, $\mathcal{F}^{\varepsilon}_{BRUE}$ is generally non-convex.*

Proof. An immediate result from inequalities (4.5.2) showing that $\mathcal{F}^{\varepsilon}_k$ is a polytope. However, the union of the convex sets are not necessarily convex; furthermore, as the number of acceptable paths each polyhedron contains is different, so the union of polytope in different dimensions is surely not convex if there exists more than one subset. □

Chapter 5

Boundedly rational Braess paradox

5.1 Introduction and motivation

The network design problem (NDP) is to improve the road network performance by determining a set of plans, such as building new roads, expanding existing roads or enforcing congestion pricing, based on certain route choice behavior assumption (Yang and Bell 1998b). However, building more roads may not necessarily enhance the system performance due to the Braess paradox (Braess 1969; Braess et al. 2005). Network planners should be cautious of the Braess paradox while making a new network design.

5.1.1 Literature review on the Braess paradox

The Braess paradox was first illustrated by a real-life example in Stuttgart: A road investment failed to yield expected benefits until another street was closed (Murchland 1970). Its existence was also tested in various experimental games from the perspective of the behavioural theory (Rapoport et al. 2009, Schneider and Weimann 2004, Selten et al. 2004).

Murchland (1970) analyzed that the Braess paradox results from self routing and suggested avoiding it by reducing the discrepancy between selfish routing and optimal routing. Researchers further explored conditions when the Braess paradox occurs: Pas and Principio (1997) showed that Braess paradox only occurs when the travel demand is within a certain range. Frank (1981) and Steinberg and Zangwill (1983) studied necessary and sufficient conditions when the Braess paradox occurs for general networks with linear link cost functions; Dafermos and Nagurney (1984) proposed a positive semidefinite matrix to test whether the paradox occurs with asymmetric link travel times.

There are also many studies extending the paradox to more general contexts. Smith (1978) illustrated how an increase in the travel time on an uncongested road can lead to a reduction in the total delay. Fisk (1979) studied the paradox in a two-mode network with transit and auto, where transit travel time may decrease when the auto demand increases. Steinberg and Stone (1988) showed that an increase in one link's congestion level can lead to abandonment of another link. Yang and Bell (1998a) found that adding a new road segment might reduce the network capacity.

In addition, the Braess paradox was shown to prevail in other types of networks: computer networks (Kameda et al. 2000; Korilis et al. 1999), mechanical and electrical networks (Cohen and Horowitz 1991), large-scale random graphs (Valiant and Roughgarden 2006) and large sparse graphs (Chung and Young 2010).

5.1.2 Contribution

The contributions of this chapter are two-fold:

- This chapter generalizes the existence conditions of the Braess paradox from the classical Braess network to grid networks with Bureau of Public Roads (BPR) link performance functions and shows that the Braess paradox can easily occur in ordinary networks;

- Given the boundedly rational assumption, how travelers react to addition of new links in a network has never been explored. This chapter aims to shed light on when the Braess paradox occurs under the boundedly rational driver behavior in the classical Braess network and ordinary grid networks. Especially, the impacts

of the indifference band and the congestion sensitivity of link cost functions on the occurrence of the Braess paradox is analyzed. This study can thus offer guidelines for network planners when network design proposals are made within the boundedly rational framework.

This chapter is organized as follows. In Section 5.2, the definition of bounded rationality user equilibria (BRUE) and the methodology of characterizing the BRUE set in the classical Braess network are given. Due to non-uniqueness of the BRUE set, three attitudes, risk-averse, risk-neutral and risk-prone towards building new links are discussed, which are based on the best, the worst and the distribution of the system travel time respectively. In Section 5.3, the paradox analysis starts with the Braess network with affine linear link performance functions. The methodologies of computing the best and the worst flow patterns are introduced. When the Braess paradox happens given the demand level and the indifference band are followed. In Section 5.4, the paradox analysis is discussed in grid networks with nonlinear link performance functions and a more general condition of the occurrence of the paradox is given.

5.2 Braess paradox under boundedly rational user equilibrium

The transportation network is represented by a directed graph that includes a set of consecutively numbered nodes, $\mathcal{N}$, and a set of consecutively numbered links, $\mathcal{L}$. Let $\mathcal{W}$ denote the origin-destination (OD) pair set (with W OD pairs) connected by a set of simple paths (composed of a sequence of distinct nodes), $\mathcal{P}^w$, through the network. The traffic demand between each OD pair is $d^w \in \mathbb{R}_+$ (where $\mathbb{R}_+$ represents the set of all non-negative real numbers) and the traffic demand vector $\mathbf{d} = (d^w)_{w\in\mathcal{W}} \in \mathbb{R}_+^W$. Let f_i^w denote the flow on path $i \in \mathcal{P}^w$ for OD pair w, then the path flow vector is $\mathbf{f} = \{f_i^w\}_{i\in\mathcal{P}^w, w\in\mathcal{W}}$. The feasible path flow set is to assign the traffic demand onto the feasible paths: $\mathcal{F} \triangleq \{\mathbf{f} : \mathbf{f} \geqslant \mathbf{0}, \sum_{i\in\mathcal{P}^w} f_i^w = d^w, \forall w \in \mathcal{W}\}$. Denote x_a as the link flow on link a, then the link flow vector is $\mathbf{x} = \{x_a\}_{a\in\mathcal{L}}$. Each link $a \in \mathcal{L}$ is assigned a cost function which is a function of the link flow, written as $c(\mathbf{x})$. Let $\delta_{a,i}^w = 1$ if link a is on path i connecting OD pair w, and 0 if not; then $\Delta \triangleq \{\delta_{a,i}^w\}_{a\in\mathcal{L},i\in\mathcal{P}}^{w\in\mathcal{W}}$ denotes the

link-path incidence matrix. We have the relationship $\mathbf{x} = \Delta\mathbf{f}$. Denote $C_i^w(\mathbf{f})$ as the path cost on path i for OD pair w, then the path cost vector $C(\mathbf{f}) \triangleq \{C_i^w(\mathbf{f})\}_{i\in\mathcal{P}}^{w\in\mathcal{W}}$. So $C(\mathbf{f}) = \Delta^T c(\mathbf{x})$ under the additive path cost assumption.

Under the user equilibrium (UE), the paradox is defined as:

Definition 5.2.1. The Braess paradox happens, if the system travel time (STT) after new links are added is higher than the one without them, i.e., $STT_w > STT_{wo}$, where STT_w is the STT with new links and STT_{wo} is the one without.

Due to the non-uniqueness of the BRUE, the road network may operate at different equilibrium flow patterns with new links and without, resulting in uncertain road network operation. Network planners may hold different attitudes towards whether to build a new link or not if uncertainty exists:

- If network planners assume the worst case is most likely to happen after the new link is added, and the best case is very possible to occur without it, then we say that this planner has an attitude preference of 'risk-averse' towards building a new link;
- If network planners assume the best case is most likely to happen after the new link is built, while the worst case occurs most likely without it, then this planner holds an attitude of 'risk-prone' towards building the new link;
- If network planners' decisions are not affected by the degree of uncertainty in flow distributions and only the expected performance is considered with and without a new link, we call this attitude as 'risk-neutral.'

The worst and the best cases aforementioned can be represented by the maximum and the minimum STT values among the BRUE flow patterns:

Definition 5.2.2. In a network with W OD pairs with the traffic demand vector $\mathbf{d}$ and the indifference band vector $\boldsymbol{\varepsilon}$, the worst and the best cases are defined as the maximum and the minimum STT (denoted as 'w-STT' and 'b-STT' respectively) among the $\boldsymbol{\varepsilon}$-BRUE solution set, i.e.,

$$\text{w-}STT(\mathbf{d}, \boldsymbol{\varepsilon}) = \max_{\mathbf{f}\in\mathcal{F}_{BRUE}^{\boldsymbol{\varepsilon}}} STT(\mathbf{d}, \mathbf{f}), \tag{5.2.1a}$$

$$\text{b-}STT(\mathbf{d}, \boldsymbol{\varepsilon}) = \min_{\mathbf{f}\in\mathcal{F}_{BRUE}^{\boldsymbol{\varepsilon}}} STT(\mathbf{d}, \mathbf{f}). \tag{5.2.1b}$$

Assume there exists a distribution $g(STT)$ over the STT interval satisfying:

$$\int_{\text{b-}STT}^{\text{w-}STT} g(STT)dSTT = 1, \tag{5.2.2}$$

Then the expected performance is computed as the integral of the distribution from b-STT to w-STT, i.e.,

$$ESTT(\mathbf{d}, \boldsymbol{\varepsilon}) = \int_{\text{b-}STT}^{\text{w-}STT} STTg(STT)dSTT. \tag{5.2.3}$$

Based on different attitudes towards risk caused by non-uniqueness of the BRUE solution, the following scenarios for the Braess paradox are defined:

Definition 5.2.3. (a) Risk-averse Braess paradox happens, if the worst STT after new links are added is higher than the best one without them, i.e., w-STT_w > b-STT_{wo};

(b) Risk-prone Braess paradox happens, if the best STT after new links are added is higher than the worst one without them, i.e., b-STT_w > w-STT_{wo};

(c) Risk-neutral Braess paradox happens, provided distributions $g^w(STT), g^{wo}(STT)$ over the STT interval satisfying Equation (5.2.2),if its expectation after new links are added is higher than that without, i.e.,

$$\int_{\text{b-}STT}^{\text{w-}STT} STTg^w(STT)dSTT > \int_{\text{b-}STT}^{\text{w-}STT} STTg^{wo}(STT)dSTT.$$

Denote S_{RA} as the $(\mathbf{d}, \boldsymbol{\varepsilon})$ region for the risk-averse paradox where $(\mathbf{d}, \boldsymbol{\varepsilon}) \in \mathbb{R}_+^W \times \mathbb{R}_+^W$, S_{RP} for the risk-prone paradox and S_{RN} for the risk-neutral paradox. Mathematically,

$$S_{RA} = \{(\mathbf{d}, \boldsymbol{\varepsilon}) : \text{w-}STT_w > \text{b-}STT_{wo}\}, \tag{5.2.4a}$$

$$S_{RP} = \{(\mathbf{d}, \boldsymbol{\varepsilon}) : \text{b-}STT_w > \text{w-}STT_{wo}\}, \tag{5.2.4b}$$

$$S_{RN} = \left\{(\mathbf{d}, \boldsymbol{\varepsilon}) : \int_{\text{b-}STT}^{\text{w-}STT} STTg^w(STT)dSTT > \int_{\text{b-}STT}^{\text{w-}STT} STTg^{wo}(STT)dSTT\right\}. \tag{5.2.4c}$$

Then we have the following proposition for three paradox regions:

Proposition 5.2.1. $S_{RP} \subset S_{RN} \subset S_{RA}$.

Proof. (1) Show $S_{RP} \subset S_{RN}$.

Given $\int_{\text{b-}STT}^{\text{w-}STT} g^w(STT)dSTT = 1, \int_{\text{b-}STT}^{\text{w-}STT} g^{wo}(STT)dSTT = 1$, we have for all $(\mathbf{d}, \boldsymbol{\varepsilon}) \in \mathbb{R}_+^W \times \mathbb{R}_+^W$,

$$\text{b-}STT_w \leqslant \int_{\text{b-}STT}^{\text{w-}STT} STTg^w(STT)dSTT \leqslant \text{w-}STT_w,$$
$$\text{b-}STT_{wo} \leqslant \int_{\text{b-}STT}^{\text{w-}STT} STTg^{wo}(STT)dSTT \leqslant \text{w-}STT_{wo}.$$

If b-$STT_w >$ w-STT_{wo}, then

$$\int_{\text{b-}STT}^{\text{w-}STT} STTg^w(STT)dSTT \geqslant \text{b-}STT_w > \text{w-}STT_{wo} \geqslant \int_{\text{b-}STT}^{\text{w-}STT} STTg^{wo}(STT)dSTT.$$

Therefore $\int_{\text{b-}STT}^{\text{w-}STT} STTg^w(STT)dSTT > \int_{\text{b-}STT}^{\text{w-}STT} STTg^{wo}(STT)dSTT$ and then $S_{RP} \subset S_{RN}$.

(2) Show $S_{RN} \subset S_{RA}$. If $\int_{\text{b-}STT}^{\text{w-}STT} STTg^w(STT)dSTT > \int_{\text{b-}STT}^{\text{w-}STT} STTg^{wo}(STT)dSTT$, then

$$\text{w-}STT_w \geqslant \int_{\text{b-}STT}^{\text{w-}STT} STTg^w(STT)dSTT > \int_{\text{b-}STT}^{\text{w-}STT} STTg^{wo}(STT)dSTT \geqslant \text{b-}STT_{wo}.$$

So w-$STT_w >$ b-STT_{wo} and thus $S_{RN} \subset S_{RA}$.

□

Remark. The above proposition states that the risk-averse planners are the most conservative among three types of planners. Therefore a risk-averse paradox must be a risk-neutral or a risk-prone paradox; however, a risk-neutral or a risk-prone paradox is not necessarily a risk-averse one. The similar statement holds for the risk-neutral and the risk-prone paradox.

When the following conditions are satisfied, we have a "strong" definition of the Braess paradox:

Definition 5.2.4. (a) Braess paradox happens, if the best case after new links are added is higher than the worst one without them, i.e., b-$STT_w >$ w-STT_{wo};

(b) Braess paradox does not happen, if the worst case after new links are added is lower than the best one without them, i.e., w-$STT_w <$ b-STT_{wo}.

No matter which extremal values we use to determine the occurrence of the paradox, it is prerequisite to compute the worst and the best STTs. Given BRUE NCP formulation in Equation (4.2.6), solving the extremal cases is equivalent to solving mathematical programs with equilibrium constraints (MPEC):

$$
\begin{aligned}
&\min / \max \quad STT(\mathbf{d}, \mathbf{f}) \\
&s.t. \\
&0 \leqslant f_i^w \perp C_i^w(\mathbf{f}) + \rho_i^w - \pi^w \geqslant 0, \forall i \in \mathcal{P}^w, \forall w \in \mathcal{W}, \\
&0 \leqslant \pi^w \perp d^w - \sum_{i \in \mathcal{P}^w} f_i^w \geqslant 0, \forall w \in \mathcal{W}.
\end{aligned}
$$

5.3 Braess paradox analysis on the Braess network

We will first study the Braess paradox under BRUE in the classical Braess network (Braess 1969), because:

- The Braess paradox under bounded rationality is fairly new and no research efforts have been conducted. A simpler network will be a good starting point to investigate its properties;
- A simple network allows us to present the analysis in a more intuitive way by illustrating results graphically.

The classical Braess network is shown in Figure (5.1): link 1 (from node 1 to 3), 2 (from node 1 to 2), 3 (from node 3 to 4) and 4 (from node 2 to 4) form the basic network; while link 5 (from node 3 to 2) is a new link to be added. The link travel time function is listed by each link, where a_1, a_2, b_1, b_2 are cost function parameters. The total demand traveling from origin node 1 to destination node 4 is denoted as d.

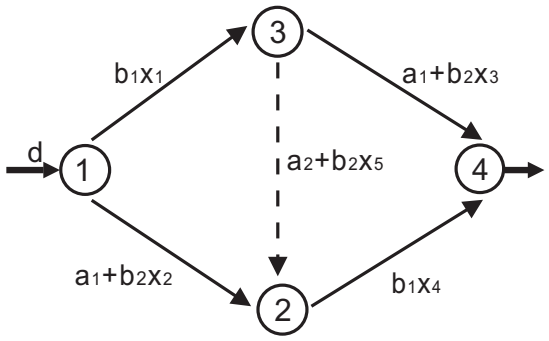

Figure 5.1: Braess network illustration

When link 5 is not added, there are two alternative paths: 1-3-4 (path 1) and 1-2-4 (path 2), called '2-path scenario'. Two path costs are computed as:

$$C_1 = (b_1 + b_2)f_1 + a_1, \tag{5.3.1a}$$

$$C_2 = (b_1 + b_2)f_2 + a_1. \tag{5.3.1b}$$

When link 5 is added, there are three alternative paths: 1-3-4 (path 1), 1-2-4 (path 2) and 1-3-2-4 (path 3), called '3-path scenario.' Three path costs are computed as:

$$C_1 = (b_1 + b_2)f_1 + b_1 f_3 + a_1, \tag{5.3.2a}$$

$$C_2 = (b_1 + b_2)f_2 + b_1 f_3 + a_1, \tag{5.3.2b}$$

$$C_3 = b_1(f_1 + f_2) + (2b_1 + b_2)f_3 + a_2. \tag{5.3.2c}$$

In the following, all variables related to the 2-path scenario will have a subscript 2, while those related to the 3-path scenario will have a subscript 3.

5.3.1 UE and BRUE

In this simple case, the user equilibrium (UE) flow pattern for both scenarios can be calculated by letting all path costs equal. Assume $a_1 \geqslant a_2, b_1 > b_2$. In the 2-path

scenario, $UE_2(d) = \left[\frac{d}{2}, \frac{d}{2}\right]^T$. In the 3-path scenario:

$$UE_3(d) = \begin{cases} \left[0, 0, d\right]^T, 0 \leqslant d < \frac{a_1 - a_2}{b_1 + b_2}, \\ \left[\frac{-a_1 + a_2 + (b_1 + b_2)d}{b_1 + 3b_2}, \frac{-a_1 + a_2 + (b_1 + b_2)d}{b_1 + 3b_2}, \frac{2(a_1 - a_2) - (b_1 - b_2)d}{b_1 + 3b_2}\right]^T, \frac{a_1 - a_2}{b_1 + b_2} \leqslant d < \frac{2(a_1 - a_2)}{b_1 - b_2}, \\ \left[\frac{d}{2}, \frac{d}{2}, 0\right]^T, d \geqslant \frac{2(a_1 - a_2)}{b_1 - b_2}. \end{cases} \tag{5.3.3}$$

Interested readers can refer to Pas and Principio (1997) for detailed calculation of these two UEs.

Remark. 1. The assumptions of $a_1 \geqslant a_2$ and $b_1 > b_2$ guarantee that there exist three cases of UE_3 defined in Equation (5.3.3), when the travel demand varies from zero to infinity (Pas and Principio 1997).

2. These two assumptions also ensure that the new link is attractive, due to lower a_2, b_2 coefficients in its cost function. Moreover, $b_1 > b_2$ necessitates the existence of the Braess paradox under UE. As the new link is connected by two links whose marginal cost with one more unit of flow is higher than that of the new link, when more travelers use the new link, congestions on these two connecting links may cancel out time saving brought by the new link. If this is the case, the Braess paradox happens.

In the 2-path scenario, by definition of the BRUE, if path 1 is shorter and path 2 is utilized, then $C_2 - C_1 \leqslant \varepsilon$; If path 2 is shorter and path 1 is utilized, then $C_1 - C_2 \leqslant \varepsilon$. Therefore the BRUE flow patterns in 2-path scenario must satisfy a system of inequalities, given both paths are utilized:

$$BRUE_2^{\varepsilon} = \{\mathbf{f} : C_i(\mathbf{f}) - C_j(\mathbf{f}) \leqslant \varepsilon, i, j = 1, 2, i \neq j\}. \tag{5.3.4}$$

Although Equation (5.3.4) is initially obtained by assuming both paths are utilized, it also holds for any BRUE flow pattern with only one path utilized. That is, for the 2-path scenario, due to its special symmetric structure, when only one path is utilized, the non-utilized path is always shorter, and thus there does not exist a BRUE flow pattern such that $C_i(\mathbf{f}) - C_j(\mathbf{f}) > \varepsilon$ while $f_i = 0$. In summary, Equation (5.3.4) holds for any BRUE flow pattern, whether both paths are utilized or only one path is utilized.

In the 3-path scenario, if path 1 is the shortest and paths 2 and 3 are utilized, then $C_i - C_1 \leqslant \varepsilon, i, j = 2, 3$; If path 2 is the shortest and paths 1 and 3 are utilized, then $C_i - C_2 \leqslant \varepsilon, i, j = 1, 3$; Similarly, if path 3 is the shortest and path 1 and 2 are utilized, then $C_i - C_3 \leqslant \varepsilon, i, j = 1, 2$. In summary, the BRUE flow patterns in 3-path scenario must satisfy a system of inequalities, given all three paths are utilized:

$$S = \{\mathbf{f} : C_i(\mathbf{f}) - C_j(\mathbf{f}) \leqslant \varepsilon, i, j = 1, 2, 3, i \neq j\}. \tag{5.3.5}$$

However, S may be a subset of the BRUE set due to the assumption that all three paths are utilized. That is, there might be a BRUE flow pattern such that $C_i(\mathbf{f}) - C_j(\mathbf{f}) > \varepsilon$ while $f_i = 0$, i.e., a non-utilized path is outside the indifference band, which does not belong to S yet is still BRUE. In the following, we will identify such special BRUE flow patterns with a non-utilized path outside the indifference band.

We first look into the case when only one path is utilized, i.e., the traffic demand is assigned to only one path. In this case, if the utilized path is either path 1 or path 2, it can be easily verified that the utilized path is the longest path, and thus there does not exist a non-utilized path outside the indifference band. If the utilized path is path 3, then the flow pattern is BRUE with path 3 being the shortest path and path 1 and path 2 being the non-utilized paths outside the indifference band if and only if the following conditions hold: $d < \frac{a_1 - a_2}{b_1 + b_2}$ and $\varepsilon < -(b_1 + b_2)d + a_1 - a_2$. Under these conditions, $S = \emptyset$ and the BRUE set is a singleton, i.e., $BRUE_3^\varepsilon = \left[0, 0, d\right]^T$.

We then look into the case when only two paths are utilized, i.e., the traffic demand is assigned to two of the three paths with one path being non-utilized. In this case, if the non-utilized path is path 1 and thereby path 2 is utilized, $C_1 < C_2$ holds due to the symmetry between path 1 and path 2. Thus under BRUE, the non-utilized path (path 1) cannot be outside the indifference band, otherwise the utilized path 2 would be "even more" outside the indifference band which contradicts BRUE. The same analysis holds if path 2 is the non-utilized one. If the non-utilized path is path 3, then the flow pattern can be BRUE with path 3 being a non-utilized path outside the indifference band if and only if the following conditions hold: $d > \frac{2(a_1 - a_2)}{b_1 - b_2}, \varepsilon < (b_1 - b_2)d - 2(a_1 - a_2)$, under which there exists a special BRUE subset $\{\mathbf{f} \in \mathcal{F} : f_3 = 0, |C_1(\mathbf{f}) - C_2(\mathbf{f})| \leqslant \varepsilon\}$. This subset is actually $BRUE_2^\varepsilon$ and $BRUE_2^\varepsilon \subseteq BRUE_3^\varepsilon$ in this case. Note that this special BRUE subset is never completely within S, i.e., $BRUE_2^\varepsilon \not\subseteq S$, because at least part of

this subset is comprised of BRUE flow patterns such that path 3 is not utilized yet is the longest path outside the indifference band. Therefore the BRUE set is the union of two convex sets $BRUE_2^\varepsilon$ and S, i.e., $BRUE_3^\varepsilon = BRUE_2^\varepsilon \bigcup S$. Although the BRUE flow set is generally non-convex, it still has a simple enough structure for us to graphically solve for the best and worst cases.

Based on the above discussion, we can say that it holds $S = BRUE_3^\varepsilon$ except for two special cases identified above. Therefore,

$$BRUE_3^\varepsilon = \begin{cases} \left[0, 0, d\right]^T, \text{ if } d < \frac{a_1 - a_2}{b_1 + b_2}, \varepsilon < -(b_1 + b_2)d + a_1 - a_2, \\ BRUE_2^\varepsilon \bigcup S, \text{ if } d > \frac{2(a_1 - a_2)}{b_1 - b_2}, \varepsilon < (b_1 - b_2)d - 2(a_1 - a_2), \\ S, \text{ o.w.} \end{cases} \tag{5.3.6}$$

In summary, the BRUE set for the Braess network is either convex (a singleton is also convex) or the union of two convex subsets. Therefore it is closed and bounded and thus compact. Given affine linear cost functions, it is also connected. This property will be used in the next section when we identify the best and the worst path flow patterns.

5.3.2 Graphical solutions of the best and the worst cases

The paradox under BRUE is defined upon the best and the worst flow patterns in the BRUE set. To identify the minimum and the maximum of STTs, we first need to study the properties of the STT function. Given affine linear cost functions, the STT is a quadratic function and the BRUE set is convex or non-convex with simple structure. Solving extremal flow patterns in Equation (5.2.5) is equivalent to solving positive-definite quadratic programs over a convex set or the union of two convex sets. The Braess network only contains two or three paths, therefore these two extremal cases can be solved graphically.

Two-path scenario

The STT associated with a specific flow pattern is computed as the product of flows and its associated travel costs. The system travel time for the 2-path scenario, denoted

as 'STT_2', is computed as:

$$STT_2(d, \mathbf{f}) = \sum_{i=1}^{2} C_i f_i = (b_1 + b_2)(f_1^2 + f_2^2) + a_1 d. \tag{5.3.7}$$

STT_2 is a quadratic function with respect to flow patterns. Since STT is a continuous function with respect to path flows while the BRUE set is compact, the STT over the BRUE set constitutes a closed interval, called the "STT interval." The STT interval can be represented graphically by a line segment connecting the best and the worst values.

Before finding the minimum flow pattern defined in Equation (5.2.1b), it is important to discuss the system optimal (SO), the feasible flow distribution with the minimum STT given a pre-determined traffic demand. Mathematically,

$$SO(d) = \min_{\mathbf{f} \in \mathcal{F}} \mathrm{STT}(d, \mathbf{f}).$$

If $SO \in \mathcal{F}^{\epsilon}_{BRUE}$, then SO is the best flow pattern.

In the 2-path scenario, $SO_2(d) = \left[\frac{d}{2}, \frac{d}{2}\right]^T$. It is UE and is therefore BRUE. Thus it is also the best flow pattern.

Solving the worst flow pattern is equivalent to maximizing a positive definite quadratic program over a convex set. Therefore the worst flow pattern should occur on one corner of $BRUE^{\varepsilon}_2$. Its corner point is a feasible flow pattern satisfying $C_1(\mathbf{f}) - C_2(\mathbf{f}) = \varepsilon$ or $C_2(\mathbf{f}) - C_1(\mathbf{f}) = \varepsilon$.

Three-path scenario

In the 3-path scenario, due to flow conservation, the feasible flow set can be characterized by two path flows, i.e., $f_3 = d - f_1 - f_2$. Then STT_3 can be computed as follows:

$$\begin{aligned} STT_3(d, \mathbf{f}) &= \sum_{i=1}^{3} C_i f_i \\ &= (b_1 + 2b_2)(f_1^2 + f_2^2) + 2b_2 f_1 f_2 + [a_1 - a_2 - 2(b_1 + b_2)d]\,(f_1 + f_2) \\ &+ \left[(2b_1 + b_2)d^2 + a_2 d\right]. \end{aligned} \tag{5.3.8}$$

Given a certain demand level, STT_3 is also a quadratic equation with respect to path flows on the first two paths. SO_3 depends on the demand level:

$$SO_3(d) = \begin{cases} \left[0, 0, d\right]^T, 0 \leqslant d < \frac{a_1 - a_2}{2(b_1 + b_2)}, \\ \left[\frac{\frac{-a_1+a_2}{2} + (b_1+b_2)d}{b_1+3b_2}, \frac{\frac{-a_1+a_2}{2} + (b_1+b_2)d}{b_1+3b_2}, \frac{(a_1-a_2)-(b_1-b_2)d}{b_1+3b_2}\right]^T, \frac{a_1-a_2}{2(b_1+b_2)} \leqslant d < \frac{a_1-a_2}{b_1-b_2}, \\ \left[\frac{d}{2}, \frac{d}{2}, 0\right]^T, d \geqslant \frac{a_1-a_2}{b_1-b_2}. \end{cases} \tag{5.3.9}$$

As aforementioned, if $SO_3 \in BRUE_3$, it is the best flow pattern; or else the best flow pattern has to be identified otherwise.

For the worst flow patterns, there are two cases:

1. If $BRUE_3$ is convex, the worst flow patterns must occur at one corner point;

2. if $BRUE_3$ is the union of two convex subsets, the worst flow patterns also occur at one corner point of one subset. However, calculation is needed to compare which subset's corner point carries higher STT value.

UE_3 is a special case of $BRUE_3$, which can help to locate the BRUE set. SO_3 has the minimum STT value, which facilitates finding the extremal cases. As the demand level varies, UE_3 and SO_3 have five possible relative positions shown in Figure (5.2). The triangle area encompassed by two axes and the line $f_1 + f_2 = d$ is the feasible region. STT_3 is a conic function with respect to the first two path flows and thus its contours (i.e., all flow patterns with the same STT_3 values) are ellipses, centered at SO_3. The best and the worst flow patterns are those BRUE which are located at the nearest and the farthest STT contours from SO_3.

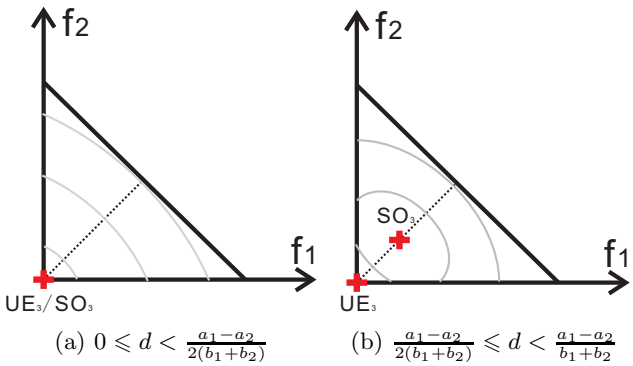

(a) $0 \leqslant d < \frac{a_1-a_2}{2(b_1+b_2)}$ (b) $\frac{a_1-a_2}{2(b_1+b_2)} \leqslant d < \frac{a_1-a_2}{b_1+b_2}$

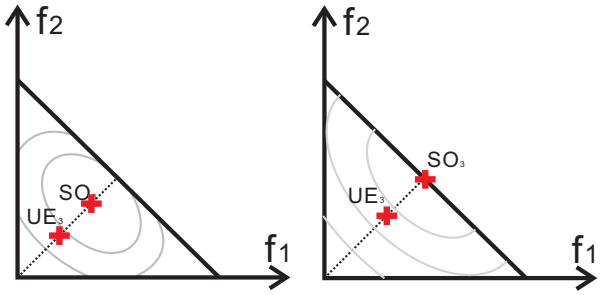

(c) $\frac{a_1-a_2}{b_1+b_2} \leqslant d < \frac{a_1-a_2}{b_1-b_2}$ (d) $\frac{a_1-a_2}{b_1-b_2} \leqslant d < \frac{2(a_1-a_2)}{b_1-b_2}$

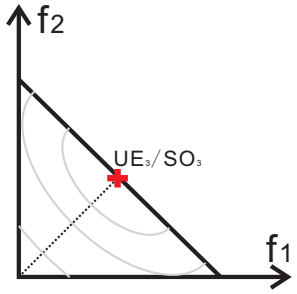

(e) $d \geqslant \frac{2(a_1-a_2)}{b_1-b_2}$

Figure 5.2: Relative positions of UE_3 and SO_3

In Figure (5.2b-5.2c), SO_3 may be closer to UE_3 or closer to the boundary of the feasible region $f_1 + f_2 = d$. When SO_3 is closer to UE_3, as ε varies, the worst and the best flow patterns are different from those when SO_3 is closer to $f_1 + f_2 = d$. Therefore, it is further split into two scenarios. Similarly UE_3 may be closer to the origin or to SO_3 in Figure (5.2d). In conclusion, to capture all possibilities of the worst and the best flow patterns, the demand level should be divided into eight intervals (shown in

Figure (5.3 and A.1-A.7)). Within each demand interval, the best and the worst flow patterns depend on the value of ε and we will discuss them as ε increases from zero to ∞. In the following, Case 1 when $0 \leqslant d < \frac{a_1-a_2}{2(b_1+b_2)}$ (shown in Figure (5.3)) will be elaborated upon.

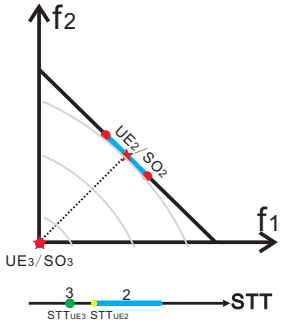

(a) $0 \leqslant \varepsilon < (b_1 + b_2)d$

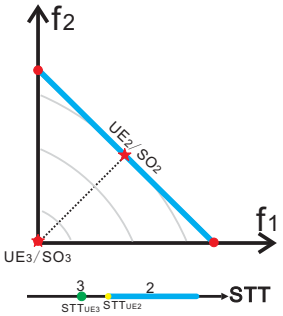

(b) $(b_1+b_2)d \leqslant \varepsilon < -(b_1+b_2)d+a_1-a_2$

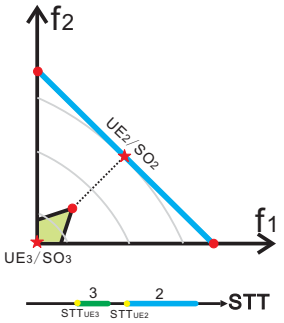

(c) $-(b_1 + b_2)d + a_1 - a_2 \leqslant \varepsilon < \frac{-(b_1-b_2)d}{2} + a_1 - a_2$

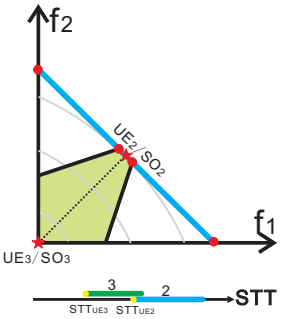

(d) $\frac{-(b_1-b_2)d}{2}+a_1-a_2 \leqslant \varepsilon < b_2d+a_1-a_2$

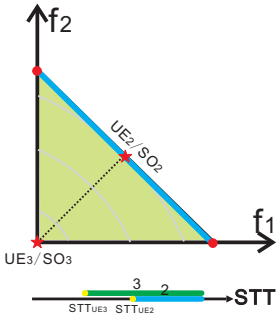

(e) $\varepsilon \geqslant b_2d + a_1 - a_2$

Figure 5.3: Case 1: $0 \leqslant d < \frac{a_1-a_2}{2(b_1+b_2)}$

Figure (5.3a)-(5.3e) illustrate the worst and the best cases when $0 \leqslant d < \frac{a_1-a_2}{2(b_1+b_2)}$, as ε gradually increases. The slanted line and the triangle are the feasible sets for two scenarios respectively. The blue line segment is $BRUE_2$ and the green polytope is $BRUE_3$. Grey elliptical lines are STT contours, facilitating identification of the best and the worst cases. A star represents the best-case flow pattern, while circles indicate the worst cases on the corner points of the BRUE set. There exist two worst flow patterns because of symmetry of the BRUE set.

When $0 \leqslant \varepsilon < (b_1 + b_2)d$ (shown in Figure (5.3a)), ε is too small to divert flows from path 3 to path 1 or 2, so $BRUE_3$ contains only one flow pattern-the origin and therefore the worst and the best cases are the same. The worst flow patterns for 2-path scenario are corner points of $BRUE_2$. As ε grows till $(b_1+b_2)d$ (shown in Figure (5.3b)), any feasible flow pattern under 2-path scenario belongs to $BRUE_2$, so the worst flow patterns for 2-path scenario are corner points of the line $f_1 + f_2 = d$. If ε continues to grow up to $-(b_1+b_2)d+a_1-a_2$ (shown in Figure (5.3c)), $BRUE_3$ starts to expand and the best flow pattern is the upper right corner point which is closest to SO_3, indicated by a circle. Continue this analysis until ε is so large that every feasible flow pattern under 3-path scenario is $BRUE_3$. Similar analysis can be applied to other seven cases under different demand levels shown in Appendix.

In Figure (5.3a-5.3b), below the path flow coordinates is an axis representing the STT, with its value increasing to the right. STT values for both scenarios are plotted on this axis. STT_3 is a single value and STT_2 interval locates on the right side of STT_3, denoting that STT_2 is higher than STT_3. Thus the Braess paradox never happens. Similar analysis can be applied to Figure (5.3c). In Figure (5.3d-5.3e), two STT intervals overlap. So whether the paradox happens or not depends on which BRUE flow pattern is used for the analysis (i.e., which attitude planners hold). This will be discussed in detail in the next section.

Remark. In Case 8 shown in Figure (A.7b), $BRUE_3$ is non-convex which reflects the only non-convex situation discussed in Section 5.3.1. $BRUE_2$ is one subset of $BRUE_3$, therefore it is hidden. The other subset S is indicated by a green triangle. After calculation, we find out that the worst flow pattern is the corner point of $BRUE_2$ not that of S.

5.3.3 Paradox synthesis over (d, ε) region

After analyzing the STT functions as the demand level or the indifference band varies respectively, we are ready to explore how STTs vary with both variables.

One (d, ε) pair determines a BRUE set, among which each flow pattern is associated with a STT value. As analyzed in Section 5.3.2, the STT values over a BRUE set constitutes a compact interval. Figure (5.4) summarizes the STT intervals in two scenarios within the (d, ε) region. The x-axis is the demand level and the y-axis represents the indifference band level. Same colors are used to indicate STT intervals in two scenarios as in Figure (5.3): the blue line segment represents STT_2 while the green line segment indicates STT_3.

Though there exist a STT_2 interval and a STT_3 interval for each (d, ε) pair, under certain combinations of d and ε, the STT intervals in two scenarios display similar "patterns". The pattern here we mean that the STT interval is either a single value or an interval, and two STT intervals have similar relative positions. When two STTs display similar patterns over a set of (d, ε) pairs, only one pattern is plotted. For example, when $0 \leqslant d < \frac{a_1 - a_2}{2(b_1+b_2)}$ and $0 \leqslant \varepsilon < -(b_1 + b_2)d + a_1 - a_2$, STT_3 is a single value while STT_2 is an interval lying on the right side of STT_3 (i.e., every STT value in 2-path scenario is larger than that in 3-path scenario). Therefore we can illustrate this pattern in one set of STT_2 and STT_3 intervals, shown in the left bottom region in pink color.

Under various combinations of d and ε, STT_2 and STT_3 have different values and different relative positions (as illustrated in Figure (5.3,A.1-A.7)). Therefore the points over the (d, ε) region can be grouped into multiple subregions. In Figure (5.4), the vertical dividing lines indicate critical values of d, while the horizontal lines and oblique ones represent critical values of ε with the formula listed next to the separating lines. The pink region is when the paradox does not happen while the yellow region is when the paradox always happens. The green region is when three attitudes are needed to determine whether the paradox happens or not.

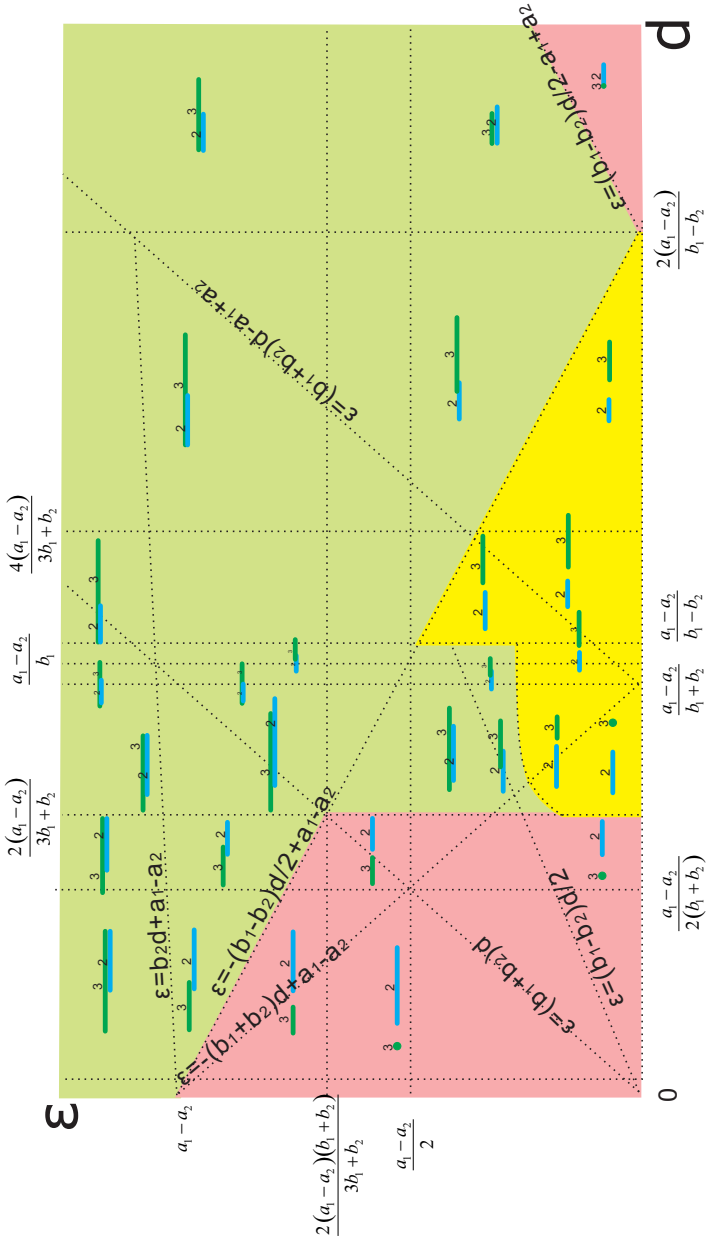

Figure 5.4: STT intervals over (d, ε) region

5.3.4 Braess paradox regions under three different attitudes

In this subsection, we will plot S_{RP}, S_{RN}, S_{RA} for the Braess network and study their relationships, given cost parameters $a_1 = 50, a_2 = 10, b_1 = 10, b_2 = 1$.

Summarizing the analysis of the best and the worst STTs for eight cases in Section 5.3.2 will give us complete STT functions. As STTs are functions of both d and ε, 3-dimensional surfaces over (d, ε) region are used to illustrate them. In Figure (5.5), the red surface denotes w-STT_3 and the yellow one denotes b-STT_2. The region where the red is above the yellow surface is when the paradox happens. Since we are comparing the worst value with link 5 to the best one without, this represents the risk-averse attitude.

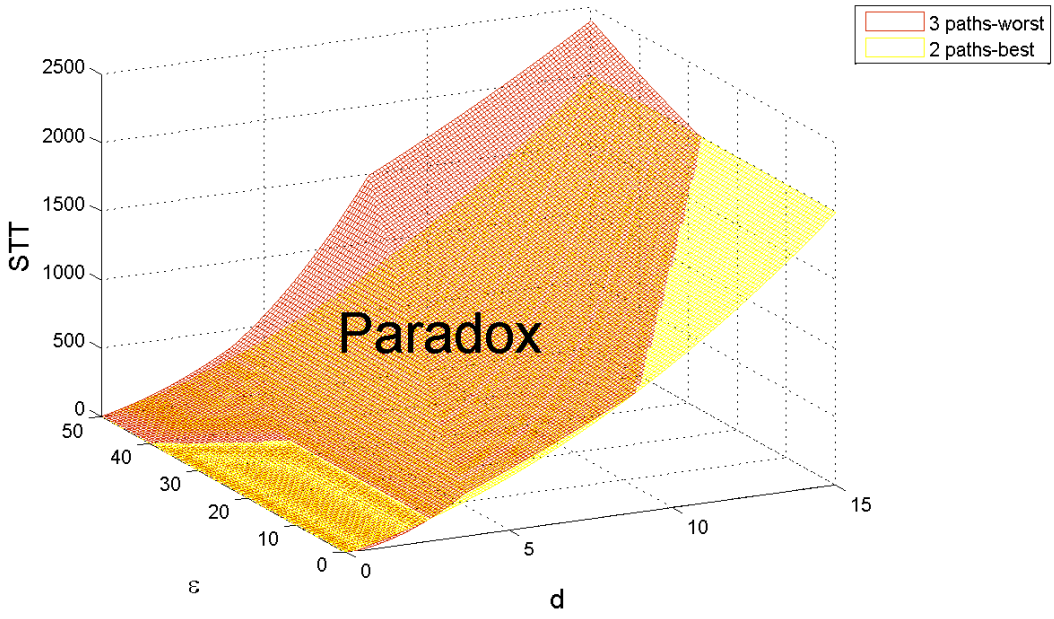

Figure 5.5: Risk-averse paradox

For ease of visualization, we project these two surfaces onto the 2-dimensional (d, ε) plane in Figure (5.6a). The paradox happens over the red region. The demand level is divided into eight intervals, with each interval representing one case discussed in Section 5.3.2. Under each demand interval, C is short for 'Case' and the number following

it denotes the case number. When $\varepsilon = 0$, the risk-averse paradox only occurs when the demand falls within an intermediate level (i.e., $2.6 \leqslant d \leqslant 8.8$), which is consistent with the paradox analysis under UE in Pas and Principio (1997).

In Figure (5.6c), the red surface refers to b-STT_3 and the yellow one represents w-STT_2. The red region is when the paradox happens. This represents the risk-prone attitude. Similarly, when $\varepsilon = 0$, the risk-prone paradox only occurs when $2.6 \leqslant d \leqslant 8.8$. Increasing ε may cause the risk-prone paradox to disappear when the demand level is too low and to happen when the demand level is high.

Assuming a uniform distribution over the STT interval, i.e., $g(STT) = \frac{1}{STT}$, the mean of the STT is the arithmetic average of the best and the worst values. The Braess paradox with the risk-neutral attitude is shown in Figure (5.6b). Similarly, the risk-neutral paradox only occurs when $2.6 \leqslant d \leqslant 8.8$ given $\varepsilon = 0$. Increasing ε may cause the risk-prone paradox to disappear, because the indifference band can help improve the system performance in the best scenario.

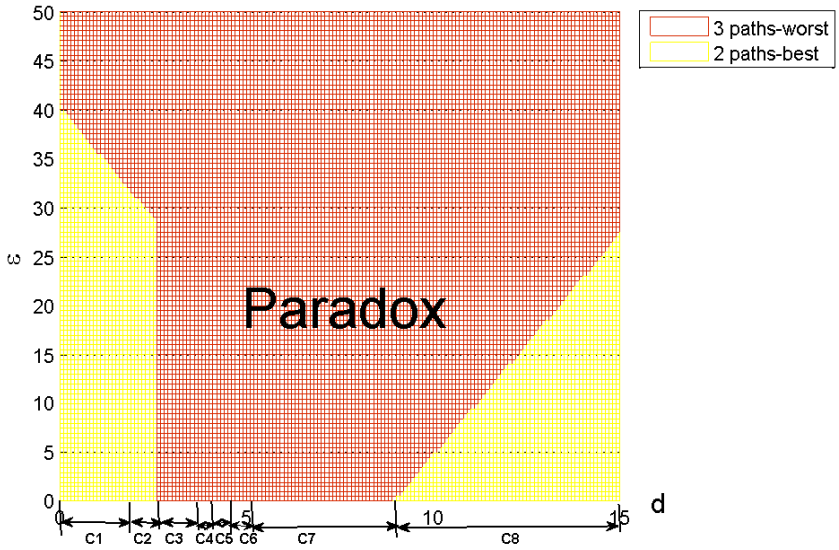

(a) Risk-averse region S_{RA}

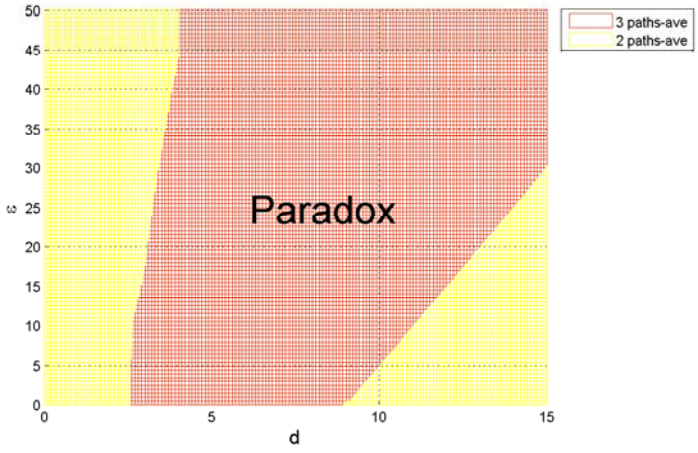

(b) Risk-neutral region S_{RN}

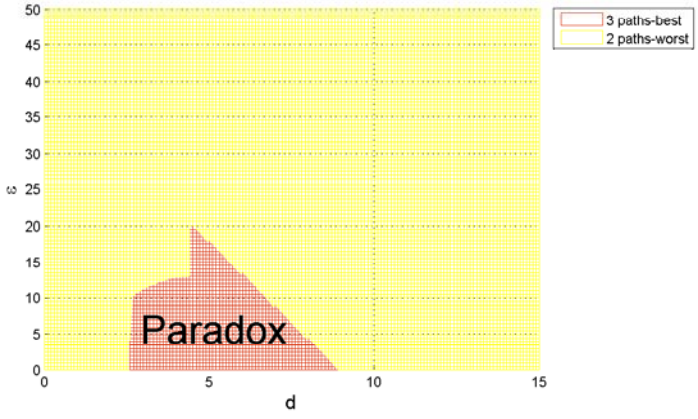

These three paradox regions satisfy the relationship shown in Proposition (5.2.1). Given $\varepsilon = 0$, the demand level under which three paradoxes happen are the same. When the paradox under UE happens, the risk-averse paradox surely occurs with $\varepsilon > 0$, but the risk-prone or risk-neutral paradox does not necessarily occur; on the other hand, even when the paradox under UE does not happen, it may occur when $\varepsilon > 0$.

5.4 Braess paradox analysis in grid networks

Section 5.3 mainly focuses on deriving existence conditions of the Braess paradox analytically in the classical Braess network. Although this network structure makes it easy to illustrate the paradox graphically, the structure itself is unusual or extreme (at least in transportation networks), which gives the implication that Braess paradox can happen only in this kind of extreme networks, or at least it is unclear whether it can happen in other more "ordinary" networks. In this section, we will generalize the paradox conditions under BRUE to simple and ordinary grid networks with regular BPR link performance functions, to further demonstrate the potential of the Braess paradox occurring in real transportation networks.

5.4.1 A grid network with one OD pair

Consider a simple grid network as shown in Figure (5.7). To make the network "ordinary", we consider that all links have the same commonly used BPR link cost function. The link cost structure in this example simply represents a usual case that all roads in the network are of similar standards. Consider that there is one OD pair from Node O to Node D with a demand level $d = 2$. For this network, the UE flow on each link is $x = 1$, and the UE travel time between OD is 3.45.

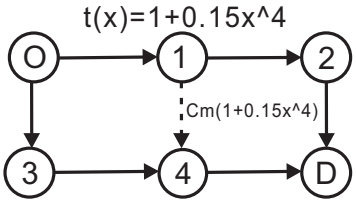

Figure 5.7: A grid network with BPR link cost functions

Now consider one middle link is added from node 1 to 4, indicated as dotted line in Figure (5.7). We shall demonstrate that, if the newly added middle link is faster than the existing links, then Braess paradox could occur, i.e. the new UE travel time between OD could be higher than 3.45. For simplicity, let the newly added middle link have a BPR link cost function $t(x) = c_m(1 + 0.15x^4)$, where c_m is the free flow travel time of the new middle link. Here we use c_m to represent the fast degree of the new link, i.e. the new link is the same with existing links if $c_m = 1$, is slower if $c_m > 1$, and is faster if $c_m < 1$. Under UE, the relationship of c_m and the new UE travel time is plotted in Figure (5.8). In Figure (5.8), the x-axis is the free flow travel time of the new link, while the y-axis is the new UE travel time between OD. As c_m decreases (the new link becomes faster), the new UE travel time first decreases and then increases. In particular, when the new link is so fast that $c_m < 0.75$, the new UE travel time will be higher than the original level 3.45, which means that the Braess paradox happens. If the new link is ideally fast with a zero travel time, i.e., $c_m = 0$, then the new UE travel time will be 16 % higher than the original level 3.45.

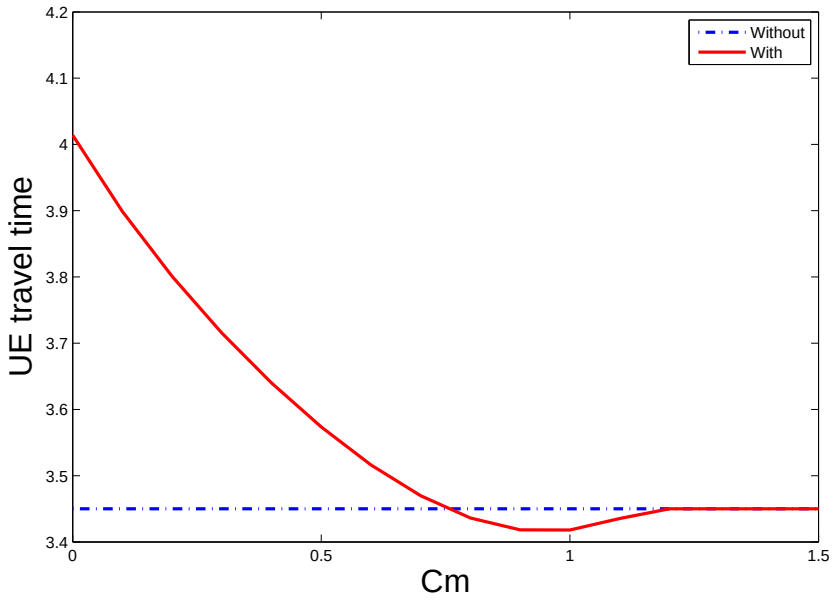

Figure 5.8: UE travel time comparison without and with the new link

Because the network is a normal grid network with regular BPR link cost functions, our result indicates that the Braess paradox can happen in the real world, especially in grid networks. Retrospectively, the reason for the occurrence of the Braess paradox in an ordinary grid network is simple: *when a new fast link is added (or more generally, some improvement is completed for some part of the network), users will be attracted to use the new link, which will result in flow concentration on links connected to the new link. The detrimental congestion effect of the flow concentration could outweigh the beneficial effect of the fastness of the new link. When this is the case, the Braess paradox simply occurs.* With this underlying philosophy, it is clear that, as long as the new link is fast enough to attract users and thereby causes flow concentration in its vicinity, there is a possibility of the Braess paradox occurring.

The above argument is especially true for transportation networks with BPR link cost functions, because BPR cost functions are convex functions such that the congestion effect increases nonlinearly (more than linearly) with the level of flow concentration. On the other hand, the fastness of the new link reduces travel times only linearly with its fast degree. Therefore, as the new link becomes faster, the congestion effect of the attracted flow concentration increases at a higher rate than the fastness effect itself does, which means that, if the new link is too fast, the attracted congestion effect could outweigh the fastness effect itself and thus the Braess paradox could occur. This implies that, a "middle" link in a grid network with BPR link cost functions (like the one in Figure (5.7)), if much faster than other links, could be a paradox link.

With the above example and analysis, and in view of the popularity and practicality of BPR link cost functions and grid-kind networks in transportation field, it is safe to say that the occurrence of Braess paradox in transportation networks should not be too surprising.

Because the congestion effect of link cost functions plays an important role in the occurrence of the paradox, we introduce a term named 'congestion sensitivity' to describe this congestion effect. The congestion sensitivity of link i's travel time, denoted as p_i, is measured by the power of the link flow x_i in its cost function $t_i(\mathbf{x})$. For example, if the BPR function is used, i.e., $t(\mathbf{x}) = 1 + 0.15x^4$, the congestion sensitivity is $p = 4$.

To better understand the impact of the congestion effect on the paradox, in the following, we would like to study the relationship of the link cost congestion sensitivity

and the occurrence of the risk-averse paradox. The reason we mainly focus on the risk-averse paradox is that it represents the worst scenario given a new link is built. Under BRUE, the worst STT can be solved from Equations (5.2.5) with GAMS software (General Algebraic Modeling System, see Rosenthal and Brooke 2007).

Remark. As the BRUE set is non-convex, the best and the worst STTs computed by GAMS may be sub-optima and deviate from actual best and worst values, but the relative gap between the solution and the optimum is 10% by default in computation. For such a small network optimization, GAMS can actually provide very accurate solutions by employing two reliable approaches (Ferris et al. 2002). Therefore the accuracy of the computed STTs is controlled to be within 90% of optima in the following numerical examples. The sensitivity analysis of the solution accuracy can be discussed but it goes beyond the scope of this study, which will be our future investigation.

In the grid network shown in Figure (5.7), assume the demand level $d = 2$, the new link travel time is $c_m(1 + 0.15x^p)$ and other links' travel times are $1 + 0.15x^p$, where $p \geqslant 0$. Note that when $p = 0$, the cost function reduces to a constant 1.15; while when $p = 1$, the cost function reduces to the linear function $1 + 0.15x$.

In Figure (5.9), each line represents a frontier of the risk-averse paradox region as the function of (ε, p), given a certain c_m. When (ε, p) falls on the right upper part of the frontier, the risk-averse paradox happens. When c_m varies from 0 to 1.5 (the range when the paradox first happens and then disappears under UE), the occurrence of the paradox may be affected by both ε and p or dominated by either of them.

When $c_m = 0$ (indicated by the red line with star markers), the paradox happens if $p \geqslant 2.4$ regardless of ε, because the new link is so fast that many travelers are attracted to use it and two links connecting it suffer from the congestion effect if the congestion sensitivity is high.

When $c_m = 0.7$ (indicated by the black dotted line with square markers) and 0.9 (indicated by the yellow line with circle markers), in general, the larger the congestion sensitivity is, the more likely the risk-averse paradox happens given a smaller indifference band. In other words, bounded rationality plays a diminishing role in the occurrence of the paradox if the congestion sensitivity is higher, because the link cost is highly sensitive to the flow increase if the congestion sensitivity is large. However, when $c_m = 1.1$ (indicated by the cyan line with cross markers) and 1.5 (indicated by the magenta line

with diamond markers), the larger the congestion sensitivity is, the more likely the risk-averse paradox happens with a larger indifference band. In other words, bounded rationality plays a more important role in the occurrence of the paradox given the congestion sensitivity is higher. This is because the paradox is dominated by ε when c_m is longer.

Therefore, there exists a critical travel cost of the newly built road so that the indifference band and the congestion sensitivity play different roles in the occurrence of the paradox under and above this value. In the grid network shown in Figure (5.7), $c_m = 1$ is the threshold. In practice, the indifference band is determined by people's route choice behavior and the congestion sensitivity is one of the road characteristics, so these two values are difficult to modify. To reduce the likelihood of the occurrence of the paradox, we need to carefully choose the travel cost of the new link.

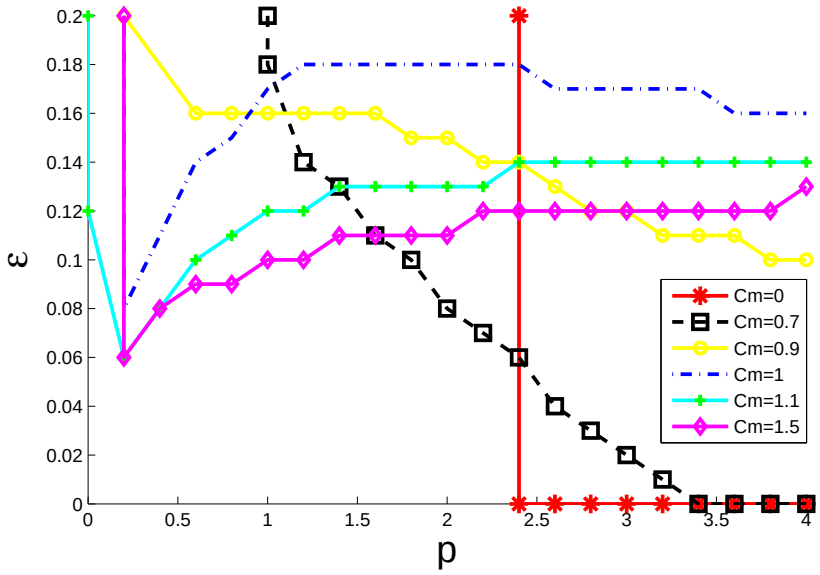

Figure 5.9: Risk-averse Braess paradox frontier over (p, ε) region

5.4.2 A grid network with four OD pairs

Here we give a multiple-OD network to further demonstrate the Braess paradox in transportation networks. Figure (5.10) shows a grid network with four OD pairs, from node 1 to 6 (OD 1), from 1 to 9 (OD 2), from node 4 to 6 (OD 3), and from 4 to 9

(OD 4). The demand level for each OD pair is $d = 0.7$. All current links have the same BPR cost function: $t(x) = 1 + 0.15x^4$. The new link is added from node 2 to 5 with a BPR link cost function $t(x) = c_m(1 + 0.15x^4)$, where the free flow cost c_m reflects the fast degree of the new link.

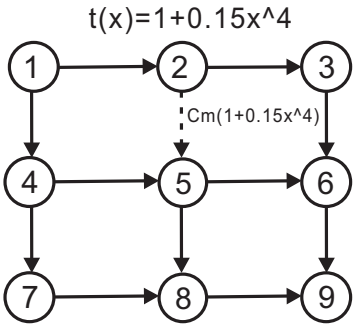

Figure 5.10: A grid network connecting four OD pairs with BPR link cost functions

Figure (5.11) plots the UE travel time of the four OD pairs as a function of the free flow travel time of the new middle link, c_m. From our numerical results (also can be seen from Figure (5.11)), when the new link has a free flow travel time $0.10 < c_m < 0.84$ (faster than the existing links), the UE travel times of all the four OD pairs are higher than the original costs without the new link, which means that the addition of the new fast link increases the UE travel time of every road user. Thus it is clear that the newly added link could easily be a "paradox" link if its fast degree is not carefully designed.

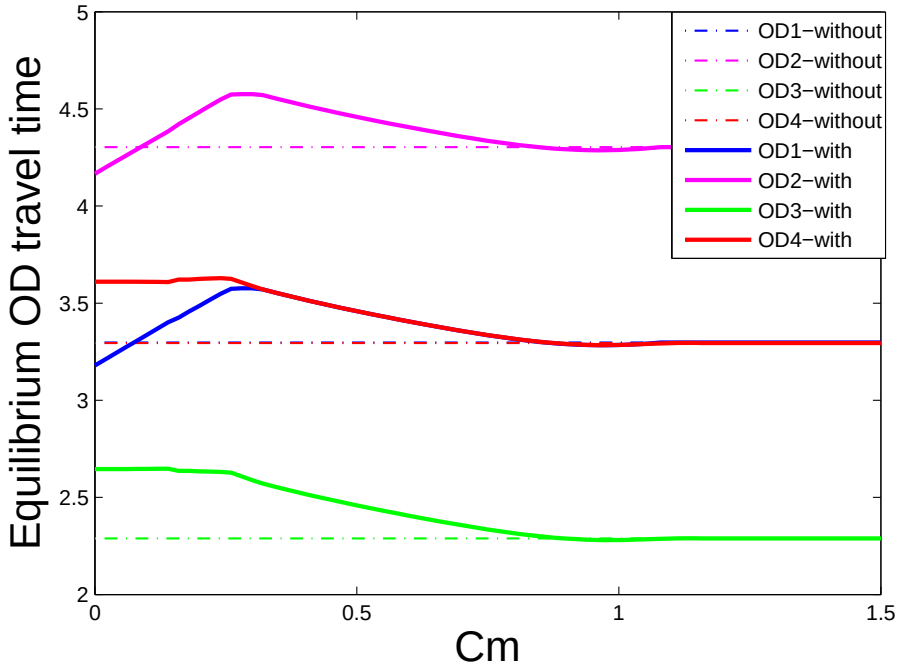

Figure 5.11: Paradox analysis in the grid network connecting four OD pairs

It should be mentioned here that the above multiple-OD network example is not constructed by much effort, as we simply incorporate the elementary network of Figure (5.7) into this larger network. The point here is that, no matter how complex a network is, as long as it is a grid-kind network with BPR-kind convex link cost functions, a fast "middle" link could be a "paradox" link, due to the same reasons mentioned in the small single-OD example.

To examine the impact of BRUE on Braess paradox, let us now consider that the indifference band for OD pair 1 is 0.1 and zero for other OD pairs. In this network, we only discuss the paradox conditions when the new link free flow travel time c_m varies, provided the fixed demand levels and the indifference bands for four OD pairs. Figure (5.12) shows the best and the worst STT functions with respect to c_m without and with the new link. The blue dotted lines represent the worst and the best STTs without the new link, and the red lines represent those with the new link. We can decompose c_m into multiple intervals and the occurrence of the paradox is indicated within each

interval: 'No BP' means the paradox does not happen, 'BP' means the paradox definitely happens and 'BP_{RA}' means the risk-averse paradox happens. When the new link is too fast (i.e., $c_m \in [0, 1]$), i.e., the congestion effect outweighs the beneficial effect brought by the new link, either the paradox always happen (i.e., $c_m \in [0, 0.79]$) or the risk-averse paradox happens (i.e., $c_m \in [0.79, 1]$). If the new link is too long (i.e., $c_m \geqslant 1.18$), no one will use it and there is no reason to build it. Thus, if we plan to build this new link, $c_m \in [1, 1.06]$ is recommended in this case.

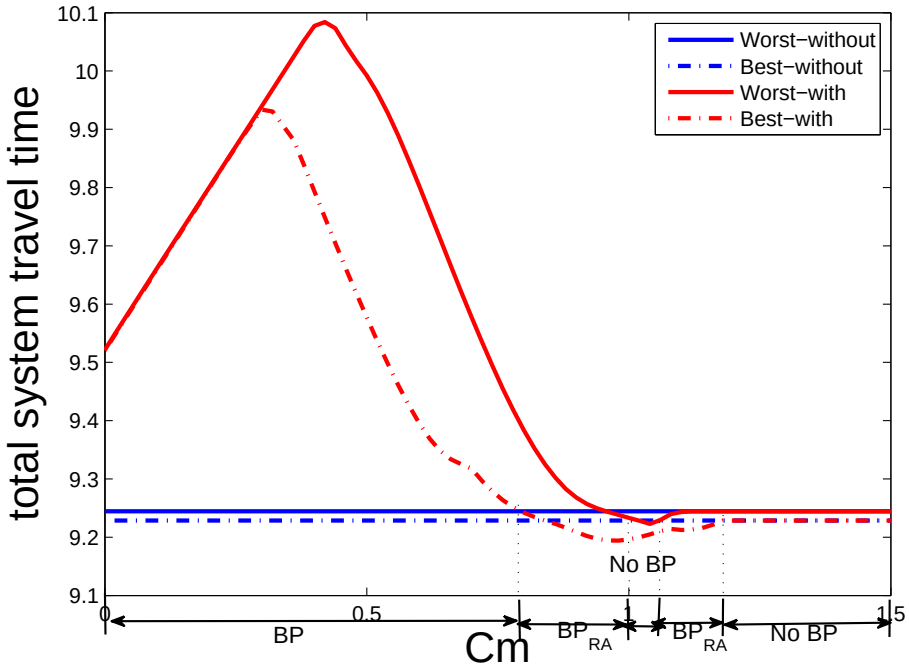

Figure 5.12: Paradox analysis in the grid network connecting four OD pairs

Remark. When $c_m < 0.4$, the best and the worst STT functions seems overlapping but their values are a little different. When the new link is quite fast given the indifference band $\varepsilon = 0.1$, most people traveling between OD pair 1 use the new link and only a few use other routes. Thus, the worst scenario deviates only slightly from the best one and the indifference band plays a very small role.

Chapter 6

Conclusions and Future Research Directions

In this chapter, we will first summarize three significant research findings of this dissertation in empirical validation, theoretical modeling and application of boundedly rational route choice behavior. Then research gaps of this dissertation will be pinpointed. As a growing research field in travel behavior study, several promising research directions will also be provided.

6.1 Conclusions

This dissertation is motived by the irreversible response to a network change due to the reopening of the I-35W Bridge in Minneapolis. To explain this anomalous phenomenon, a boundedly rational route choice framework is proposed. Within this framework, empirical analysis and theoretical modeling are developed, as well as its implication for transportation planning.

First, by analyzing route choices of commuters in the Twin Cities before and after the reopening of the I-35W Bridge, we reveal that there exists a time saving threshold under which drivers will not switch to the new bridge. This threshold results from people's stickiness of driving habits and is characterized by an indifference band. A probit model is used to estimate this indifference band by utilizing GPS travel data. As bounded rationality successfully explains observed anomaly, this empirical work

provides insights into the cause of the irreversible network change and sheds lights on route choice behavior estimation with empirical data.

Second, by analyzing the interior structure of the BRUE set, this dissertation shows that the BRUE set can be decomposed into finite subsets and each subset is convex if affine linear link performance functions are employed. As a result, a systematic methodology of obtaining BRUE solutions is proposed for networks with fixed demands. The topological properties of the BRUE set are also studied.

The theoretical aspects of BRUE solutions help predict BRUE link flow patterns in a network, paving the way for bounded rationality related applications. The most crucial application is the Braess paradox analysis under bounded rationality. This dissertation studies the general existence condition of the Braess paradox in ordinary networks and analyzed the Braess paradox based on boundedly rational route choice behavior assumption. The analysis shows that Braess Paradox can easily occur in ordinary networks and the impact of BRUE on the Braess Paradox varies as the newly built link cost changes. In contrast to the previous Braess paradox analysis which is only influenced by the demand level, the occurrence of the boundedly rational Braess paradox becomes more complicated and depends on both the demand level and the indifference band.

6.2 Research gaps of this dissertation

Though this dissertation provides a comprehensive framework of boundedly rational travel behavior modeling and estimation, there are several research directions which need to be extended.

6.2.1 Empirical verification and estimation

Though it is the first effort in estimating the indifference band by utilizing empirical GPS data collected in the Twin Cities, the empirical study is subject to limitations. According to the distribution of estimated time saving brought by using the new bridge, stayers are decomposed into two groups: stayers from one group do not switch because the saved time is marginal; the other group of stayers decides to stay even when saved time is substantial. This may result from the relatively small sample size or the

behavioral heterogeneity among travelers.

Nowadays, not only aggregated detector data at fixed locations, but also mobile sensor data from GPS or smart-phones for individual travelers are available. With travel behavioral data from various sources in place, empirical verification of bounded rationality should continue and bounded rationality parameters need to be estimated for more metropolitan areas.

6.2.2 Mathematical properties of BRUE

One of the contribution of this dissertation is that the BRUE set can be decomposed into multiple convex subsets provided with affine linear link cost functions. However, it is still a big challenge to understand the topological properties of the BRUE set with general link cost functions. Deeper understanding of the equilibrium set's mathematical properties will provide better prediction of traffic flow patterns and facilitate bounded rationality applications.

Furthermore, existing studies on analytical properties of BRUE assume that deterministic flow-dependent travel time is the only factor influencing route choices. Two other major contributing factors, travel time reliability and monetary cost, have been incorporated into perfect rationality models and accordingly UE is subjected to many variants: Stochastic UE (SUE), Probabilistic UE (PUE) (Lo et al. 2006), Late arrival penalized UE (LAPUE) (Watling 2006), Mean-excess traffic equilibrium (METE) (Chen and Zhou 2010; Chen et al. 2011), Stochastic bicriterion user-optimal (Dial 1996, 1997), Bi-objective UE (BUE) (Wang et al. 2009). Significant contributions can be made if these two factors are also incorporated into BRUE.

6.2.3 Transportation network design under bounded rationality

New methodologies are needed regarding the transportation network design problem (NDP) with boundedly rational travel behavior. The classical network design problem is usually formulated as a bi-level program: the upper level is the decision made to either enhance capacities of the established links, apply congestion pricing, or add new links to an existing road network; the lower level is an equilibrium problem, describing how travelers are distributed within the new road network. Due to the existence of

the indifference band, travelers may respond differently to a network design proposal, leading to non-uniqueness of the equilibrium and causing difficulties in BRUE link flow pattern prediction and proposal evaluation. Therefore a new network design framework needs to be established to accommodate boundedly rational route choice behavior.

The above three directions are mainly focused on generalizing findings of this dissertation. Boundedly rational travel behavior is still understudied and broader research directions need to be provided.

6.3 Future Research Directions

In this section, we will point out research gaps which need to be filled in the existing literature.

6.3.1 Cognitive process

Bounded rationality, involving extensive psychology and behavorial aspects, has been well-studied in economics and psychology for decades. However, the cognitive process of boundedly rational travel behavior remains understudied in transportation. The travel behavior decision-making is a complicated cognitive process and borrowing models from these established fields can expedite BR research in transportation.

6.3.2 Game-theoretical BRUE model

The boudedly rational game-theoretical model results in boundedly rational equilibria and its analytical properties are generally tractable. There is no such literature on exploring boundedly rational user equilibria with the game theoretical approach. Great contributions will be made if the boundedly rational finite game can be borrowed to model travel behavior. In addition, travelers are usually treated as infinitesimals and large population approximation may also be needed to generalize boundedly rational Nash equilibria to user equilibria.

6.3.3 Boundedly rational multi-modal and route choice

Most existing dynamic travel behavioral models incorporated bounded rationality into both departure-time and route choices and these two choices are jointly estimated. Mode choice is always treated as a separate decision apart from these two choices. In future, a unifying framework of boundedly rational multi-modal departure-time and route choices should be developed to integrate all travel decisions.

References

Akiva, M. E. B., 1994. Modeling heterogeneity in discrete choice processes application to travel demand. Ph.D. thesis, Massachusetts Institute of Technology.

Bamberg, S., Schmidt, P., 2003. Incentives, morality, or habit? Predicting students car use for university routes with the models of Ajzen, Schwartz, and Triandis. Environment and Behavior, 35 (2), 264–285.

Bekhor, S., Ben-Akiva, M., Ramming, M., 2006. Evaluation of choice set generation algorithms for route choice models. Annals of Operations Research, 144 (1), 235–247.

Bell, M., Iida, Y., 1997. Transportation network analysis.

Ben-Akiva, M., Bergman, M., Daly, A., Ramaswamy, R., 1984. Modeling inter-urban route choice behaviour. In: Proceedings from the 9th International Symposium on Transportation and Traffic Theory, VNU Science Press, Utrecht, Netherlands. pp. 299–330.

Ben-Akiva, M., Bolduc, D., 1996. Multinomial probit with a logit kernel and a general parametric specification of the covariance structure. D'epartement d'economique, Universit'e laval with Department of Civil and Environmental Engineering, Massachusetts Institute of Technology.

Ben-Akiva, M., Ramming, S., 1998. Lecture notes: Discrete choice models of traveler behavior in networks. Prepared for Advanced Methods for Planning and Management of Transportation Networks, 25.

Ben-Akiva, M. E., Koutsopoulos, H. N., Mishalani, R. G., Yang, Q., 1997. Simulation

laboratory for evaluating dynamic traffic management systems. Journal of Transportation Engineering, 123 (4), 283–289.

Bogers, E. A., Viti, F., Hoogendoorn, S. P., 2005. Joint modeling of advanced travel information service, habit, and learning impacts on route choice by laboratory simulator experiments. Transportation Research Record, 1926 (1), 189–197.

Bovy, P., Fiorenzo-Catalano, S., 2007. Stochastic route choice set generation: behavioral and probabilistic foundations. Transportmetrica, 3 (3), 173–189.

Braess, D., 1969. ber ein paradoxon aus der verkehrsplanung. Unternehmensforschung 12, 258–268.

Braess, D., Nagurney, A., Wakolbinger, T., 2005. On a paradox of traffic planning. Transportation Science, 39 (4), 446–450.

Cantarella, G. E., Cascetta, E., 1995. Dynamic processes and equilibrium in transportation networks: towards a unifying theory. Transportation Science, 29 (4), 305–329.

Cantillo, V., de Dios Ortúzar, J., Williams, H. C., 2007. Modeling discrete choices in the presence of inertia and serial correlation. Transportation Science, 41 (2), 195–205.

Cantillo, V., Heydecker, B., de Dios Ortúzar, J., 2006. A discrete choice model incorporating thresholds for perception in attribute values. Transportation Research Part B, 40 (9), 807–825.

Carrion, C., Levinson, D., 2012. Route choice dynamics after a link restoration. Tech. rep.

Cascetta, E., 1989. A stochastic process approach to the analysis of temporal dynamics in transportation networks. Transportation Research Part B, 23 (1), 1–17.

Cascetta, E., Nuzzolo, A., Russo, F., Vitetta, A., 1996. A modified logit route choice model overcoming path overlapping problems: Specification and some calibration results for interurban networks. In: Proceedings of the 13th International Symposium on Transportation and Traffic Theory. Lyon, France, Elsevier Science, pp. 697–711.

Chen, A., Zhou, Z., 2010. The α-reliable mean-excess traffic equilibrium model with stochastic travel times. Transportation Research Part B, 44 (4), 493–513.

Chen, A., Zhou, Z., Lam, W. H., 2011. Modeling stochastic perception error in the mean-excess traffic equilibrium model. Transportation Research Part B, 45 (10), 1619–1640.

Chen, H.-C., Friedman, J. W., Thisse, J.-F., 1997. Boundedly rational Nash equilibrium: a probabilistic choice approach. Games and Economic Behavior, 18 (1), 32–54.

Chen, R., Mahmassani, H. S., 2004. Travel time perception and learning mechanisms in traffic networks. Transportation Research Record, 1894 (1), 209–221.

Chung, F., Young, S., 2010. Braesss paradox in large sparse graphs. Internet and Network Economics, 194–208.

Clark, A. J., 1933. The mode of action of drugs on cells.

Cohen, J., Horowitz, P., 1991. Paradoxical behaviour of mechanical and electrical networks. Nature, 352, 699–701.

Conlisk, J., 1996. Why bounded rationality? Journal of Economic Literature, 34 (2), 669–700.

Contini, B., Morini, M., 2007. Testing bounded rationality against full rationality in job changing behavior. Tech. rep., IZA Discussion Papers.

Cottle, R., Pang, J., Stone, R., 2009. The linear complementarity problem. No. 60. Society for Industrial Mathematics.

Cox, C., 1987. Threshold dose-response models in toxicology. Biometrics, 511–523.

Dafermos, S., Nagurney, A., 1984. On some traffic equilibrium theory paradoxes. Transportation Research Part B, 18 (2), 101–110.

Daganzo, C. F., Bouthelier, F., Sheffi, Y., 1977. Multinomial probit and qualitative choice: A computationally efficient algorithm. Transportation Science, 11 (4), 338–358.

Danczyk, A., Liu, H., Levinson, D., 2010. Unexpected cause, unexpected effect: Empirical observations of Twin Cities traffic behavior after the I-35W Bridge collapse and reopening. Submitted to Transportation. Availible online http://www. ce. umn. edu/˜ liu/I-35W/Empirical_Findings_I-35W_Final. pdf.

Davis, G., Nihan, N., 1993. Large population approximations of a general stochastic traffic assignment model. Operations Research, 41 (1), 169–178.

Di, X., Liu, H. X., Ban, X. J., 2014a. Second best toll pricing within the framework of bounded rationality.

Di, X., Liu, H. X., Pang, J.-S., Ban, X. J., 2013. Boundedly rational user equilibria (BRUE): Mathematical formulation and solution sets. Transportation Research Part B, (57), 300–313.

Di, X., Liu, H. X., Pang, Ban, X. J., Yu, J., 2014b. On the stability of a boundedly rational day-to-day dynamic. Networks and Spatial Economics, DOI:10.1007/s11067-014-9233-y.

Dial, R., 1996. Bicriterion traffic assignment: Basic theory and elementary algorithms. Transportation Science, 30 (2), 93–111.

Dial, R., 1997. Bicriterion traffic assignment: Efficient algorithms plus examples. Transportation Research Part B, 31 (5), 357–379.

Ferris, M. C., Dirkse, S. P., Meeraus, A., 2002. Mathematical programs with equilibrium constraints: Automatic reformulation and solution via constrained optimization.

Fisk, C., 1979. More paradoxes in the equilibrium assignment problem. Transportation Research Part B, 13 (4), 305–309.

Fonzone, A., Bell, M. G., 2010. Bounded rationality in hyperpath assignment: The locally rational traveler model.

Frank, M., 1981. The Braess paradox. Mathematical Programming, 20 (1), 283–302.

Friesz, T., Bernstein, D., Mehta, N., Tobin, R., Ganjalizadeh, S., 1994. Day-to-day dynamic network disequilibria and idealized traveler information systems. Operations Research, 42 (6), 1120–1136.

Gabaix, X., Laibson, D., Moloche, G., Weinberg, S., 2006. Costly information acquisition: Experimental analysis of a boundedly rational model. The American Economic Review, 1043–1068.

Gao, S., Frejinger, E., Ben-Akiva, M., 2011. Cognitive cost in route choice with real-time information: An exploratory analysis. Transportation Research Part A, 45 (9), 916–926.

Gifford, J. L., Checherita, C., 2007. Bounded rationality and transportation behavior: Lessons for public policy. In: Transportation Research Board 86th Annual Meeting. No. 07-2451.

Guilford, J. P., 1954. Psychometric methods.

Guo, X., Liu, H., 2011. Bounded rationality and irreversible network change. Transportation Research Part B, 45 (10), 1606–1618.

Hato, E., Asakura, Y., 2000. Incorporating bounded rationality concept into route choice model for transportation network analysis. PTRC-Publications, 1–12.

Haurie, A., Marcotte, P., 1985. On the relationship between NashCournot and Wardrop equilibria. Networks, 15 (3), 295–308.

He, X., 2010. Modeling the traffic flow evolution process after a network disruption. Ph.D. thesis, University of Minnesota.

He, X., Guo, X., Liu, H., 2010. A link-based day-to-day traffic assignment model. Transportation Research Part B, 44 (4), 597–608.

He, X., Liu, H. X., 2012. Modeling the day-to-day traffic evolution process after an unexpected network disruption. Transportation Research Part B, 46 (1), 50–71.

Hemmingsen, A., 1933. The accuracy of insulin assay on white mice. Quarterly Journal of Pharmacy and Pharmacology, 6, 39–80.

Hiraoka, T., Iritani, I., Okabe, K., Kumamoto, H., 2002. Route choice behavior model based on bounded rationality. In: Proc. of 10th ITS World Congress, CD-ROM.

Hu, T., Mahmassani, H., 1997. Day-to-day evolution of network flows under real-time information and reactive signal control. Transportation Research Part C, 5 (1), 51–69.

Jager, W., 2003. Breaking bad habits: A dynamical perspective on habit formation and change. Human Decision-Making and Environmental Perception: Understanding and Assisting Human Decision-Making in Real Life Settings.

Jan, O., Horowitz, A. J., Peng, Z.-R., 2000. Using global positioning system data to understand variations in path choice. Transportation Research Record, 1725 (1), 37–44.

Jayakrishnan, R., Mahmassani, H., Hu, T., 1994a. An evaluation tool for advanced traffic information and management systems in urban networks. Transportation Research Part C, 2 (3), 129–147.

Jayakrishnan, R., Tsai, W., Prashker, J., Rajadhyaksha, S., 1994b. A faster path-based algorithm for traffic assignment. Transportation Research Record, 75–75.

Jha, M., Madanat, S., Peeta, S., 1998. Perception updating and day-to-day travel choice dynamics in traffic networks with information provision. Transportation Research Part C, 6 (3), 189–212.

Jotisankasa, A., Polak, J. W., 2006. Framework for travel time learning and behavioral adaptation in route and departure time choice. Transportation Research Record, 1985 (1), 231–240.

Kameda, H., Altman, E., Kozawa, T., Hosokawa, Y., 2000. Braess-like paradoxes in distributed computer systems. IEEE Transactions on Automatic Control, 45 (9), 1687–1691.

Khisty, C. J., Arslan, T., 2005. Possibilities of steering the transportation planning process in the face of bounded rationality and unbounded uncertainty. Transportation Research Part C, 13 (2), 77–92.

Korilis, Y. A., Lazar, A. A., Orda, A., 1999. Avoiding the Braess paradox in non-cooperative networks. Journal of Applied Probability, 36 (1), 211–222.

Krishnan, K., 1977. Incorporating thresholds of indifference in probabilistic choice models. Management Science, 23 (11), 1224–1233.

Lo, H., Luo, X., Siu, B., 2006. Degradable transport network: Travel time budget of travelers with heterogeneous risk aversion. Transportation Research Part B, 40 (9), 792–806.

Lotan, T., 1997. Effects of familiarity on route choice behavior in the presence of information. Transportation Research Part C, 5 (3-4), 225–243.

Lou, Y., Yin, Y., Lawphongpanich, S., 2010. Robust congestion pricing under boundedly rational user equilibrium. Transportation Research Part B, 44 (1), 15–28.

Lu, C., Mahmassani, H., 2008. Modeling user responses to pricing: Simultaneous route and departure time network equilibrium with heterogeneous users. Transportation Research Record, 2085 (1), 124–135.

Mahmassani, H., Chang, G., 1987. On boundedly rational user equilibrium in transportation systems. Transportation Science, 21 (2), 89–99.

Mahmassani, H., Jayakrishnan, R., 1991. System performance and user response under real-time information in a congested traffic corridor. Transportation Research Part A, 25 (5), 293–307.

Mahmassani, H., Jou, R., 2000. Transferring insights into commuter behavior dynamics from laboratory experiments to field surveys. Transportation Research Part A, 34 (4), 243–260.

Mahmassani, H., Liu, Y., 1999. Dynamics of commuting decision behaviour under advanced traveler information systems. Transportation Research Part C, 7 (2-3), 91–107.

Mahmassani, H., Stephan, D., 1988. Experimental investigation of route and departure time choice dynamics of urban commuters. No. 1203.

Mahmassani, H., Zhou, X., Lu, C., 2005. Toll pricing and heterogeneous users: approximation algorithms for finding bicriterion time-dependent efficient paths in large-scale traffic networks. Transportation Research Record, 1923 (1), 28–36.

Marsden, G., Frick, K. T., May, A. D., Deakin, E., 2012. Bounded rationality in policy learning amongst cities: Lessons from the transport sector. Environment and Planning A, 44 (4), 905–920.

McKelvey, R. D., Palfrey, T. R., 1995. Quantal response equilibria for normal form games. Games and Economic Behavior, 10 (1), 6–38.

Morikawa, T., Miwa, T., Kurauchi, S., Yamamoto, T., Kobayashi, K., 2005. Driver's route choice behavior and its implications on network simulation and traffic assignment. Simulation Approaches in Transportation Analysis, 341–369.

Murchland, J., 1970. Braesss paradox of traffic flow. Transportation Research, 4 (4), 391–394.

Nagurney, A., Zhang, D., 1997. Projected dynamical systems in the formulation, stability analysis, and computation of fixed-demand traffic network equilibria. Transportation Science, 31 (2), 147–158.

Nakayama, S., Kitamura, R., Fujii, S., 2001. Drivers' route choice rules and network behavior: Do drivers become rational and homogeneous through learning? Transportation Research Record, 1752 (1), 62–68.

Parthasarathi, P., Levinson, D., Hochmair, H., 2013. Network structure and travel time perception. PloS one, 8 (10), e77718.

Pas, E., Principio, S., 1997. Braess' paradox: Some new insights. Transportation Research Part B, 31 (3), 265–276.

Patriksson, M., 1994. The traffic assignment problem: models and methods. VSP Intl Science.

Peeta, S., Ziliaskopoulos, A. K., 2001. Foundations of dynamic traffic assignment: The past, the present and the future. Networks and Spatial Economics, 1 (3-4), 233–265.

Prato, C. G., Bekhor, S., 2006. Applying branch-and-bound technique to route choice set generation. Transportation Research Record, 1985 (1), 19–28.

Ramming, M. S., 2001. Network knowledge and route choice. Ph.D. thesis, Massachusetts Institute of Technology.

Rapoport, A., Kugler, T., Dugar, S., Gisches, E., 2009. Choice of routes in congested traffic networks: Experimental tests of the Braess paradox. Games and Economic Behavior, 65 (2), 538–571.

Ridwan, M., 2004. Fuzzy preference based traffic assignment problem. Transportation Research Part C, 12 (3), 209–233.

Rosenthal, R., Brooke, A., 2007. GAMS: A User's Guide. GAMS Development Corporation.

Samuelson, W., Zeckhauser, R., 1988. Status quo bias in decision making. Journal of Risk and Uncertainty, 1 (1), 7–59.

Schneider, K., Weimann, J., 2004. Against all odds: Nash equilibria in a road pricing experiment. Human Behaviour and Traffic Networks, 133–53.

Seim, K., 2006. An empirical model of firm entry with endogenous product-type choices. The RAND Journal of Economics, 37 (3), 619–640.

Selten, R., Schreckenberg, M., Chmura, T., Pitz, T., Kube, S., Hafstein, S., Chrobok, R., Pottmeier, A., Wahle, J., Schreckenberg, M., et al., 2004. Experimental investigation of day-to-day route-choice behavior and network simulations of autobahn traffic in north rhine-westphalia. Human Behavior and Traffic Networks. Berlin: Springer, 1–21.

Simon, H. A., 1957. Models of man: Social and rational; Mathematical essays on rational human behavior in a social setting.

Simon, H. A., 1982. Models of bounded rationality: Empirically grounded economic reason. Vol. 3. MIT Press (MA).

Simon, H. A., 1986. Rationality in psychology and economics. Journal of Business, 209–224.

Sivak, M., 2002. How common sense fails us on the road: Contribution of bounded rationality to the annual worldwide toll of one million traffic fatalities. Transportation Research Part F, 5 (4), 259–269.

Smith, M., 1978. In a road network, increasing delay locally can reduce delay globally. Transportation Research, 12 (6), 419–422.

Smith, M., 1979. The existence, uniqueness and stability of traffic equilibria. Transportation Research Part B, 13 (4), 295–304.

Srinivasan, K., Mahmassani, H., 1999. Role of congestion and information in trip-makers' dynamic decision processes: Experimental investigation. Transportation Research Record, 1676 (1), 44–52.

Steinberg, R., Stone, R., 1988. The prevalence of paradoxes in transportation equilibrium problems. Transportation Science, 22 (4), 231–241.

Steinberg, R., Zangwill, W., 1983. The prevalence of Braess' paradox. Transportation Science, 17 (3), 301–318.

Szeto, W., Lo, H., 2006. Dynamic traffic assignment: Properties and extensions. Transportmetrica, 2 (1), 31–52.

Tversky, A., 1972. Elimination by aspects: A theory of choice. Psychological review, 79 (4), 281–299.

Tversky, A., Kahneman, D., et al., 1981. The framing of decisions and the psychology of choice. Science, 211 (4481), 453–458.

Valiant, G., Roughgarden, T., 2006. Braess's paradox in large random graphs. In: Proceedings of the 7th ACM conference on Electronic commerce. ACM, pp. 296–305.

Vovsha, P., Bekhor, S., 1998. Link-nested logit model of route choice: overcoming route overlapping problem. Transportation Research Record, 1645 (1), 133–142.

Walker, J. L., 2001. Extended discrete choice models: Integrated framework, flexible error structures, and latent variables. Ph.D. thesis, Massachusetts Institute of Technology.

Wang, J., Raith, A., Ehrgott, M., 2009. Tolling analysis with bi-objective traffic assignment. In: Multiple Criteria Decision Making for Sustainable Energy and Transportation Systems: Proceedings of the 19th International Conference on Multiple Criteria Decision Making, Auckland, New Zealand, 7th-12th January 2008. Vol. 634. Springer, p. 117.

Wardrop, J., 1952. Some theoretical aspects of road traffic research. Proceedings of the Institution of Civil Engineers, 1, 325–378.

Watling, D., 1999. Stability of the stochastic equilibrium assignment problem: A dynamical systems approach. Transportation Research Part B, 33 (4), 281–312.

Watling, D., 2006. User equilibrium traffic network assignment with stochastic travel times and late arrival penalty. European Journal of Operational Research, 175 (3), 1539–1556.

Wu, J., Sun, H., Wang, D. Z., Zhong, M., Han, L., Gao, Z., 2013. Bounded-rationality based day-to-day evolution model for travel behavior analysis of urban railway network. Transportation Research Part C, 31, 73–82.

Yang, H., Bell, M., 1998a. A capacity paradox in network design and how to avoid it. Transportation Research Part A, 32 (7), 539–545.

Yang, H., Bell, M., 1998b. Models and algorithms for road network design: A review and some new developments. Transport Reviews, 18 (3), 257–278.

Yanmaz-Tuzel, O., Ozbay, K., 2009. Modeling learning impacts on day-to-day travel choice. In: Transportation and Traffic Theory 2009. Springer, pp. 387–401.

Zhang, L., 2011. Behavioral foundation of route choice and traffic assignment. Transportation Research Record, 2254 (1), 1–10.

Zhao, Z., 1994. The ϵ-equilibrium in transportation networks. Fuzzy sets and systems, 68 (2), 195–202.

Zhu, S., 2011. The roads taken: Theory and evidence on route choice in the wake of the I-35W Mississippi River Bridge collapse and reconstruction. Ph.D. thesis, University of Minnesota.

Zhu, S., Levinson, D., Liu, H. X., Harder, K., 2010. The traffic and behavioral effects of the I-35W Mississippi River bridge collapse. Transportation research part A, 44 (10), 771–784.

Zhu, S., Levinson, D. M., 2012. Disruptions to transportation networks: A review. In: Network Reliability in Practice. Springer, pp. 5–20.

Ziliaskopoulos, A. K., Waller, S. T., 2000. An internet-based geographic information system that integrates data, models and users for transportation applications. Transportation Research Part C, 8 (1), 427–444.

Appendix A

Acronyms and Appendix

Table A.1: Notation

$\mathcal{N}$	A set of consecutively numbered nodes
$\mathcal{L}$	A set of consecutively numbered links
$a \in \mathcal{L}$	Link index
$\mathcal{W}$	Origin-destination (OD) pair set connected by a set of simple paths
$\mathcal{P}^w$	Simple paths (composed of a sequence of distinct nodes) connecting OD pair $w \in \mathcal{W}$
d^w	Traffic demand for OD pair w
$\mathbf{d}$	Traffic demand vector
f_i^w	Flow on path $i \in \mathcal{P}^w$ for OD pair w
$\mathbf{f} = \{f_i^w\}_{i \in \mathcal{P}^w}^{w \in \mathcal{W}}$	Path flow vector
$\mathcal{F}$	Feasible path flow set is to assign the traffic demand on the feasible paths
x_a	Link flow on link a
$\mathbf{x} = \{x_a\}_{a \in \mathcal{L}}$	Link flow vector
$c(\mathbf{x})$	Link performance function
$\delta_{a,i}^w$	Link-path incidence indicator, 1 if link a is on path i connecting OD pair w, and 0 if not
$\Delta \triangleq \{\delta_{a,i}^w\}_{a \in \mathcal{L}, i \in \mathcal{P}}^{w \in \mathcal{W}}$	Link-path incidence matrix

Table A.1 – continued from previous page

$C(\mathbf{f}) \triangleq \{C_i^w(\mathbf{f})\}_{i\in\mathcal{P}}^{w\in\mathcal{W}}$	Path cost vector
$\perp$	Orthogonal sign representing the inner product of two vectors is zero
$(\varepsilon^w)_{w\in\mathcal{W}}$	Indifference band for OD pair $w \in \mathcal{W}$
$\boldsymbol{\varepsilon} = (\varepsilon^w)_{w\in\mathcal{W}}, \varepsilon^w \geqslant 0$	Indifference band vector
π^w	Maximum path cost within ε^w for OD pair w
ρ_i^w	Indifference function for path $i \in \mathcal{P}$ connecting OD pair $w \in \mathcal{W}$
$\mathcal{P}_l^\varepsilon$	Largest ε-acceptable path set
$\mathcal{P}_{UE}$	User equilibrium shortest path set
$\mathcal{F}_{BRUE}^{\boldsymbol{\varepsilon}}$	$\boldsymbol{\varepsilon}$-BRUE path flow solution set
w-$STT(\mathbf{d}, \boldsymbol{\varepsilon})$	the maximum STT among the $\boldsymbol{\varepsilon}$-BRUE solution set
b-$STT(\mathbf{d}, \boldsymbol{\varepsilon})$	the minimum STT among the $\boldsymbol{\varepsilon}$-BRUE solution set
S_{RP}	$(\mathbf{d}, \boldsymbol{\varepsilon})$ region for the risk-prone paradox
S_{RN}	$(\mathbf{d}, \boldsymbol{\varepsilon})$ region for the risk-neutral paradox
S_{RA}	$(\mathbf{d}, \boldsymbol{\varepsilon})$ region for the risk-averse paradox

Table A.2: Acronyms

Acronym	Meaning
PR	Perfect rationality
BR	Bounded rationality
OD	Origin-destination pair
BRD	Boundedly rational day-to-day dynamic
UE	User equilibrium
DUE	Dynamic user equilibrium
DUO	Dynamic user optimal
DTA	Dynamic traffic assignment
BRUE	Boundedly rational user equilibrium
STT	system travel time
MPEC	Mathematical programs with equilibrium constraints

Continued on next page

Table A.2 – continued from previous page

Acronym	Meaning
RUM	Random utility maximization
i.i.d.	Independently identically distributed
m	meter

Table A.3: Bridge usage distribution for each subject

Subject ID	Franklin	I94	Washington	10th	35W	TH65	Hennepin	Plymouth	Broadway	37th	I694	Most frequently used bridge
2003					1.0			1.0				Plymouth 35W
2006				1.0	1.0							10th 35W
2010				1.0	1.0							10th 35W
2011				1.0	1.0							10th 35W
2015			1.0		1.0							Washington 35W
2020			1.0		1.0							Washington 35W
2021			1.0 0.3		0.7							Washington 35W
2028			1.0 0.1		0.9							Washington 35W
2034				1.0	1.0							10th 35W
2037				1.0	1.0							10th 35W

2079		1.0 0.5			0.5							I94 35W
2080					0.9			0.1	0.3	0.7 0.1		36th 35W
2087	0.3		1.0 0.3		0.3							Washington 35W
2089					1.0			1.0				Plymouth 35W
2109			1.0		1.0							Washington 35W
2110				1.0 0.0	1.0							10th 35W
2125			1.0 0.1		0.8				0.1			Washington 35W
2132			1.0		1.0							Washington 35W
2137			0.9	0.1	1.0							Washington 35W
2141		0.1	0.8		1.0				0.1			Washington 35W
1001			0.5 0.1	0.1	0.3	0.1	0.5 0.5					Hennepin 35W
1002			1.0 0.1		1.0							Washington 35W
1003				1.0								10th

				0.0	1.0							35W
1004			1.0									Washington
					1.0							35W
1005			1.0									Washington
					1.0							35W
1006		1.0										I94
					1.0							35W
1008		1.0										I94
		0.1			0.9							35W
1012				1.0								10th
					1.0							35W
1013									1.0			Broadway
		0.1	0.1		0.5				0.3			35W
1014				1.0								10th
				0.5	0.5							35W
1015			1.0									Washington
			0.2	0.0	0.8							35W
1016				1.0								10th
					1.0							35W
1017				1.0								10th
				0.0	1.0	0.0						35W
1020			1.0									Washington
			0.1		0.9							35W
1021			0.7	0.3								Washington
			0.2		0.8							35W
1022				1.0								10th

				0.0	1.0							35W
1023				1.0								10th
					1.0							35W
1024			0.3	0.8								10th
				0.0	1.0							35W
1026						1.0						TH65
					1.0							35W
1028				1.0								10th
		0.2		0.4	0.5							35W
1033						1.0						TH65
					0.9	0.1						35W
1035			1.0									Washington
					1.0							35W
1040	1.0											Franklin
	0.4	0.2			0.4							35W
1041				1.0								10th
				0.1	0.7		0.3					35W
1042				1.0								10th
				0.1	0.9							35W
1043				1.0								10th
					1.0							35W
1047				1.0								10th
					1.0							35W
2009									1.0			Broadway
									1.0			Broadway
2022		0.9							0.1			I94

		0.8						0.1	0.2			I94
2023			1.0									Washington
			1.0									Washington
2030	0.1	0.6	0.3									I94
	0.2	0.7	0.1									I94
2035	0.6			0.4								10th
	0.4			0.5	0.1							10th
2038				1.0								10th
				0.9	0.1							10th
2040			1.0									Washington
			1.0									Washington
2041			1.0									Washington
			0.5	0.2	0.2							Washington
2044		1.0										I94
		0.6	0.4									I94
2053				1.0								10th
				1.0								10th
2070			1.0									Washington
			1.0									Washington
2073		1.0										I94
		1.0										I94
2077			1.0									Washington
			1.0									Washington
2093		0.9	0.1									I94
		0.9	0.0			0.0						I94
2095			1.0									Washington

		0.1	0.9									Washington
2112			1.0									Washington
			1.0									Washington
2119				0.8				0.3				10th
				0.8				0.2				10th
2122							1.0					Hennepin
		0.5			0.5		0.1					I94
2124			1.0									Washington
			1.0									Washington
2127			1.0									Washington
			1.0									Washington
2128			1.0									Washington
			1.0									Washington
2139		0.1	0.8				0.1					Washington
			0.6		0.4							Washington
2148		0.6	0.4									I94
		0.8	0.2									I94
1009							1.0					Hennepin
							1.0					Hennepin
1011			1.0									Washington
			0.8		0.2							Washington
1019				1.0								10th
		0.1		0.9								10th
1027				1.0								10th
	0.2			0.8								10th
1030		0.2	0.8									Washington

		0.0	0.9		0.0							Washington
1039		1.0										I94
		0.9			0.1							I94
1044			1.0									Washington
			0.9		0.1							Washington
1046											1.0	I694
					0.2	0.1					0.7	I694

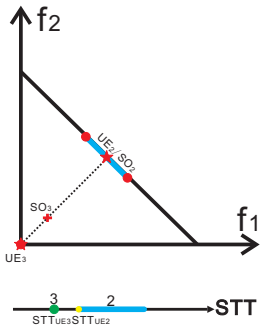

(a) $0 \leqslant \varepsilon < -(b_1 + b_2)d + a_1 - a_2$

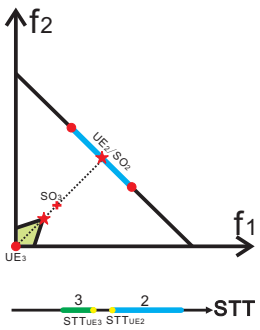

(b) $-(b_1 + b_2)d + a_1 - a_2 \leqslant \varepsilon < \frac{a_1 - a_2}{2}$

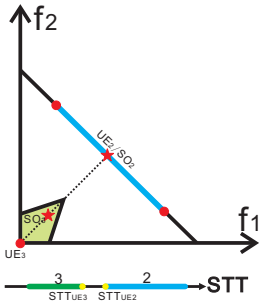

(c) $\frac{a_1 - a_2}{2} \leqslant \varepsilon < (b_1 + b_2)d$

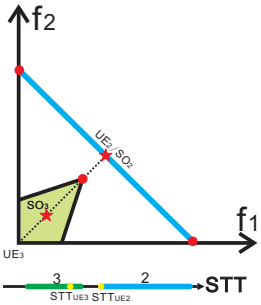

(d) $(b_1 + b_2)d \leqslant \varepsilon < \frac{-(b_1 - b_2)d}{2} + a_1 - a_2$

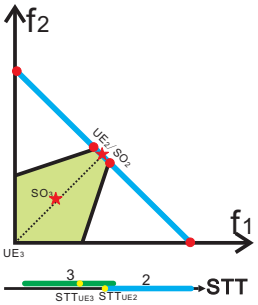

(e) $\frac{-(b_1 - b_2)d}{2} + a_1 - a_2 \leqslant \varepsilon < b_2 d + a_1 - a_2$

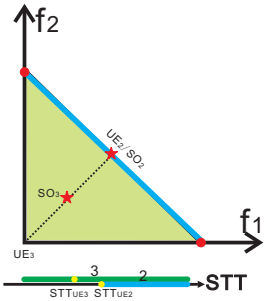

(f) $\varepsilon \geqslant b_2 d + a_1 - a_2$

Figure A.1: Case 2: $\frac{a_1 - a_2}{2(b_1 + b_2)} \leqslant d < \frac{2(a_1 - a_2)}{3b_1 + b_2}$

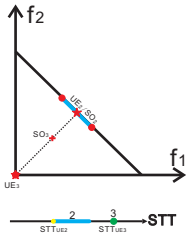

(a) $0 \leqslant \varepsilon < -(b_1 + b_2)d + a_1 - a_2$

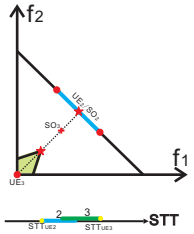

(b) $-(b_1+b_2)d+a_1-a_2 \leqslant \varepsilon < \frac{(b_1-b_2)d}{2}$

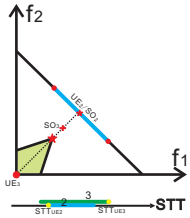

(c) $\frac{(b_1-b_2)d}{2} \leqslant \varepsilon < \frac{a_1-a_2}{2}$

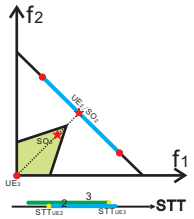

(d) $\frac{a_1-a_2}{2} \leqslant \varepsilon < \frac{-(b_1-b_2)d}{2} + a_1 - a_2$

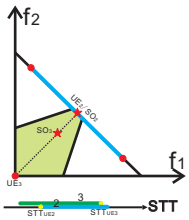

(e) $\frac{-(b_1-b_2)d}{2} + a_1 - a_2 \leqslant \varepsilon < (b_1 + b_2)d$

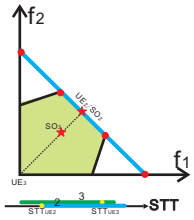

(f) $(b_1 + b_2)d \leqslant \varepsilon < b_2d + a_1 - a_2$

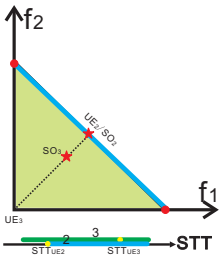

(g) $\varepsilon \geqslant b_2d + a_1 - a_2$

Figure A.2: Case 3: $\frac{2(a_1-a_2)}{3b_1+b_2} \leqslant d < \frac{a_1-a_2}{b_1+b_2}$

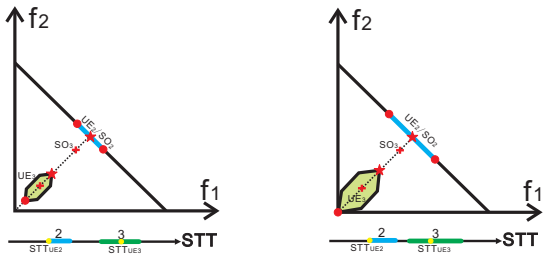

(a) $0 \leqslant \varepsilon < (b_1+b_2)d-a_1+a_2$ (b) $(b_1+b_2)d-a_1+a_2 \leqslant \varepsilon < \frac{(b_1-b_2)d}{2}$

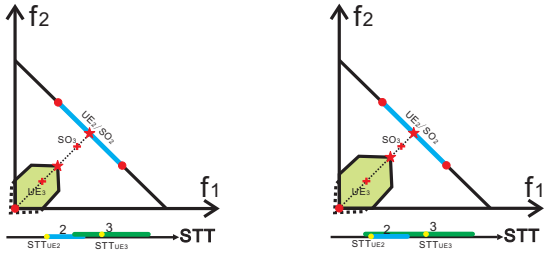

(c) $\frac{(b_1-b_2)d}{2} \leqslant \varepsilon < \frac{a_1-a_2}{2}$ (d) $\frac{a_1-a_2}{2} \leqslant \varepsilon < (b_1+b_2)d$

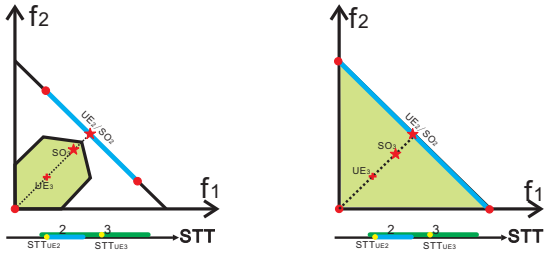

(e) $(b_1+b_2)d \leqslant \varepsilon < b_2d+a_1-a_2$ (f) $\varepsilon \geqslant b_2d+a_1-a_2$

Figure A.3: Case 4: $\frac{a_1-a_2}{b_1+b_2} \leqslant d < \frac{a_1-a_2}{b_1}$

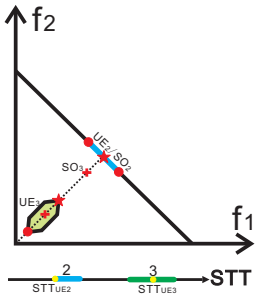

(a) $0 \leqslant \varepsilon < (b_1 + b_2)d - a_1 + a_2$

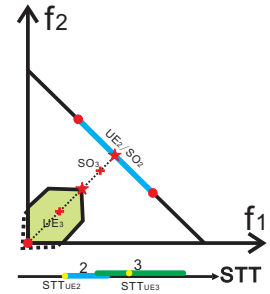

(b) $(b_1+b_2)d-a_1+a_2 \leqslant \varepsilon < \frac{a_1-a_2}{2}$

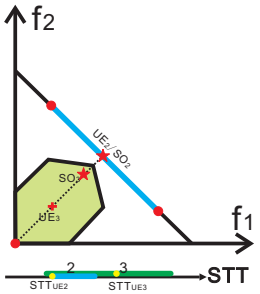

(c) $\frac{a_1-a_2}{2} \leqslant \varepsilon < b_2d + a_1 - a_2$

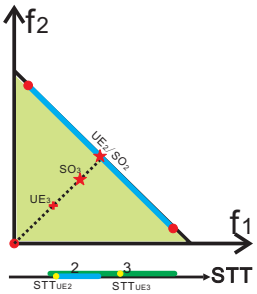

(d) $b_2d + a_1 - a_2 \leqslant \varepsilon < (b_1 + b_2)d$

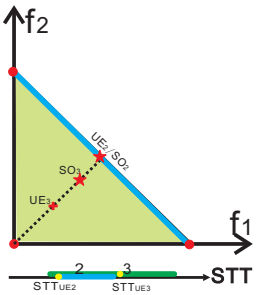

(e) $\varepsilon \geqslant (b_1 + b_2)d$

Figure A.4: Case 5: $\frac{a_1-a_2}{b_1} \leqslant d < \frac{a_1-a_2}{b_1-b_2}$

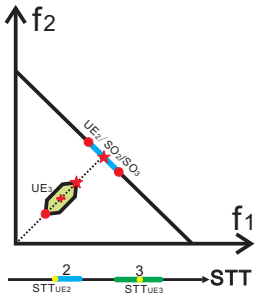

(a) $0 \leqslant \varepsilon < (b_1 + b_2)d - a_1 + a_2$

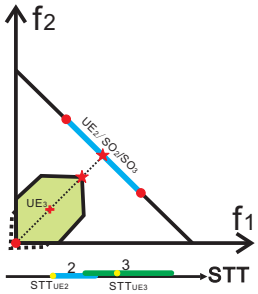

(b) $(b_1 + b_2)d - a_1 + a_2 \leqslant \varepsilon < \frac{-(b_1-b_2)d}{2} + a_1 - a_2$

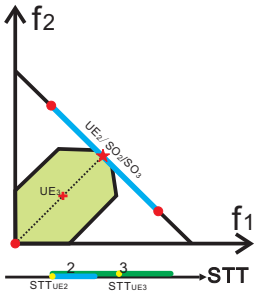

(c) $\frac{-(b_1-b_2)d}{2} + a_1 - a_2 \leqslant \varepsilon < (b_1 + b_2)d$

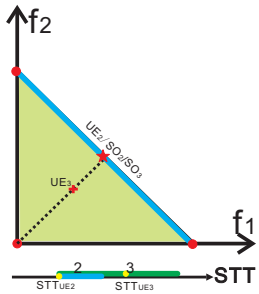

(d) $\varepsilon \geqslant (b_1 + b_2)d$

Figure A.5: Case 6: $\frac{a_1-a_2}{b_1-b_2} \leqslant d < \frac{4(a_1-a_2)}{3b_1+b_2}$

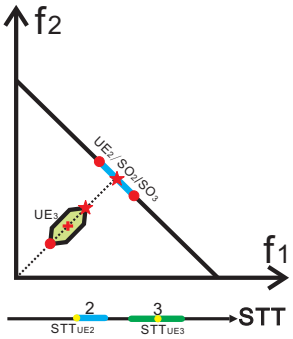

(a) $0 \leqslant \varepsilon < -\frac{(b_1-b_2)d}{2} + a_1 - a_2$

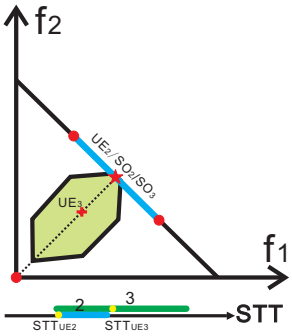

(b) $-\frac{(b_1-b_2)d}{2} + a_1 - a_2 \leqslant \varepsilon < (b_1+b_2)d - a_1 + a_2$

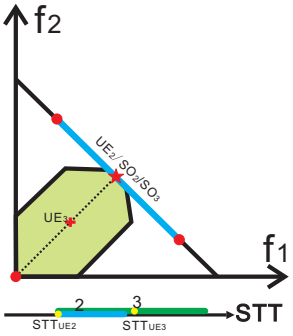

(c) $(b_1+b_2)d - a_1 + a_2 \leqslant \varepsilon < (b_1+b_2)d$

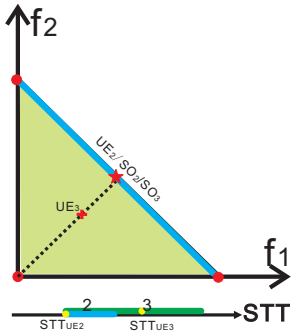

(d) $\varepsilon \geqslant (b_1+b_2)d$

Figure A.6: Case 7: $\frac{4(a_1-a_2)}{3b_1+b_2} \leqslant d < \frac{2(a_1-a_2)}{b_1-b_2}$

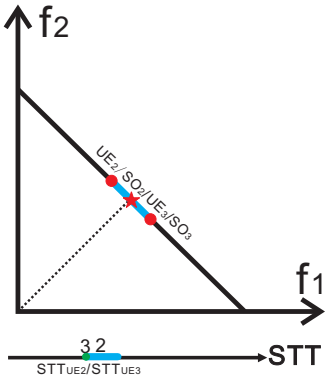

(a) $0 \leqslant \varepsilon < \frac{(b_1-b_2)d}{2} - a_1 + a_2$

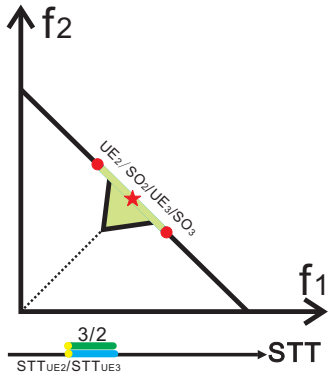

(b) $\frac{(b_1-b_2)d}{2} - a_1 + a_2 \leqslant \varepsilon < (b_1-b_2)d - 2(a_1 - a_2)$

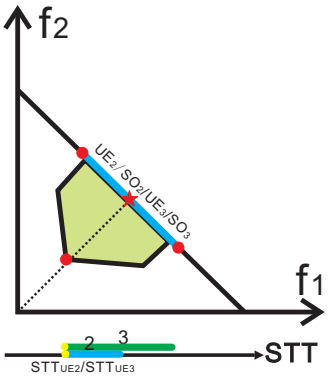

(c) $(b_1 - b_2)d - 2(a_1 - a_2) \leqslant \varepsilon < (b_1 + b_2)d - a_1 + a_2$

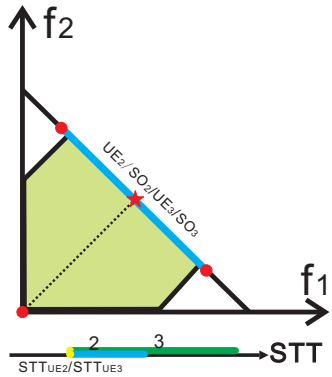

(d) $(b_1 + b_2)d - a_1 + a_2 \leqslant \varepsilon < (b_1 + b_2)d$

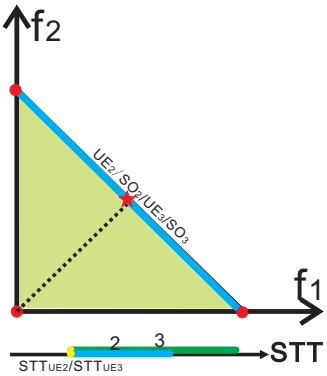

(e) $\varepsilon \geqslant (b_1 + b_2)d$

Figure A.7: Case 8: $d \geqslant \frac{2(a_1-a_2)}{b_1-b_2}$